Rockefeller University
Digital Commons @ RU

Student Theses and Dissertations

2018

Cell Cycle Control by Cyclin-CDKS in Chlamydomonas ReinhardtII

Kenneth C. Atkins

Follow this and additional works at: https://digitalcommons.rockefeller.edu/student_theses_and_dissertations

 Part of the Life Sciences Commons

Recommended Citation
Atkins, Kenneth C., "Cell Cycle Control by Cyclin-CDKS in Chlamydomonas ReinhardtII" (2018). *Student Theses and Dissertations*. 424.
https://digitalcommons.rockefeller.edu/student_theses_and_dissertations/424

This Thesis is brought to you for free and open access by Digital Commons @ RU. It has been accepted for inclusion in Student Theses and Dissertations by an authorized administrator of Digital Commons @ RU. For more information, please contact mcsweej@mail.rockefeller.edu.

CELL CYCLE CONTROL BY CYCLIN-CDKS

IN *CHLAMYDOMONAS REINHARDTII*

A Thesis Presented to the Faculty of

The Rockefeller University

in Partial Fulfillment of the Requirements for

the degree of Doctor of Philosophy

by

Kenneth C. Atkins

June 2018

© Copyright by Kenneth C. Atkins 2018

CELL CYCLE CONTROL BY CYCLIN-CDKS IN *CHLAMYDOMONAS REINHARDTII*

Kenneth C. Atkins, Ph.D.

The Rockefeller University 2018

The cell cycle consists of a series of events, including replication and segregation of the genome, that occurs in order to ensure successful reproduction of cells. In fungi and animals, this process is carefully regulated by a set of protein complexes with alternating, oscillating activity. A well-established model has been developed for animals and fungi in which the activities of various cyclin-dependent kinases (CDKs) and the anaphase promoting complex (APC) drive the events of the cell cycle at the appropriate time and in the appropriate order. While this model has been extremely useful for understanding cell division in these lineages, it is not necessarily applicable to other groups of eukaryotes. Animals and fungi belong to a relatively recently diverged group called the Opisthokonts, so their shared features do not necessarily extend to their eukaryotic cousins, including plants, a very important lineage of particular concern to humanity.

Chlamydomonas reinhardtii is a unicellular member of the plant kingdom. Its simple genome (compared to land plants) and easily observed cell division cycle have facilitated the collection of a large number of conditional mutations that block the cell cycle at high temperature. Mutations in two CDKs, CDKA1 and CDKB1, and two subunits of the APC are included in this set. The phenotypes of these mutants at restrictive-temperature revealed that CDKA1, unlike its ortholog in the Opisthokonts, is not required for mitosis, and instead plays a role in cell cycle initiation. CDKB1, on the other hand, is a plant-specific CDK and is required

for promoting the events of mitosis. The APC plays a similar role to its counterpart in Opisthokonts in driving the metaphase-to-anaphase transition.

In this thesis, we present the results of our efforts to better understand the function and regulation of the kinases CDKA1 and CDKB1 and two *Chlamydomonas* cyclins, CYCA1 and CYCB1. We characterize the role of these molecules in cell division timing, DNA replication, spindle formation, and cytokinesis and explore the nature of their regulatory interactions and their control by the APC. We also describe a genetic screen to identify parallel pathways that promote cell cycle initiation alongside CDKA1 and speculate on a possible common thread among the identified mutations.

A genetic screen for genes involved in cell cycle initiation uncovers many null mutations in *CDKA1*, showing definitively that CDKA1 is inessential for cell division in *Chlamydomonas*, and likely all plants. Disruption of both *CDKA1* and *CYCA1* results in a delay in cell division, and CYCA1 is specifically required for biochemical activity of CDKA1, suggesting they may act as a complex to promote the initiation of cell division. CYCB1 is required for timely DNA replication and mitotic spindle formation in a similar manner to CDKB1, and, consistently, is also required for biochemical activation of CDKB1. We propose that CYCB1 and CDKB1 form a complex and together constitute the primary mitotic inducer in *Chlamydomonas*. Both CDKA1 and CDKB1 are downregulated by the APC, and CDKA1 kinase activity is inhibited by CYCB1-CDKB1. A model is presented incorporating these and prior findings concerning the function and regulatory interaction among these cell cycle regulators. Several possible positive and negative feedback loops become apparent which may ensure switch-like activation or appropriate ordering of the activity of various complexes.

ACKNOWLEDGMENTS

The efforts of many people contributed to the realization of this work, but I would like to thank those who are both known to me and who I think have made a substantial contribution. Fred Cross provided guidance throughout, wrote many of the programs used, and helped conduct analyses. Most importantly, however, our discussions have made me a more careful and critical thinker and communicator, and I hope that is reflected in this thesis. The members of my thesis committee, Fred Cross, Shai Shaham, and Hiro Funabiki, have provided valuable insights and helped guide the direction of the work. Both Frej Tulin and Michal Breker, in addition to sharing useful ideas, isolated many of the mutants described in this work. Kresti Pecani helped prepare samples analyzed in this work and provided technical support. Sam Obado performed mass spectrometry analysis on CDKA1 and CDKB1 immunoprecipitates. Svetlana Mazel and Alison North taught me various techniques and helped design protocols. I especially thank my boyfriend Eric Petschek for his patience and support, and for advice on writing and figure preparation.

TABLE OF CONTENTS

LIST OF FIGURES

LIST OF TABLES

Chapter 1 Introduction

Cyclin-CDKs regulate key cell cycle phase transitions in eukaryotes

All cells must replicate their components and segregate them appropriately into daughter cells in order to reproduce. This process is quite sophisticated in eukaryotic cells and depends on a complex set of events whose timing correlates with specific conditions in the external environment and the internal state of the cell. It is now well established that both the timing and the order of many events in the cell division cycle is not an intrinsic feature; it is instead imposed externally by a set of ancient regulatory molecules.

The molecular underpinnings of cell cycle regulation were discovered in various fungi and animals, and findings from these systems have established a consensus model for cell cycle control (Morgan 2007). The enzymatic activity of cyclin-dependent kinases (CDKs), activated by regulatory cyclins, is critical for the early stages of the cell cycle, including replication of the genome and the formation of a mitotic spindle. The separation of sister chromosomes and other late events are ensured by the activity of the anaphase promoting complex (APC), whose activity as an E3 ubiquitin ligase targets various proteins for destruction. The two critical targets of the APC are the anaphase inhibitor securin and the mitotic cyclins (Thornton and Toczyski 2003). Inter-regulation between the cyclin-CDKs and the APC ensures the correct ordering and separation of their activity. Cyclin-CDKs activate the APC and the APC in turn targets cyclins for destruction, thus eliminating cyclin-CDK activity. This negative feedback loop is a central feature of eukaryotic cell cycle control and is partly responsible for the alternating activity of these two complexes.

In fungi, a single CDK called CDK1, which binds at different times to various B-type cyclins, drives both DNA replication and mitosis. Animal cells use several different CDKs to regulate the cell cycle. CDK2, a close relative of CDK1, drives DNA replication in complex with cyclins E or A. Animal CDK1, activated by cyclin B, promotes mitosis. CDK1 is the only essential CDK in fungi, and in animals it is capable of driving all the events of the cell cycle in the absence of CDK2, CDK3, CDK4, and CDK6 (Santamaría et al. 2007). Fungal and animal genomes typically encode many different cyclins. The regulation and function of these cyclins is diverse, with some overlap (Bloom and Cross 2007), probably enabling flexible control of the cell cycle in different environmental and developmental scenarios and providing modularity to the execution of related events in different cell cycle stages. Despite this diversification of function, a single B-type cyclin can drive both DNA replication and mitosis in fission yeast (Fisher and Nurse 1996). In animals, absence of certain A and B-type cyclins results in impaired division (Murphy et al. 1997; Brandeis et al. 1998), whereas E and D-type cyclins are largely dispensable for normal cell proliferation (Kozar et al. 2004; Geng et al. 2003).

Cell cycle control in land plants

Although the precise rooting is unclear, deep phylogenetic analysis suggests that divergence between photosynthetic and non-photosynthetic eukaryotes occurred very early (Rogozin et al. 2010). Within the eukaryotes, fungi and animals comprise the Opisthokont clade. Other eukaryotic groups diverged from the Opisthokonts early in the evolution of the eukaryotes (Fig. 1.1). Because animals and fungi are closely related, their shared features do not necessarily extend to other eukaryotes. The consensus model for cell cycle control is largely derived from the study of Opisthokonts and does not necessarily apply to the plant kingdom or any other

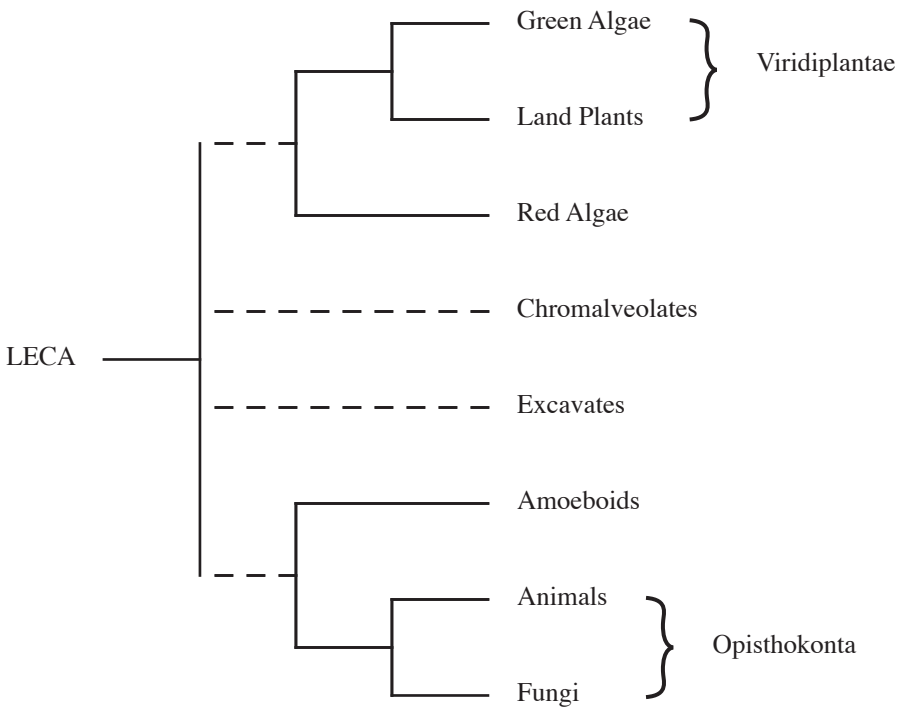

Figure 1.1 A phylogenetic tree of the eukaryotes.

Adapted from (Rogozin et al. 2010).

In this tree, fungi and animals comprise a group called Opisthokonta. Other eukaryotic groups diverged before the split of fungi and animals. Although the exact rooting is unclear, plants clearly form an outgroup to Opisthokonta and likely diverged from this group early in the evolution of the eukaryotes. Land plants and green algae together comprise the group Viridiplantae. Branch lengths are arbitrary. Dahsed lines indicate unclear divergences. LECA: last eukaryotic common ancestor.

non-Opisthokont group. There may be significant divergences. As primary producers, plants play a critical role in the biosphere and provide vast quantities of food and fiber for humanity, and thus it may be of great utility to understand such divergences where they exist.

Plant genomes encode many homologs of genes with known roles in cell cycle control in the Opisthokonts (Vandepoele et al. 2002; Robbens et al. 2005; Bisova et al. 2005; Guo et al. 2007). These include various CDKs, cyclins, CDK inhibitors (CKIs), and the transcriptional regulators Rb, E2F, and DP. This conservation of sequence, however, belies a considerable level of divergence in function (Harashima et al. 2013). For instance, phosphoregulation of CDK1 by WEE1 and CDC25, which is critical for the transition to mitosis in animals and fission yeast, is not involved in normal cell cycle regulation in plants (Dissmeyer et al. 2009). The role of WEE1 in this context is restricted to arresting the cell cycle in response to replication stress (Cools et al. 2011). CDC25 is absent in plants. It may have become inessential due to the evolution of the plant-specific B-type CDKs or new regulatory circuits involving CKIs (Boudolf et al. 2006; Dissmeyer et al. 2010; Zhao et al. 2012). Plants also possess cell cycle regulators that are not found in animals or fungi. For example, the plant-specific CDK inhibitors SMR and EL2 and several plant-specific APC inhibitors including UVI4, GIG1, and SAMBA have no recognizable homologs in either animals or fungi (Churchman et al. 2006; Peres et al. 2007; Heyman et al. 2011; Iwata et al. 2011; Eloy et al. 2012).

In one of the more surprising examples of divergence, CDKA1, the plant kingdom ortholog of CDK1, is inessential in *Arabidopsis*, although cell proliferation is substantially attenuated in its absence (Nowack et al. 2012). Members of the CDKB family may provide essential function in the absence of CDKA1 (Nowack et al. 2012).

CDKB is a plant-specific cyclin-dependent kinase. Best reciprocal BLAST (BRB) analysis (Remm et al. 2001) demonstrates that CDKA and CDKB form gene families across plant genomes (Fig. 1.2). CDKA forms a BRB pair with Opisthokont CDK1, but CDKB lacks a BRB partner in Opisthokonts. CDKB may have been acquired early in the plant lineage sometime after the separation from Opisthokonts. Alternatively, it may have been present in the last common ancestor of both plants and Opisthokonts and was simply lost in an early ancestor of the Opisthokonts.

Multiple polyploidization events in the evolutionary history of land plants (Adams and Wendel 2005) have littered plant genomes with multiple copies of many genes, creating an abundance of redundancy. This is a complicating factor for the analysis of gene function since phenotypes due to single gene mutations may be quite subtle. The *Arabidopsis* genome encodes around 30 A-, B-, and D-type cyclins altogether (Vandepoele et al. 2002). The molecular function of the various cyclins is still mostly unclear. Nevertheless, it is clear that different subgroups of A- and D-type cyclins have specialized roles in responding to nutrient availability (Riou-Khamlichi et al. 2000; Lorenz et al. 2003), plant hormones (Dewitte et al. 2007; Sanz et al. 2011; Polko et al. 2015), or developmental signals (Cruz-Ramírez et al. 2012; Forzani et al. 2014; Vanneste et al. 2011) to control cell proliferation in specific tissues and at different developmental stages.

During the development of many plant organs, cells must exit the proliferative meristem and begin expanding in volume. The concomitant transition from mitotic to endocycles, and thus the generation of polyploidy in mature cells, may be required for creating these very large cells (Mendell et al. 2008; Melaragno et al. 1993; Chevalier et al. 2014). A- and D-type cyclins in *Arabidopsis* can delay the onset or duration of this transition (Dewitte et al. 2007; Imai et al.

Figure 1.2[*] *Chlamydomonas* CDKA1 is an ortholog of land plant CDKA and animal CDK1; *Chlamydomonas* CDKB1 is an ortholog of land plant CDKB and lacks an animal ortholog.

The figure illustrates best reciprocal BLAST analysis (Remm et al. 2001) of CDKs. Cre: *Chlamydomonas reinhardtii*, Ath: *Arabidopsis thaliana* (dicot), Bdi: *Brachypodium distachyon* (monocot), Mmu: *Mus musculus*. Top left: Cre vs. Ath. Top right: Ath vs. Bdi. Bottom left: Cre vs. Bdi. Bottom right: Cre vs. Mmu. BLAST scores are provided for all alignments. Heavy blue arrows indicate a best reciprocal BLAST (BRB) relationship: each gene in the pair finds the other gene as the highest-scoring BLAST hit in the other genome. Light blue arrows indicate a non-BRB BLAST hit. CDKA and CDKB genes form BRB-pairs in Viridiplantae comparisons (Cre-Ath, Ath-Bdi, Cre-Bdi). Cre CDKA forms a BRB-pair with Mmu CDK1 or CDK2 equivalently (as expected if CDK1 and CDK2 diverged from each other within the animal lineage). Cre CDKB does not form a BRB pair with any gene in the mouse genome. The greatest divergence in this set is between CDKA/CDK1 and CDKB. If divergence is neutral, this implies that CDKB split from CDKA/CDK1 before Viridiplantae split from Opisthokonts, in which case the ortholog must have been lost early in the Opisthokont lineage. Or, CDKB might have split from CDKA/CDK1 within the Viridiplantae lineage, in which case divergence of CDKB could have been positively selected.

[*] Sequence analysis performed by F. Cross.

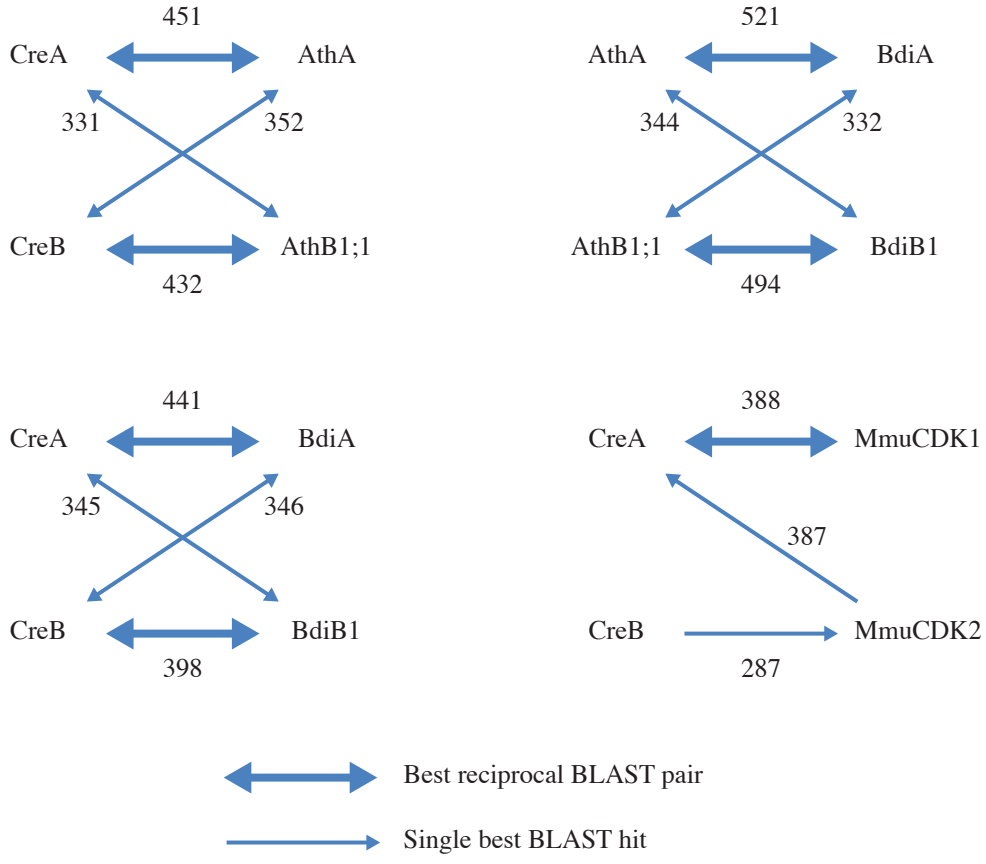
451
CreA
AthA
331
352
CreB
AthB1;1
432
521
AthA
BdiA
344
332
AthB1;1
BdiB1
494
441
CreA
BdiA
345
346
CreB
BdiB1
398
388
CreA
MmuCDK1
387
CreB
MmuCDK2
287
Best reciprocal BLAST pair
Single best BLAST hit

2006) and B1-type cyclins, when inappropriately expressed, can induce mitotic cycles in endoreduplicating cells (Schnittger et al. 2002).

Evidently, the expansion of the cyclin family in land plants has afforded opportunities for diversification of function and the ability to regulate division in specific tissues, perhaps contributing to or enhancing the evolution of multicellularity in Viridiplantae. Unfortunately, this radiation has introduced a complicated tangle of redundant genes with overlapping functions and presents a formidable barrier to genetic analysis.

Molecular players in the *Chlamydomonas* cell cycle

Chlamydomonas reinhardtii is a green alga and a member of the clade Chlorophyta, which diverged from the Streptophytes (land plants and their close relatives) very early in the evolution of Viridiplantae (Karol et al. 2001; Lemieux et al. 2000). This divergence occurred before the multiple polyploidization events in land plants and thus most genes in the *Chlamydomonas* genome are present in single copy (Merchant et al. 2007). In addition, *Chlamydomonas* propagates with a haploid genome. This make it an ideal system for loss-of-function genetics—mutant phenotypes are immediately apparent since they are not masked by a functioning copy of the mutated gene, whether a paralog or a wild type copy from a homologous chromosome.

The *Chlamydomonas* cell division cycle is synchronizable and growth and division are readily observed microscopically. These features enabled the isolation of many conditional mutations inactivating various components of the cell cycle machinery in *Chlamydomonas* (Tulin and Cross 2014; Breker et al. 2016). This work revealed the presence of many conserved elements, including CDKs, subunits of the APC, and genes whose homologs in Opisthokonts carry out the execution of DNA replication and mitotic spindle assembly. A few plant-specific

genes were also identified; their precise role is not yet entirely clear. The consequences of mutational inactivation of *CDKA1* and *CDKB1* suggest a divergence of function compared to Opisthokonts (see below). The spindle assembly checkpoint in *Chlamydomonas* is either weak or absent altogether since mutants with impaired microtubule function undergo multiple rounds of DNA rereplication.

The ciliary and mitotic cycles are integrated in some manner in *Chlamydomonas*. At the end of the growth phase the basal bodies detach from the flagella and migrate away from one another. They are eventually found at the spindle poles during mitosis, but it is unclear whether they act as microtubule organizing centers (Dutcher and O'Toole 2016). Cells lacking basal bodies show defects in the relative orientation of the mitotic spindle and the cytokinetic cleavage furrow, revealing a critical role for basal bodies in the spatial regulation of cell division (Ehler et al. 1995). The basal bodies are connected to four sets of acetylated microtubule bundles called rootlets, and the position of these rootlets is thought to direct the formation of the cytokinetic furrow (Holmes and Dutcher 1989; Ehler et al. 1995; Ehler and Dutcher 1998). Molecular regulation of the temporal coordination between the ciliary and mitotic cycles is still unclear.

The *Chlamydomonas* cell cycle begins with an extended growth phase during which cells can undergo many doublings in cell size before dividing. After 'n' doublings, a rapid series of sequential cycles of DNA replication, mitosis, and cell division occur within the mother cell wall to create a cluster of 2^n cells which then hatch from the mother cell wall to start the cycle anew (see wild type in Fig. 2.3A). The conserved transcriptional regulators RBR1, E2F1, and DP1 act together to control this process, determining either when to begin cell divisions, how many cycles to perform, when to stop them, or some combination of these (Fang et al. 2006; Fang and Umen 2008; Olson et al. 2010). The precise mechanism is unclear. Conditional inactivating

mutations in these genes would likely be helpful for determining which steps in the cycle are regulated. CDKG1 is thought to act upstream of these regulators. Its concentration in pre-division mother cell nuclei and subsequent dilution and degradation during cell divisions may underlie the coordination between mother cell size and number of divisions (Li et al. 2016b).

In order to maintain cell size over generations, the cell division cycle must be coordinated with cell growth in some manner (Jorgensen and Tyers 2004). As might be expected since *Chlamydomonas* is a photosynthetic microbe, the timing of cell divisions in *Chlamydomonas* is regulated by light. In cultures of *Chlamydomonas* grown with alternating periods of light and dark, cells divide synchronously—growing during the light period and dividing during the dark period. During the early growth period, cell cycle progression is light-dependent. After a certain point, however, cells will proceed to divide even if they are transferred to the dark (Spudich and Sager 1980). This point, at which cell cycle progression is no longer light-dependent, is called 'commitment.' Blue light, but not red light, can induce a delay in cell division (Münzner and Voigt 1992). Delay upon blue light exposure is due to a later onset of the commitment point (Oldenhof et al. 2004). The effect of blue light is seen even in the presence of the photosynthesis inhibitor DCMU and thus may be directly mediated by a light sensor. The molecular underpinnings of commitment are unknown, although models with sizer and timer mechanisms (Donnan and John) and circadian control (Goto and Johnson 1995) have been proposed.

CDKA1 and CDKB1 drive distinct cell cycle phase transitions in *Chlamydomonas*

Mutations in both *CDKA1* and *CDKB1* were identified in a screen for essential cell cycle mutants in *Chlamydomonas* (Tulin and Cross 2014). The temperature-sensitive *cdka1-1* mutant exhibits a long delay before cell division, but ultimately undergoes normal divisions. This delay

in division is accompanied by a similar delay in DNA replication. The *cdkb1-1* mutant, on the other hand, initiates DNA replication with a slight delay compared to wild type and arrests with once-replicated DNA and a single, undivided nucleus. Thus, CDKA1 and CDKB1 have distinct functions. CDKA1 acts early to promote the transition from growth to cell division and CDKB1 act later to promote mitotic events.

Most genes in *Chlamydomonas* exhibit periodicity in expression during synchronous culturing, with a strong induction of over 2000 transcripts coincident with cell division (Tulin and Cross 2015; Zones et al. 2015). Careful analysis of transcript accumulation during cell divisions revealed a large cohort of genes whose activation depends on CDKA1 (Tulin and Cross 2015). This group includes *CDKB1* and the cyclins *CYCA1* and *CYCB1*. Many transcripts in this cohort are elevated in the *cdkb1-1* mutant. Together, these results suggest that CDKA1 may initiate the cell division program in part by inducing the transcription of genes required for cell division, including *CDKB1*. CDKB1 acts later and is required for the downregulation of CDKA1-induced transcripts. This may represent a transcriptional negative feedback loop.

Organization of the thesis

Initial characterization of mutations in *CDKA1* and *CDKB1* in *Chlamydomonas* showed that CDKA1 functions early in the cell cycle to promote cell cycle initiation, and CDKB1 acts later to promote mitosis. Early results also suggested the possibility of a negative feedback loop operating between these kinases. In this thesis, we describe results from a variety of microscopic, genetic, and biochemical approaches to better understand the function and regulation of CDKA1 and CDKB1 and their putative activating cyclin subunits. We present a model based on these findings which may represent the core cell cycle control circuitry in Viridiplantae.

Chapter 2 describes the isolation of many new mutations in *CDKA1*, including many null mutations, definitively showing that *CDKA1* is an inessential gene in *Chlamydomonas* and likely all Viridiplantae, in striking contrast to the Opisthokont homolog CDK1. A null mutation in *CYCA1* is characterized, showing that, like *CDKA1*, it is also inessential but is required for timely cell cycle entry. **Chapter 3** concerns the *Chlamydomonas* B-type cyclin *CYCB1*. Mutational inactivation of *CYCB1* reveals that, like *CDKB1*, *CYCB1* is an essential gene and is required specifically for mitotic events. It is inessential for DNA replication and the initiation of cytokinesis. Sequence analysis and epistasis experiments suggest that CYCB1 is likely targeted for destruction by the APC. In **Chapter 4**, we characterize control of CDKA1 and CDKB1 abundance, localization, and associated kinase activity. We analyze their behavior in various mutant backgrounds. Key findings are that cyclin activation of CDKA1 and CDKB1 is essentially modular, CYCA1 activating CDKA1 and CYCB1 activating CDKB1. Both kinases are inhibited by the APC, likely via destruction of their activating cyclin subunits. CDKA1 and CDKB1 exhibit reciprocal regulation—CDKA1 promotes the expression of CDKB1 and CYCB1/CDKB1 inhibits CDKA1 kinase activity. These results corroborate the earlier suspicion of a negative feedback loop between the kinases. Inter-regulation between CDKA1 and CDKB1 may ensure the correct order and separate timing of their activation and thus the cell cycle events they direct. In **Chapter 5**, we describe the isolation and identification of mutations that result in synthetic lethality in *cdka1* mutants and present evidence that *cdka1* mutants are hypersensitive to the TOR-inhibitor rapamycin. We propose a mostly speculative model to explain these results which posits TOR as an activator of cell cycle progression in *Chlamydomonas* alongside CDKA1. **Chapter 6** summarizes and interprets the results of the thesis and proposes new questions and potential avenues for further exploration.

Chapter 2[†] CDKA1 and CYCA1 drive the transition from growth to cell division

This chapter first describes the design and result of a screen for cell cycle delay mutants. Many null alleles of the single copy *CDKA1* gene are isolated, implying that this gene is inessential in plants. A basic characterization of disruption mutants in *CDKA1* and *CYCA1* [the predicted primary biochemical activator of CDKA1 (see Chapter 4)] follows, showing that both are required, to different degrees, for the timely transition from the extended growth phase in *Chlamydomonas* to the division phase.

A selective genetic screen yields *cdka1* null mutations that delay but do not block the cell division cycle

A temperature-sensitive mutation in the *Chlamydomonas* CDK1 ortholog, *cdka1-1*, results in a lengthy delay in cell cycle initiation at restrictive temperature, but mutant cells eventually undergo cell division and are ultimately viable (Tulin and Cross 2014). This result suggests that CDKA1, in a rather striking contrast to its Opisthokont relatives, might not be required for DNA replication or mitosis. However, it cannot be excluded that successful completion of these events is due to partial function of *cdka1-1*, limiting claims about dispensability.

Many cell cycle mutants in *Chlamydomonas* undergo cell lysis shortly after reaching their specific arrest points (Tulin and Cross 2014). Consistent with the role of CDKA1 in promoting cell cycle initiation, cell lysis due to these mutations is extensively delayed in double mutants with the *cdka1-1* mutation (Tulin and Cross 2014), presumably due to a delay in CDKA1-dependent initiation of the defective cell cycle. We assessed whether this suppression of cell

[†]Edited from (Atkins and Cross, submitted).

lysis could provide an effective selection for new mutations in genes for cell cycle initiation. The *div19-2* mutation (which occurs in a type II DNA topoisomerase) results in a substantial loss of viability at restrictive temperature, at about the time wild type cells typically begin dividing (Figure 2.1A). Lethality may be due to chromosome breakage and nondisjunction during mitosis with tangled sister chromatids (Holm et al. 1989). Inclusion of *cdka1-1* in the *div19-2* background greatly extended viability at restrictive temperature (Fig. 2.1A). Theoretically, therefore, mutations that delay the onset of cell division can be isolated by selecting for extended viability in the *div19-2* mutant.

Indeed, a positive selection screen using the *div19-2* mutant as a genetic background allowed us to identify mutations that delay the cell cycle (Fig 2.1B). Many such *top2* death delay (*tdd*) mutants are slow growing, and thus probably indirectly delay division due to the presumed cell size requirement for commitment to cell cycle entry (reviewed in Cross and Umen 2015). Some of the mutants, however, grow to a very large size, mimicking the behavior of the *cdka1-1* mutant at restrictive temperature (Fig. 2.1C). All these large-arresting mutants have mutations in *CDKA1* (Fig. 2.1D).

Many of these *cdka1* mutations are null (early nonsense, frameshift, indels, etc.), indicating that *CDKA1* is inessential for viability (Table 2.1). *CDKA1* is also inessential in *Arabidopsis* (Nowack et al. 2012). We thus infer that the CDK1 ortholog is not an essential gene in Viridiplantae, unlike in the Opisthokonts.

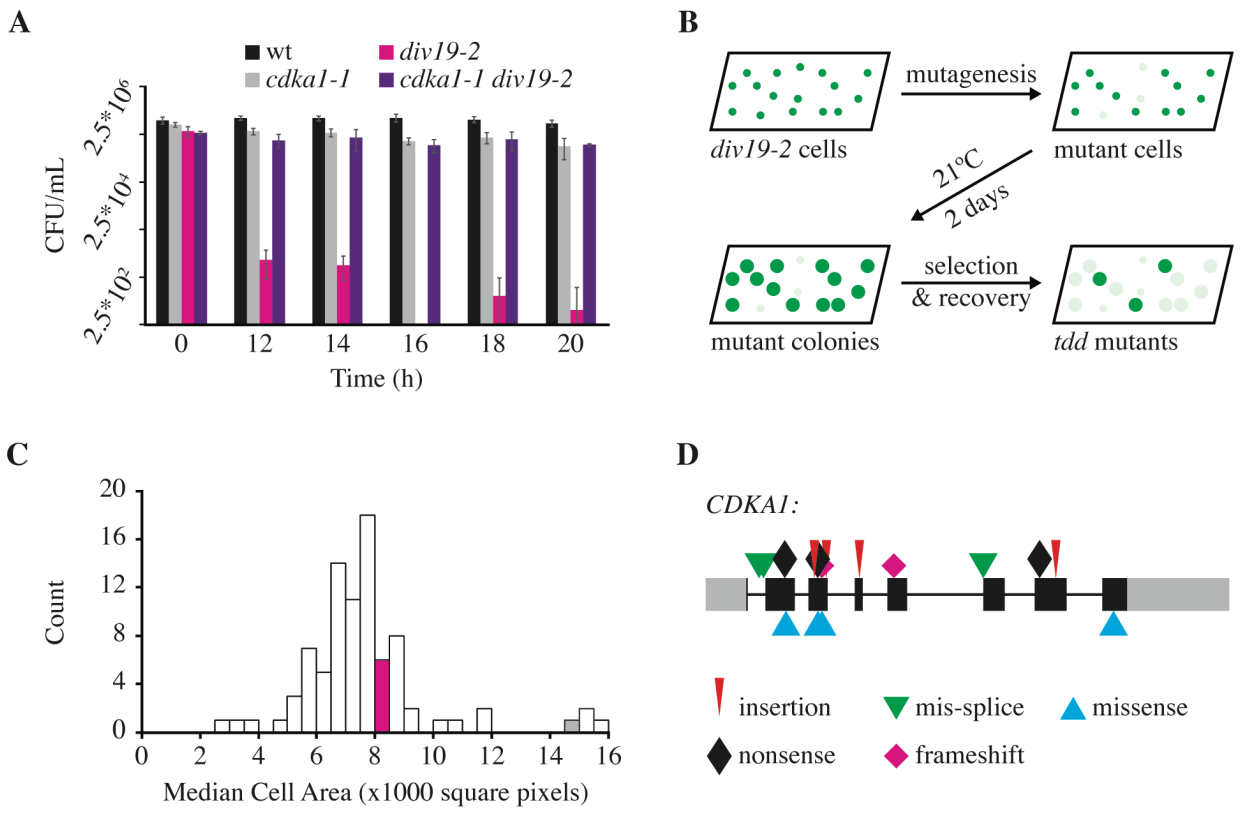

Figure 2.1 Death delay screen and mutant characterization.

(**A**) Viability of wild type, *cdka1-1*, *div19-2*, and *cdka1-1 div19-2* after exposure to 33°C for different periods of time. Error bars indiate standard deviation of four technical replicates. (**B**) Schematic of death delay screen. (**C**) Distribution of median cell area for a representative set of *tdd* mutants after 20h at 33°C. The magenta and gray bars indicate cell area of the *div19-2* and *cdka1-1 div19-2* mutants, respectively. (**D**) Mutations in *CDKA1* in large-cell arresting *tdd* mutants (>12,000 square pixels). Gray boxes indicate 5' and 3' untranslated regions. Black boxes indicate exons.

Table 2.1. Mutations in *CDKA1* in UV mutagenized *tdd* mutants.

Mutant	Mutation[a] in CDKA1[b]	Result[a]
tdd12	g.467A>T	p.Lys34>Ter
tdd11	g.715A>T	p.Lys88>Ter
tdd2	g.2098_2099CC>AT	p.Phe217>Leu, Gln218>Ter
tdd13	g.373_374GC>TT	splice-site
tdd17	g.376_377GT>TC	splice-site
tdd20	g.1746A>T	splice-site
tdd25	g.(715_719)insA	frameshift
tdd5	g.1163_1181delinsCCGCG	frameshift
tdd15	g.531T>C	p.Leu55>Pro
tdd24	g.712_713CT>TA	p.Leu87>Tyr
tdd18	g.713T>G	p.Leu87>Arg
tdd21	g.2527_2528CT>TA	p.Tyr286>Asn

[a]Mutation nomenclature is as recommended by the Human Genome Variation Society.

[b]Cre10.g465900 (Phytozome v5.5).

Both *CDKA1* and *CYCA1* are inessential for cell division, but are required for timely transition from the growth phase to cell division

Chlamydomonas has four D-type cyclins (*CYCD1-4*), one A-type cyclin (*CYCA1*), one B-type cyclin (*CYCB1*), and one 'hybrid' A/B-type cyclin (*CYCAB1*) (Bisova et al. 2005). We obtained a putative *cyca1Δ* disruption mutant from a collection of insertional mutants (Li et al. 2016a) maintained by the Chlamydomonas Library Project (CLiP, http://www.chlamylibrary.org). This disruption harbors an insertion of the paromomycin resistance cassette within sequence well conserved in cyclins. We therefore assume the mutant is null for *CYCA1* function. The *cyca1Δ* mutant is viable at both low and high temperature (Figure 2.2), but exhibits a delay in cell cycle entry, similar to though less extreme than that observed with the *cdka1Δ* disruption. We quantified this delay by time-lapse microscopy, in both single and double disruption mutants of *cyca1Δ* and *cdka1Δ* (Fig. 2.3; Table 2.2).

Wild type cells required, on average, 11.4h incubation before the first division cycle. The subsequent 2-3 division cycles were rapid, on average 0.6h each. Disruptions in both *cyca1Δ* and *cdka1Δ* caused long delays in time to the first division cycle (average increases of 2.3h and 5.3h, respectively), and more modest delays in subsequent cycles (average increases of 0.2 and 0.4h, respectively). *cyca1Δ cdka1Δ* double mutants were somewhat more severely affected than *cdka1Δ* single mutants. In addition, a substantial though variable proportion of *cdka1Δ* and *cyca1Δ cdka1Δ* double mutant cells grew very large but failed to initiate any divisions even after 35h (Fig. 2.3B, Table 2.2).

The deleterious effect of *cdka1Δ* disruption is most readily observed at 33ºC; no appreciable defect in growth or colony formation is observed at lower temperatures (Fig. 2.2). We do not understand the basis for this temperature-sensitivity of null alleles.

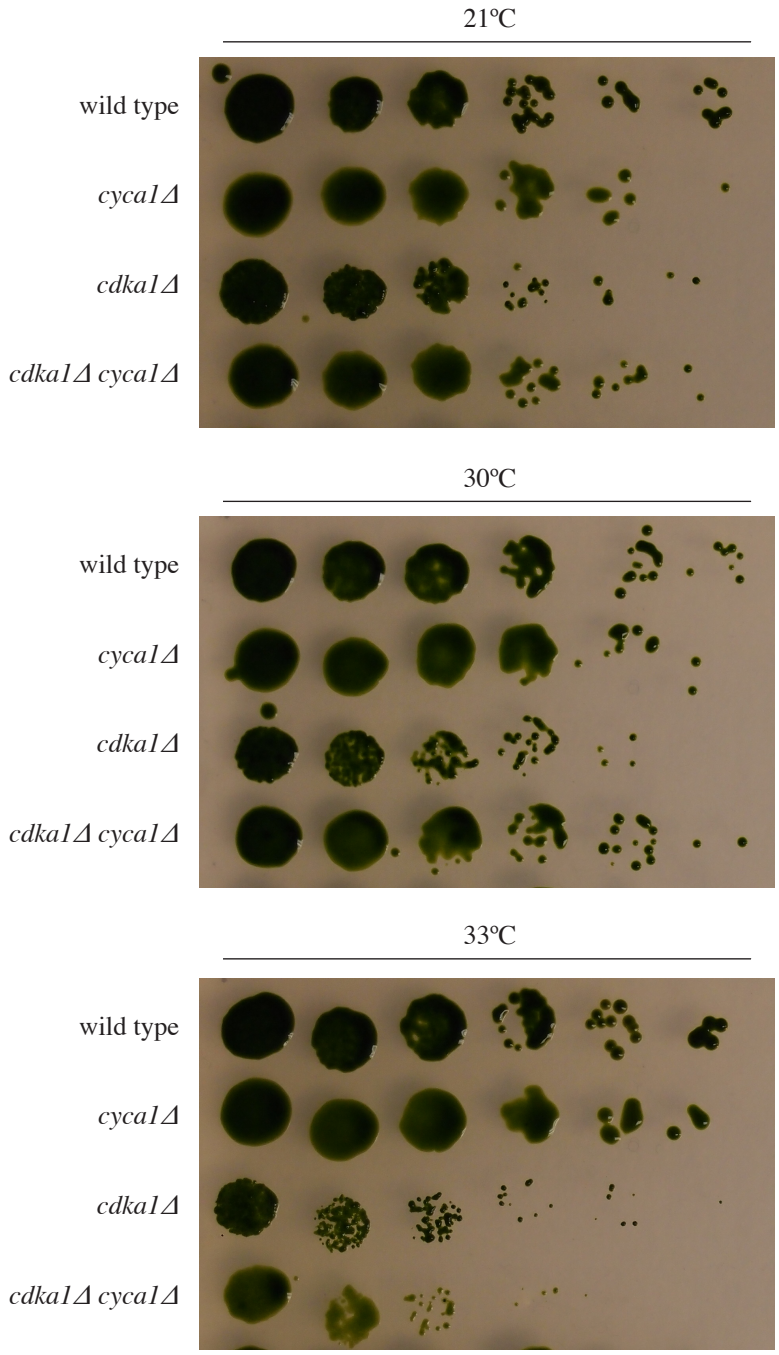

Figure 2.2 Temperature-sensitivity of the *cdka1Δ* mutant.

Both the *cdka1Δ* and *cyca1Δ cdka1Δ* mutants, but not the *cyca1Δ* mutant, exhibit a reduction in viability and form smaller colonies at 33ºC compared to 21ºC. These defects are not readily observed at 30ºC. These strains are from a single tetratype tetrad; another such tetrad exhibits similar behavior.

Fig. 2.3 Delay of cell division in *cdka1Δ* and *cyca1Δ* mutants.

(A) Montages of time-lapse microscopy. The first and last images in each montage are taken immediately after plating and after 35h exposure to 33ºC, respectively. Intervening images are taken from 10h to 22h at 0.5h intervals. Magenta arrows indicate first divisions. **(B)** Some *cdka1Δ* and *cyca1Δ cdka1Δ* cells grow very large, but fail to divide even after 35h (quantified in Table 2.2). **(C, D)** Time to first division (C) and time between divisions following the first division (D) in wild type, *cyca1Δ*, *cdka1Δ*, and *cyca1Δ cdka1Δ*. Red circles and bars indicate mean and standard deviation, respectively. Data are pooled results from two independent segregants of each genotype.

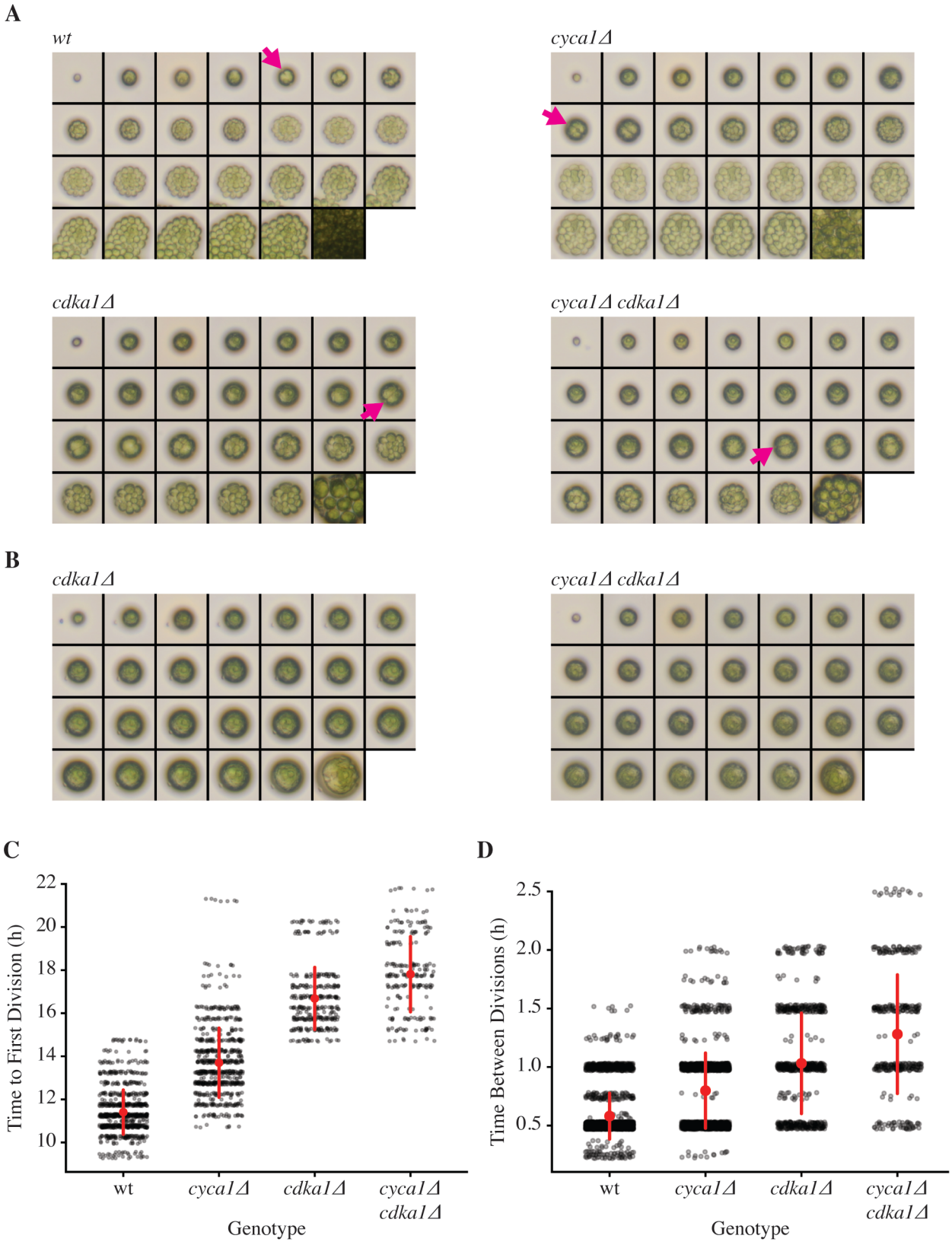
A
wt
cyca1Δ
cdka1Δ
cyca1Δ cdka1Δ
B
cdka1Δ
cyca1Δ cdka1Δ
C
Time to First Division (h)
22
20
18
16
14
12
10
wt
cyca1Δ
cdka1Δ
cyca1Δ cdka1Δ
Genotype
D
Time Between Divisions (h)
2.5
2.0
1.5
1.0
0.5
wt
cyca1Δ
cdka1Δ
cyca1Δ cdka1Δ
Genotype

Table 2.2 Summary statistics for cell cycle delay in the *cyca1Δ*, *cdka1Δ*, and *cyca1Δ cdka1Δ* mutants.

Genotype	Number of Cells that Divided[a]	Time to First Division[b]	Time b/t Divisions[c]
wt	989/997(0.99)	11.4±1.0 (n=989)	0.6±0.2 (n=3065)
cyca1Δ	784/798(0.98)	13.7±1.6 (n=784)	0.8±0.3 (n=1883)
cdka1Δ	371/476(0.78)	16.7±2.1 (n=371)	1.0±0.4 (n=883)
cyca1Δ cdka1Δ	231/560(0.41)	17.8±1.7 (n=231)	1.3±0.5 (n=399)

[a]Number of cells that divided before 35h/number counted(fraction).

[b]Mean time to first division, plus or minus standard deviation. Units are hours.

[c]Mean time between subsequent divisions, plus or minus standard deviation. Units are hours.

Previous work indicates that the delay in the first cell cycle in the *cdka1-1* mutant occurs before DNA replication (Tulin and Cross 2014). We do not know what cell cycle phase or phases are elongated in subsequent divisions.

Summary

In a screen for cell cycle delay mutants, we isolated many mutations in *CDKA1*, including many null mutations. Thus, *CDKA1* is not an essential gene in *Chlamydomonas*. Since *CDKA1* is also inessential for viability in *Arabidopsis*, we conclude that the CDK1 ortholog is likely inessential in all green plants. This is a rather remarkable result given the absolute requirement for CDK1 orthologs for carrying out mitosis in the Opisthokonts (see Introduction). Another result of this screen, which is perhaps meaningful, is that the only mutations isolated which caused cell cycle delay with unencumbered growth are in *CDKA1*. Because we know that inactivation of CDKA1 causes cell cycle delay, we expected to also isolate mutations in positive regulators of CDKA1 in the death delay screen. CDKs are dependent on the direct binding of regulatory cyclins for enzymatic activity (Connell-Crowley et al. 1993; Jeffrey et al. 1995). The fact that no cyclins were isolated in this screen suggests that any cyclin activators of CDKA1, assuming they exist, are either redundant or pleiotropic.

One model to explain this result is that CYCA1 is the primary activator of CDKA1 (see Ch. 4), but that other cyclins can activate CDKA1 in the absence of CYCA1. Genetic results are consistent with this model; we find that disruptions in both *CYCA1* and *CDKA1* result in a lengthy delay in the transition from the growth phase to cell division, although this delay is less severe in the *cyca1Δ* mutant than in the *cdka1Δ* mutant. The fact that the cell cycle of the *cyca1Δ cdka1Δ* mutant is more delayed than that of *cdka1Δ* suggests that CYCA1 also has a

CDKA1-independent capacity to promote cell cycle entry. Whether they directly interact or otherwise, both CYCA1 and CDKA1 are required for the appropriate timing of the growth to division transition in the *Chlamydomonas* cell cycle, but neither are essential for DNA replication or mitosis. This sets them apart from their counterparts in the Opisthokonts and suggests a divergence of function in the plant lineage among the CDKs and cyclins.

Chapter 3[‡] CYCB1 is required for spindle formation and is likely an APC target

Here we demonstrate the critical role of the only *Chlamydomonas* B-type cyclin *CYCB1* for mitosis as well as a nonessential role in DNA replication. Epistasis experiments with *cycb1* and *cdc27-6* mutants and primary sequence analysis suggest that CYCB1 is probably targeted for destruction by the anaphase promoting complex.

CYCB1 is required for mitotic spindle formation and plays some role in DNA replication

The *Chlamydomonas* genome encodes a single B-type cyclin—*CYCB1* (Cross and Umen 2015). The *cycb1-5* mutation (p.Glu325>Lys; Tulin and Cross, unpublished) results in lethality and a complete cell cycle block at restrictive temperature. Synchronized cultures of *cycb1-5* successfully initiate DNA replication, but with a delay compared to wild type (Fig. 3.1A). The mutant successfully completes one round of DNA replication, but arrests with 2C DNA content, failing to initiate further cycles of DNA replication and mitosis within the mother cell wall, as seen in wild type (Fig. 3.1A). Arrested cells form indentations at the periphery that are lined with microtubules, executing what seems to be an aberrant initiation of cytokinesis (Fig. 3.1B). Mitotic spindles are never observed in this mutant at restrictive temperature (Fig. 3.1B, Table 3.1). This phenotype recapitulates the behavior of the *cdkb1-1* mutant (Tulin and Cross 2014). Thus, like CDKB1, CYCB1 is specifically required for mitotic spindle formation but not for DNA replication or initiation of cytokinesis.

Since initiation of DNA replication is delayed to some degree in the *cycb1-5* mutant, CYCB1 may be a significant activator of DNA replication. Other cyclins may drive DNA

[‡]Edited from (Atkins and Cross, submitted).

Fig. 3.1 Dependence of DNA replication and spindle formation on CYCB1 and the APC.

Cells of the indicated genotype were blocked by nitrogen deprivation and released at 33ºC. **(A)** DNA content analyzed by flow cytometry. Wild type cells undergo multiple rounds of DNA synthesis and mitosis within the mother cell wall, producing cell clusters with 2, 4, 8, or 16C DNA content, before hatching to produce small 1C newborn cells (apparent DNA content of these cells compared to pre-division 1C cells is shifted to the left [Tulin and Cross 2014]). **(B)** Immunofluorescence images from a separate experiment in which cells were collected 13.5h after release from nitrogen deprivation. At this time, wild type cells had almost all divided and hatched to produce small flagellated progeny. Nearly all *cdc27-6* cells contained single bipolar spindles, indicating a block in the first metaphase after release. *cycb1-5* and *cycb1-5 cdc27-6* cells are large, reflecting cell cycle arrest (compare to size of post-division wild type cells), but uniformly lack spindles. Microtubule staining in these mutants is instead concentrated at incipient cytokinetic furrows, reflecting a probable structural role of microtubules in cytokinesis (Ehler and Dutcher 1998, Tulin and Cross 2014). Scale bars are 10μm. Quantification of phenotypes is found in Table 3.1

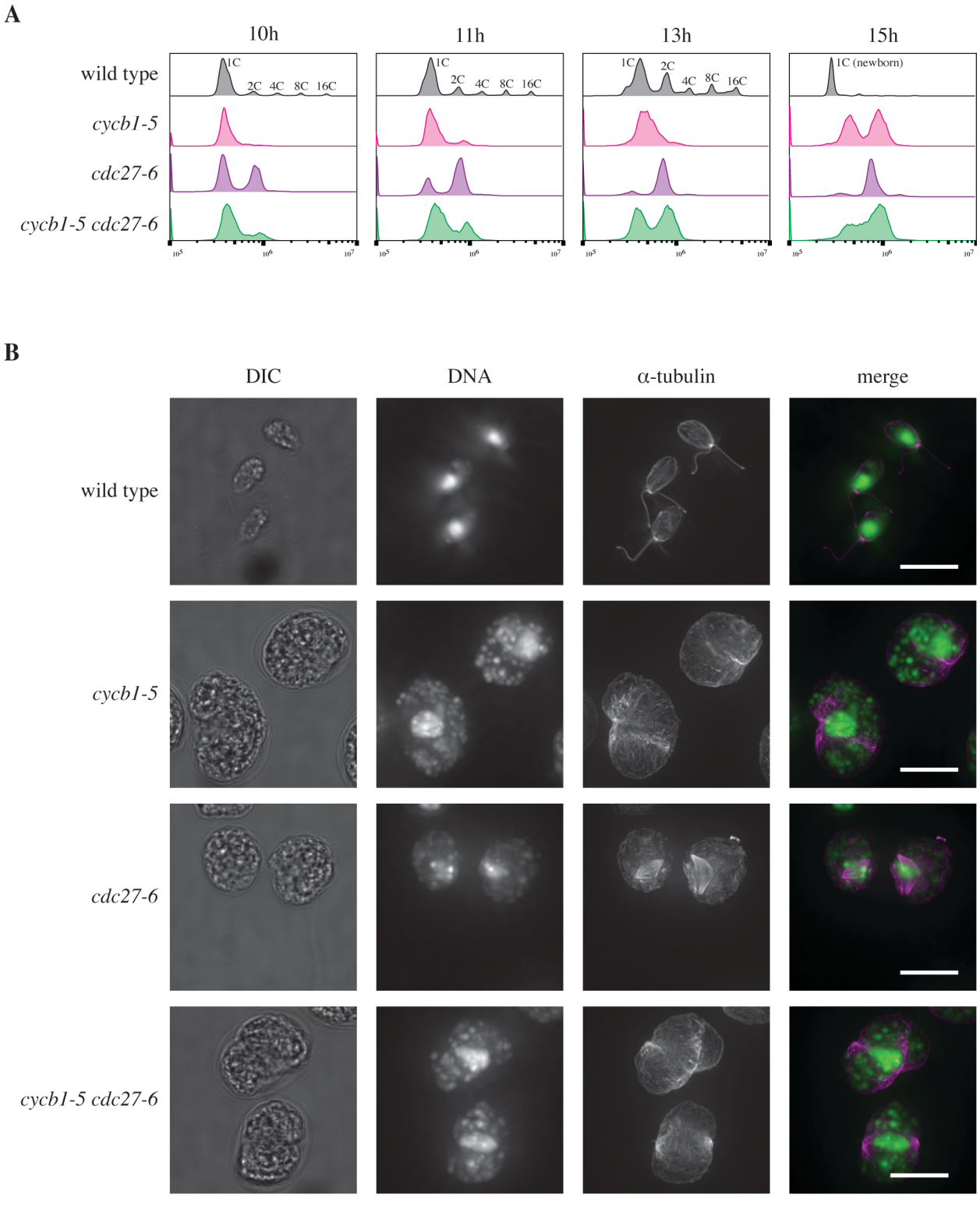
A
10h
11h
13h
15h
wild type
cycb1-5
cdc27-6
cycb1-5 cdc27-6
1C
2C
4C
8C
16C
1C (newborn)
B
DIC
DNA
α-tubulin
merge
wild type
cycb1-5
cdc27-6
cycb1-5 cdc27-6

Table 3.1 Formation of mitotic spindles and cytokinetic furrows in the *cycb1*, *cdc27*, and *cycb1 cdc27* mutants.

	Spindles	+	-	-	-
	Cytokinetic Furrows	-	+	-	-
Genotype[a]	Flagella	-	-	+	-
wt (n=241)		0.00	0.07	0.91	0.02
cycb1-5 (n=242)		0.00	0.42	0.42	0.16
cdc27-6 (n=206)		0.70	0.06	0.12	0.12
cycb1-5 cdc27-6 (n=207)		0.00	0.78	0.11	0.11

[a]For each genotype, approximately 100 cells were scored in two independent segregants. Frequency data are pooled results.

replication in the absence of CYCB1, thus accounting for its inessentiality for this process. Indeed, the *cyca1Δ cycb1-5* mutant fails to initiate DNA replication and forms many fewer incipient cytokinetic furrows (Atkins and Cross, forthcoming). Thus, in the absence of CYCB1, CYCA1 is required to promote DNA replication and for efficient initiation of cytokinesis. Similarly, DNA replication and cytokinetic initiation in the *cdkb1-1* mutant is dependent on CDKA1 (Tulin and Cross 2014), suggesting that cell cycle initiation is largely under specific control of CDKA1 and CDKB1, activated (in some combination) by CYCA1 and CYCB1.

Primary sequence and epistasis experiments suggest CYCB1 is probably an APC target

Mutants in the *Chlamydomonas* APC components APC6 and CDC27/APC3 exhibit limited mitotic progression, arresting with one or two nuclei and with 2C or 4C DNA content (Tulin and Cross 2014), probably due to partial APC function retained in these mutants at restrictive temperature. Indeed, we now find that the *cdc27-6* allele (p.Met884>Ile, Gly885>Ser) causes a uniform arrest with once-replicated DNA and metaphase spindles (Fig. 3A, B; Table 3.1). Arrested cells lack the incipient division structures seen in the *cycb1-5* mutant (Fig. 3.1B). This result demonstrates the absolute essentially of the APC for anaphase in *Chlamydomonas*.

The *cycb1-5* mutant arrests without spindles and with aborted division furrows, and the *cdc27-6* mutant arrests with the opposite phenotype. Double mutants show that *cycb1-5* is strongly epistatic to *cdc27-6*—double mutants lack mitotic spindles, and cells arrest with aberrant cytokinetic furrows (Fig. 3.1B, Table 3.1). Essentially similar results are observed with the *cdkb1-1 cdc27-6* double mutant (Atkins and Cross, forthcoming). These results indicate that the late mitotic arrest phenotype of *cdc27-6* is due to the activity of CYCB1 and CDKB1.

In Opisthokonts, the APC ubiquitinates various proteins, labeling them for destruction by the proteasome. Two of these ubiquitination targets are essential targets: the mitotic cyclins and securin, an anaphase inhibitor that maintains sister chromatid cohesion (Thornton and Toczyski 2003). The APC targets proteins harboring the destruction box motif (Glotzer et al. 1991; King et al. 1996; He et al. 2013). The recognition of this motif is conserved in plants, since APC mutants slow the degradation of a destruction box reporter in *Arabidopsis* (Kwee and Sundaresan 2003; Wang et al. 2012). Of the *Chlamydomonas* cyclins, only cyclin A and cyclin B contain canonical destruction boxes (Fig. 3.2B). If CYCB1 is an important target of the APC in *Chlamydomonas*, this could account for epistasis of *cycb1-5* to *cdc27-6*, since mutational inactivation of CYCB1 could bypass the APC requirement for cyclin degradation. Alternatively, it could be that CYCB1 is required for activation of the APC. In animals, mitotic cyclin-CDKs phosphorylate the APC and thus enable binding of the APC-activator CDC20 (Qiao et al. 2016). These two possibilities are not mutually exclusive.

Figure 3.2[§] Overall sequence and destruction box alignments for CYCA1 and CYCB1.

(A) Best reciprocal BLAST analysis (Remm et al. 2001) identifies *Chlamydomonas reinhardtii* (Cre) CYCA1 and *Arabidopsis thaliana* (Ath) CYCA2;4 as an orthologous pair. Cre CYCB1 and Ath CYCB2;4 also form an orthologous pair. *Chlamydomonas* CYCA1 has better alignment to all 10 *Arabidopsis* cyclin A proteins than to any of the 14 cyclin B proteins; the reverse is true for *Chlamydomonas* CYCB1. BLAST scores are indicated for all comparisons. These results imply divergence of cyclin A and cyclin B before the divergence of *Chlamydomonas* and *Arabidopsis*. Since the cyclin A/cyclin B divergence is also observed in animals, the cyclin A/cyclin B split predates the divergence of animals from plants. Notably, cyclin A has been lost in all fungi (Cross et al. 2011), and replaced by a radiation of cyclin B genes (Archambault et al. 2005). **(B)** Alignment of candidate destruction box (DB) sequences from *Chlamydomonas* and *Arabidopsis* cyclins to the consensus sequence of (He et al., 2013). **(C)** Distribution of number of matches to this consensus for candidate DBs across the *Chlamydomonas* proteome (searching only in the N-terminal 100 amino acids, the usual location for DBs). CYCB1, with eight matches to the consensus, has more matches than any other protein; the next-highest (22 proteins) have six matches. CYCA1 is the only predicted protein with two candidate DBs with six matches; intriguingly, *Arabidopsis* CYCA2;4 also has two candidate DBs. Overall, although it is difficult to assign a precise p-value to these alignments to the DB consensus, it is overwhelmingly likely that these alignments represent deep conservation of functional sequence.

[§] Sequence analysis performed by F. Cross.

A

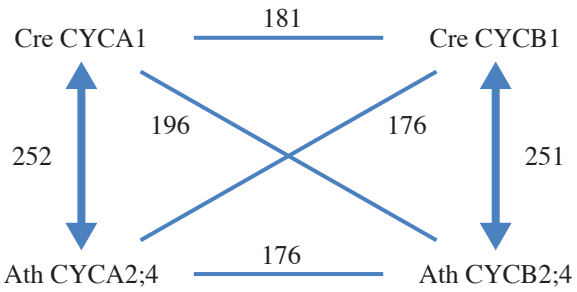

B Consensus destruction box

```
          L
      P   EIN
    RKALGDVSN

40 RRALGDLSN Cre CYCB1

48 RAMLGDLTN Cre CYCA1
67 RKALSALNA

34 RRALSNINK Ath CYCB2;4

55 RTALDEKKA Ath CYCA2;4
71 RAVLKDITN
```

C

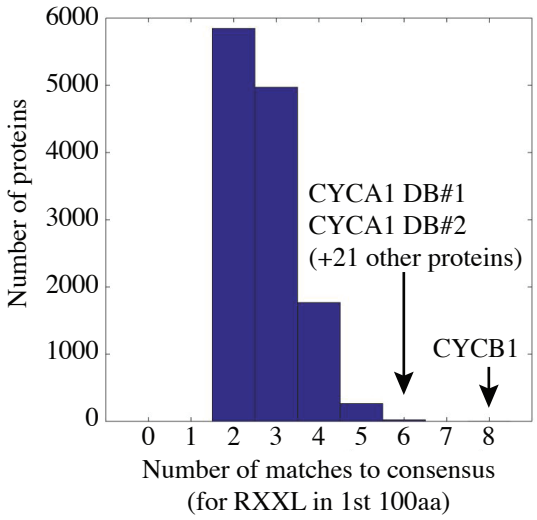

Summary

Using the simplified model system *Chlamydomonas*, which has only one B-type cyclin, we demonstrate that CYCB1 controls key cell cycle events. It is required for timely initiation of DNA replication and is absolutely required for the formation of the mitotic spindle. *Chlamydomonas* cyclin B is homologous to the family of B-type cyclins in *Arabidopsis* (Fig. 3.2A) and thus may be a good model for understanding the ancestral function of this group before its radiation into various paralogs in different land plant lineages.

Sequence analysis shows that CYCB1 harbors a canonical destruction box, a motif that is recognized by the APC. Thus, CYCB1 is a good candidate for APC-dependent destruction in *Chlamydomonas*. Supporting this notion, *cycb1-5* is strongly epistatic to the APC mutant *cdc27-6*, consistent with mutational inactivation of CYCB1 mimicking APC-dependent destruction. Other explanations, including CYCB1-dependent activation of the APC, are possible and are not mutually exclusive with APC-dependent destruction of CYCB1.

Chapter 4[**] Abundance, localization, and control of CDKA1/B1 kinase activity

To better understand the behavior and regulation of the key cell cycle regulators CDKA1 and CDKB1, we made strains expressing these kinases with a translational fusion to the fluorescent protein mCherry. Both CDKA1 and CDKB1 are found in the nucleus, and CDKA1 additionally localizes to the basal body region. A moderate induction of CDKA1 and a dramatic induction of CDKB1 is observed during cell divisions, accompanied by coincident induction of CDK-associated kinase activity. Kinase activity of CDKA1 depends on CYCA1 and not CYCB1, whereas CDKB1 kinase activity depends on CYCB1 and not CYCA1. The activity of both of these kinases is inhibited by the APC. CDKA1 induction of CDKB1/CYCB1 expression and subsequent CDKB1/CYCB1 inhibition of CDKA1 kinase activity represents a possible negative feedback loop that may ensure sequential control of cell cycle events by these two kinases.

Functional fluorescence tagging of *CDKA1* and *CDKB1*

We constructed strains expressing C-terminally tagged *CDKA1-mCherry* and *CDKB1-mCherry* transgenes. Native sequence, including the promoter, terminator, and all endogenous introns were included in the mCherry-tagged constructs (Fig. 4.1A) to increase the likelihood that expression levels and regulation of the transgene are similar to the endogenous gene.

mCherry-tagged constructs were transformed into temperature-sensitive mutants that depend on functional *CDKA1* or *CDKB1* at restrictive temperature. For *CDKA1*, we used a mutant background where *CDKA1* is essential at high temperature. The *csl89-1* mutation was isolated in a screen for enhancers of *cdka1-1* (see Ch. 5). The mutation inactivates a predicted

[**]Edited from (Atkins and Cross, submitted).

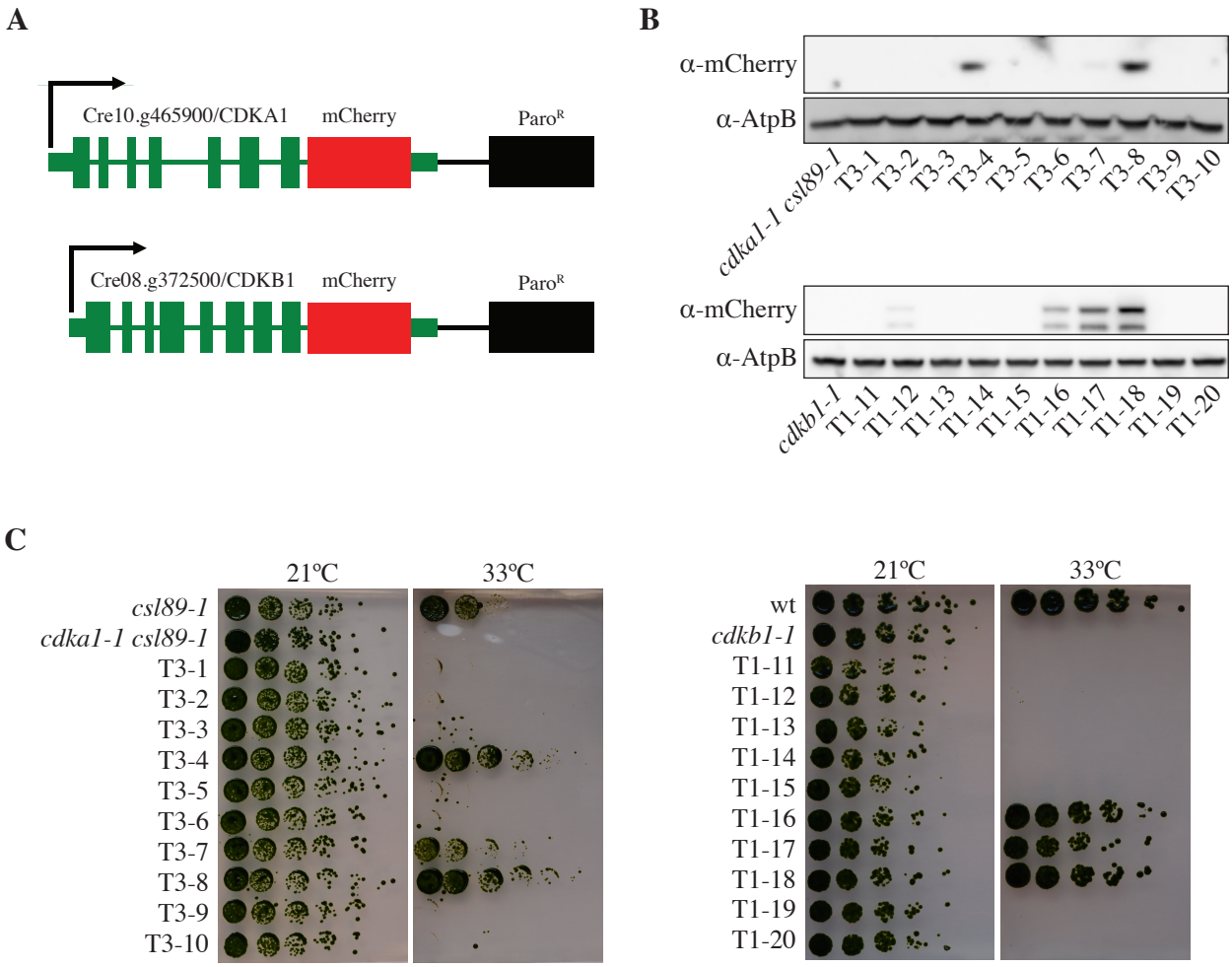

Figure 4.1 Generation of functional mCherry-tagged *CDKA1* and *CDKB1*.

(A) Plasmids used for transformation. Native sequence, including promoter, terminator, and introns are used for both *CDKA1* and *CDKB1*. Sequence encoding mCherry is added to the C-terminus after a 3x GGGGS linker sequence. Paromomycin is used to select for transformants. **(B)** Western blot showing expression of the tagged CDK transgenes in random transformants. AtpB is used as a loading control. **(C)** Complementation of temperature-sensitivity of *cdka1-1 csl89-1* and *cdkb1-1* in the transformants from (B).

tRNA methyltransferase (Cre05.g244236). For unknown reasons, *csl89-1* mutants are viable at high temperature in a *CDKA1* background but inviable in a *cdka1* background. This provides a genetic background for selection of functional tagged *CDKA1* transgene insertions. For *CDKB1*, we used the ts lethal *cdkb1-1* mutant (Tulin and Cross 2014).

Viability of transformants was tested at 33ºC. For both constructs, expression of the mCherry-tagged CDKs correlated with complementation of the ts mutations (Fig. 4.1B, C). Overall, we have noted no significant defects in cell cycle progression upon complementation by the transgenes. Functional *CDKA1-mCherry* insertions isolated in the *cdka1-1 csl89-1* background were crossed away from *csl89-1* and were found to complement the cell cycle delay phenotype of *cdka1-1* at 33ºC.

CDKA1 localizes to nuclei and possibly basal bodies

CDKA1 protein is present throughout the cell cycle, but levels increase during the multiple division phase (Fig. 4.2A, C), reflecting CDKA1 RNA abundance (Bisova et al. 2005; Tulin and Cross 2015; Zones et al. 2015). Subcellular localization of CDKA1-mCherry was determined by confocal microscopy of live, cycling cells. Nuclei were visualized using a nuclear-targeted *ble-GFP* (Li et al. 2016b). In newborn cells, CDKA1 is enriched in nuclei, and in focused puncta adjacent to the nuclei at the apical end of the cell body (Fig. 4.3A), approximately at the base of the flagella. CDKA1 and CYCA1 were previously identified by mass spectrometry as components of the ciliary transition zone, between the basal bodies and the flagellum (Diener et al. 2015). In dividing cells lacking flagella, CDKA1 is also localized to focused puncta (Fig. 4.3B). The ciliary cycle is integrated in a complex manner with the mitotic cycle, since basal bodies detach from flagella and may serve as spindle pole bodies during mitosis (Dutcher and

Fig. 4.2 Regulation of CDKA1 abundance and associated kinase activity.

Strains of the indicated genotypes were synchronized by nitrogen deprivation and released at 33ºC. **(A)** Western blot detection of CDKA1-mCherry. **(B)** Kinase activity of immunoprecipitated CDKA1-mCherry against histone H1. **(C)** Quantification of (A), (B), and fraction of cells with ≥2C DNA content as determined by flow cytometry. **(D, E)** Cyclin dependence of CDKA1-associated kinase activity. See also Fig. 4.8A. **(F, G)** CDKB1 and APC negatively regulate CDKA1-associated kinase activity.

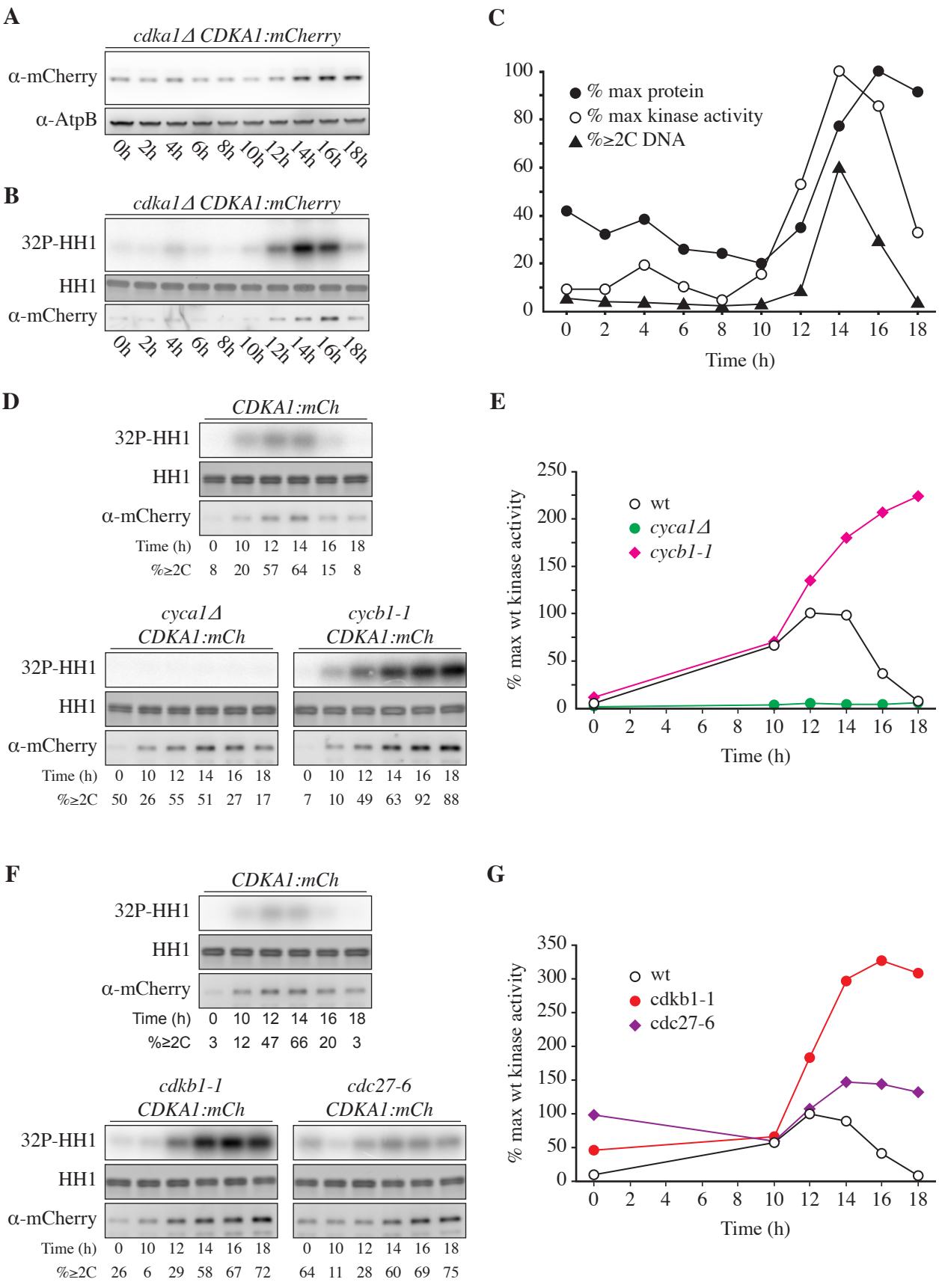
A
cdka1Δ CDKA1:mCherry
α-mCherry
α-AtpB
0h 2h 4h 6h 8h 10h 12h 14h 16h 18h
B
cdka1Δ CDKA1:mCherry
32P-HH1
HH1
α-mCherry
0h 2h 4h 6h 8h 10h 12h 14h 16h 18h
C
% max protein
% max kinase activity
%≥2C DNA
Time (h)
D
CDKA1:mCh
32P-HH1
HH1
α-mCherry
Time (h) 0 10 12 14 16 18
%≥2C 8 20 57 64 15 8
cyca1Δ CDKA1:mCh
cycb1-1 CDKA1:mCh
Time (h) 0 10 12 14 16 18 0 10 12 14 16 18
%≥2C 50 26 55 51 27 17 7 10 49 63 92 88
E
wt
cyca1Δ
cycb1-1
% max wt kinase activity
Time (h)
F
CDKA1:mCh
Time (h) 0 10 12 14 16 18
%≥2C 3 12 47 66 20 3
cdkb1-1 CDKA1:mCh
cdc27-6 CDKA1:mCh
Time (h) 0 10 12 14 16 18 0 10 12 14 16 18
%≥2C 26 6 29 58 67 72 64 11 28 60 69 75
G
wt
cdkb1-1
cdc27-6
% max wt kinase activity
Time (h)

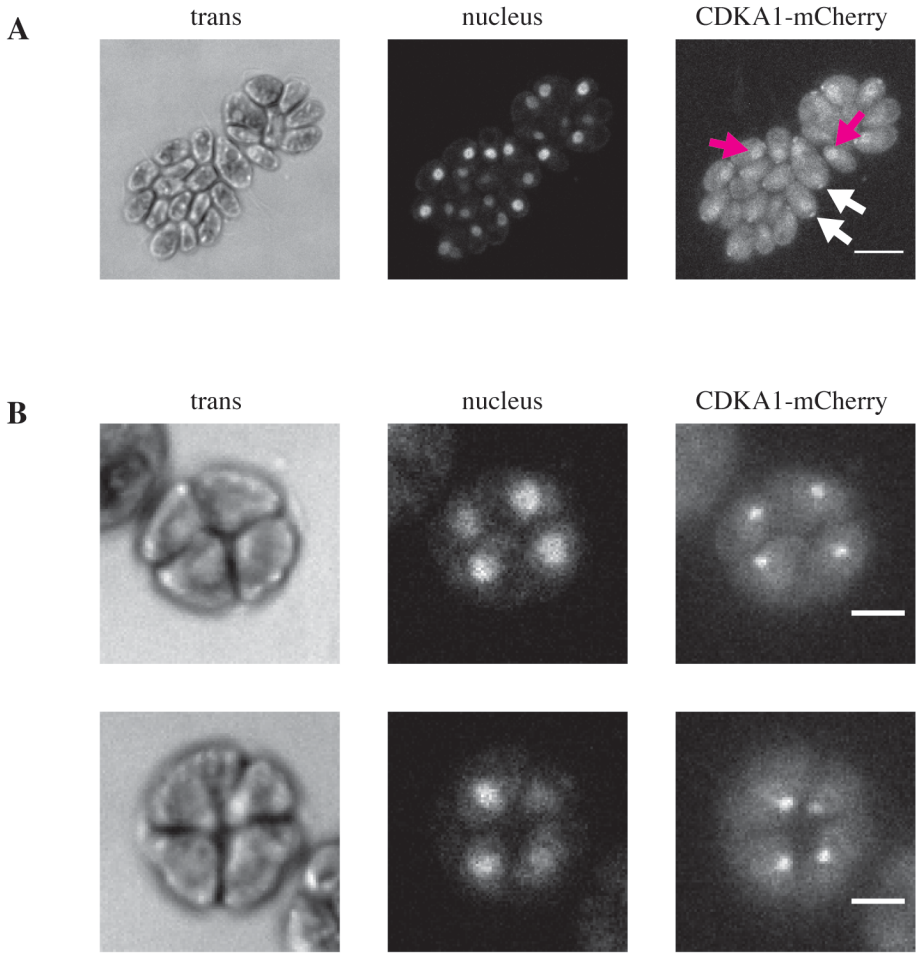

Fig. 4.3 CDKA1 is localized to the nucleus and the base of the flagella.

Confocal micrographs from a population of live, cycling *cdka1Δ CDKA1-mCherry*. All images are average intensity z-projections. Contrast is adjusted separately for each image for clarity, so intensities should not be compared across images. **(A)** In newborn cells, CDKA1 is found in nuclei (magenta arrows) and also in small puncta at the apical end of the cell body (white arrows), possibly at the base of the flagella. Scale bar is 10μm. **(B)** In dividing cells, CDKA1 is primarily found in small puncta. Scale bars are 5μm.

O'Toole 2016). We speculate that CDKA1-CYCA1 may directly regulate early steps in this process.

CDKB1 is a nuclear protein present specifically during cell divisions

CDKB1 is essentially absent during the extended growth period, is strongly induced coincident with the onset of cell division, and is degraded as cells exit the cell cycle (Fig. 4.4A, B), reflecting CDKB1 RNA abundance (Bisova et al. 2005; Tulin and Cross 2015; Zones et al. 2015). In live cell confocal microscopy, newborn cells show no detectable CDKB1 (Fig. 4.5A). After a period of cell growth, CDKB1 is detectable, with predominantly nuclear localization through multiple division cycles (Fig. 4.5B-E). When cells have completed their final divisions, CDKB1 is no longer detectable (Fig. 4.5F), suggesting rapid degradation before cells enter the next growth phase.

We have so far been unable to reliably detect CDKB1 by live-cell timelapse imaging, so we do not know whether CDKB1 is degraded during each division that takes place within the mother cell wall or only after the terminal division prior to hatching. Analysis of CDKB1 levels in cell clusters with varying numbers of nuclei (Fig. 4.5G) shows variable signal but no clearly bimodal distribution (as would be expected in the case of a long period of CDKB1 instability).

The *cdka1Δ* mutant exhibits considerably delayed cell division (see Ch. 2). Nuclear CDKB1 is not detectable in this mutant until cells become very large and begin cell division, presumably long after wild type cells accumulate CDKB1 during cell divisions that begin at a much smaller cell size (Fig. 4.6). This is consistent with the finding that CDKA1 is required for efficient accumulation of CDKB1 RNA (Tulin and Cross 2014). A similar induction of the CDKB family by CDKA1 has been proposed in *Arabidopsis* (Nowack et al. 2012).

Fig. 4.4 Regulation of CDKB1 abundance and associated kinase activity

Strains of the indicated genotypes were synchronized by nitrogen deprivation and released at 33ºC. **(A)** Western blot detection of CDKB1-mCherry. **(B)** Quantification of (A), and fraction of cells with ≥2C DNA content as determined by flow cytometry. **(C, D)** Cyclin dependence of CDKB1-associated kinase activity. See also Fig. 4.8B. **(E, F)** APC negatively regulates CDKB1-associated kinase activity.

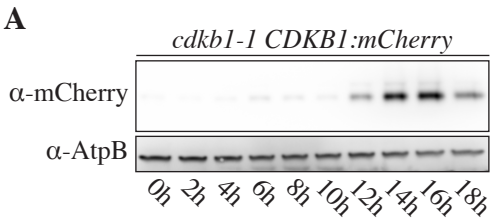
A
cdkb1-1 CDKB1:mCherry
α-mCherry
α-AtpB
0h 2h 4h 6h 8h 10h 12h 14h 16h 18h

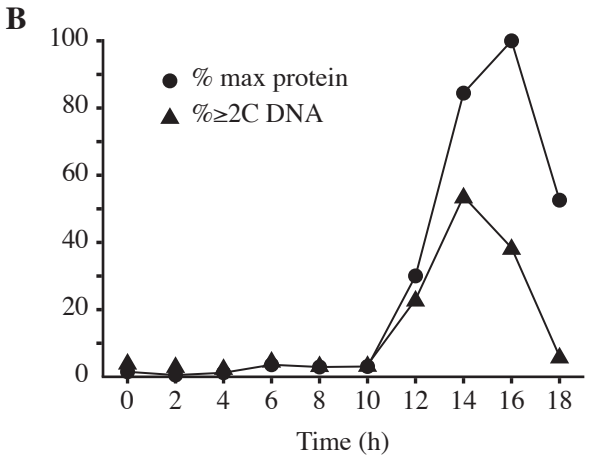
B
% max protein
%≥2C DNA
Time (h)

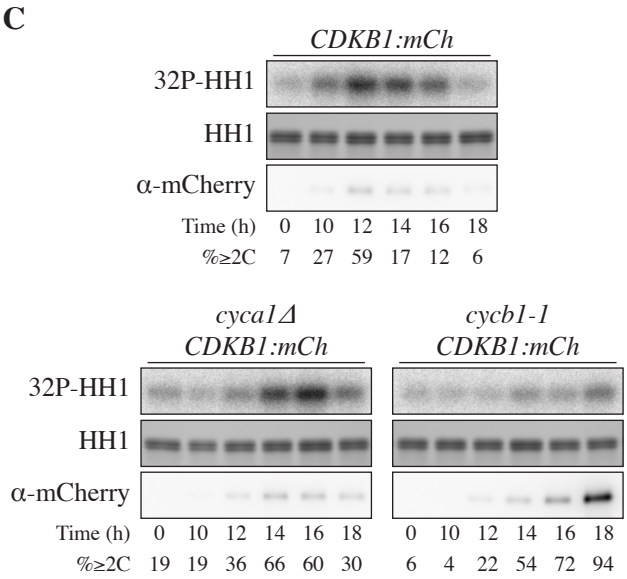
C
CDKB1:mCh
32P-HH1
HH1
α-mCherry
Time (h) 0 10 12 14 16 18
%≥2C 7 27 59 17 12 6
cyca1Δ CDKB1:mCh
cycb1-1 CDKB1:mCh
Time (h) 0 10 12 14 16 18 0 10 12 14 16 18
%≥2C 19 19 36 66 60 30 6 4 22 54 72 94

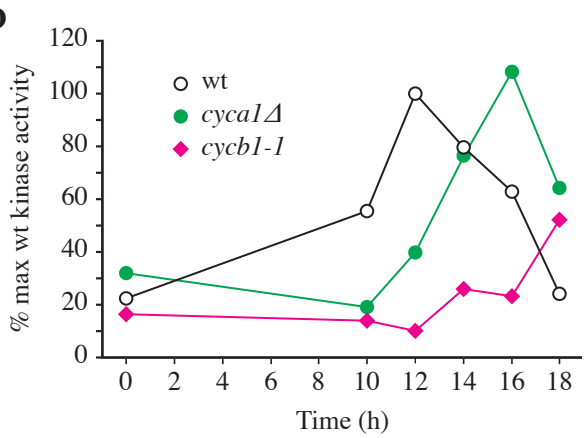
D
% max wt kinase activity
wt
cyca1Δ
cycb1-1
Time (h)

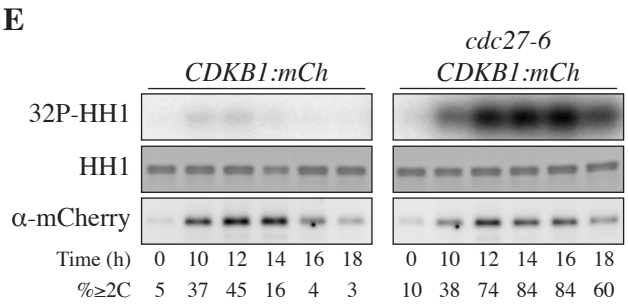
E
CDKB1:mCh
cdc27-6 CDKB1:mCh
32P-HH1
HH1
α-mCherry
Time (h) 0 10 12 14 16 18 0 10 12 14 16 18
%≥2C 5 37 45 16 4 3 10 38 74 84 84 60

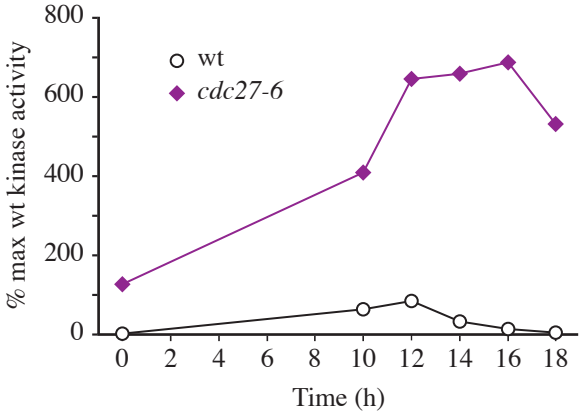
F
% max wt kinase activity
wt
cdc27-6
Time (h)

Fig. 4.5 CDKB1 is a nuclear protein during division cycles.

Confocal micrographs from a population of live cells expressing *CDKB1-mCherry* and *ble-GFP* as a nuclear marker (Li et al. 2016b). All images are average intensity z-projections. Contrast is adjusted separately for each trans and nuclear (GFP) image for clarity. CDKB1 images are contrast adjusted to the maximum of the group, so intensities can be compared. Non-nuclear signal in the mCherry channel is observed at similar levels in control strains lacking the transgene (data not shown). Scale bars are 10μm. **(A)** Newborn cell with no detectable CDKB1. **(B, C, D, E)** 1, 2, 4 and 8 cell clusters, respectively, with CDKB1 in all nuclei. **(F)** 16-cell cluster of postmitotic newborn cells (just before hatching) lack CDKB1. **(G)** Nuclear concentration of CDKB1 as a function of number of cells per cluster (see Ch. 7).

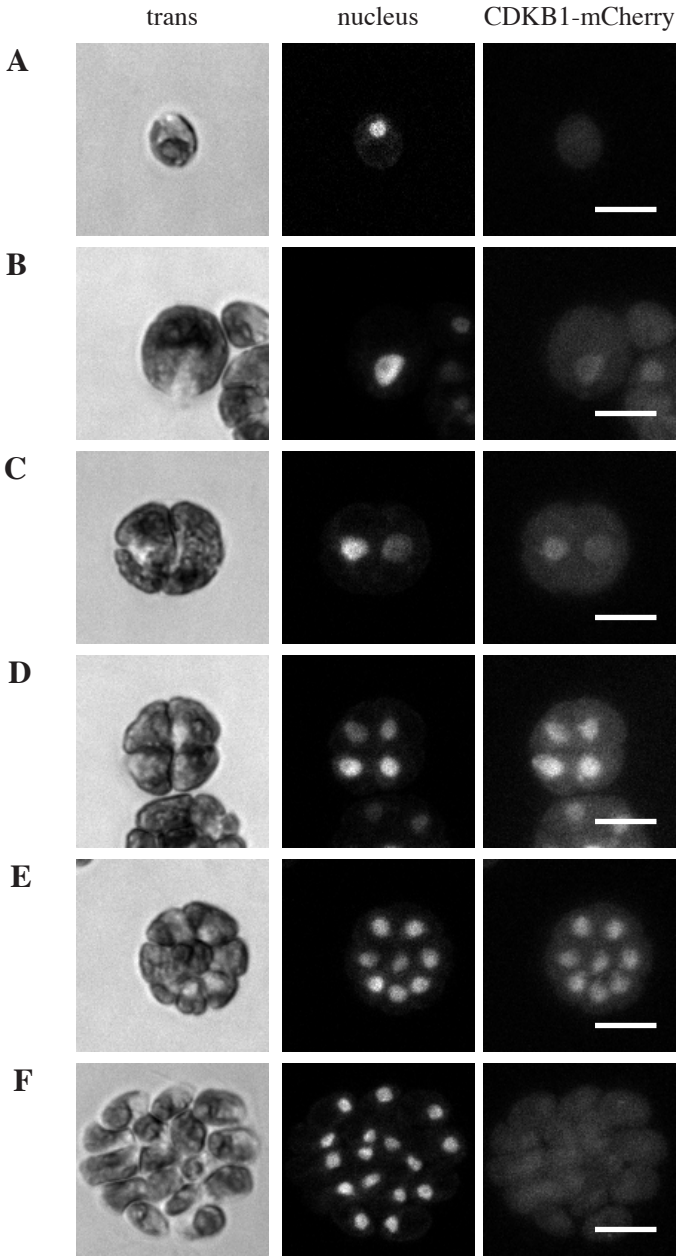
trans
nucleus
CDKB1-mCherry
A
B
C
D
E
F
G
Nuclear CDKB1-mCherry Intensity (AU)
0
2
4
6
8
10
12
14
one
two
four
eight
sixteen
Number of Nuclei per Cluster

Figure 4.6 Expression of CDKB1 is delayed and is correlated with cell division in the *cdka1Δ* mutant.

Images from unsynchronized cultures of *CDKB1-mCherry* and *cdka1Δ CDKB1-mCherry*. Since both chloroplast autofluorescence and mCherry fluorescence are acquired with the CY3 filter, fluorescence due uniquely to mCherry is inferred by computational subtraction. A multiplied FITC image (multiplier determined from images of wild type) is subtracted from the CY3 image to 'remove' chloroplast autofluorescence. Contrast is adjusted equally across images for clarity. **(A)** Nuclear CDKB1-mCherry is observed in dividing cells of wild type, but is absent from similarly sized (although not dividing) cells of the *cdka1Δ* mutant. Scale bar is 10μm. **(B)** CDKB1-mCherry only appears in the *cdka1Δ* mutant once cells have grown much larger and begun dividing. Note: this experiment was carried out with unsynchronized cells, so age of cell is inferred from size (see Fig. 2.3). Scale bar is 10μm.

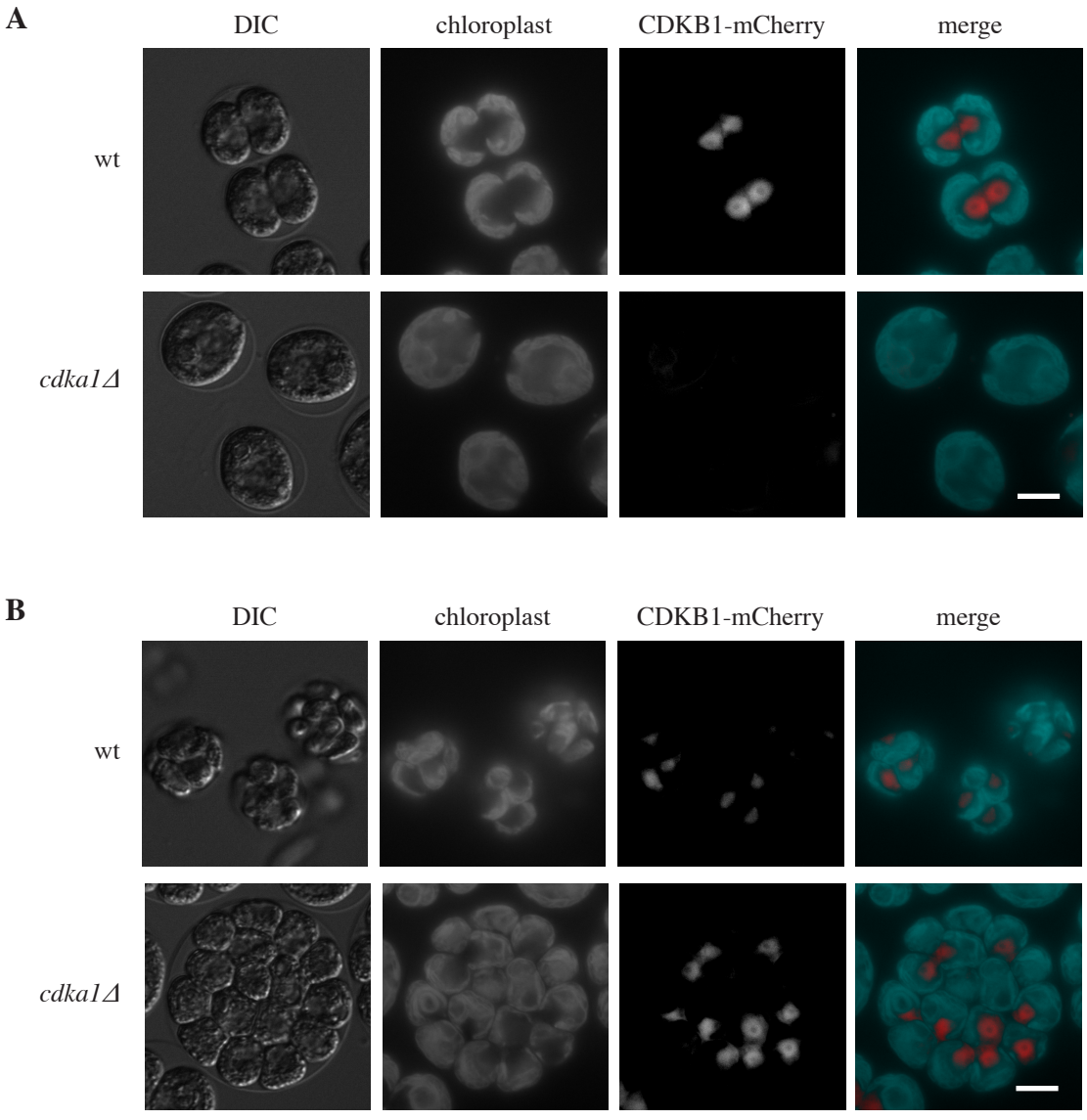
A
DIC
chloroplast
CDKB1-mCherry
merge
wt
cdka1Δ
B
DIC
chloroplast
CDKB1-mCherry
merge
wt
cdka1Δ

CDKA1 and CDKB1 have associated kinase activity that peaks in dividing cells

We examined CDKA1- and CDKB1-associated protein kinase activity in immunoprecipitates using the canonical CDK substrate histone H1. For both kinases, activity is specifically induced during cell divisions (Figs. 4.2, 4.4). As noted above, cells at all points in the cycle contain CDKA1 protein, but only dividing cells have significant associated kinase activity. CDKB1 is present and active only during cell divisions (Fig. 4.4).

CDKB1-associated activity is much lower than CDKA1-associated activity (Fig. 4.7). Many factors could explain this behavior, including differential substrate preference or sensitivity of the kinases to the conditions of the assay. We tested variations in mono- and divalent cations, pH, and extraction buffer. These manipulations affected overall activity but none significantly increased the relative activity of CDKB1 to CDKA1 (data not shown). Importantly, even though CDKB1-associated kinase activity measured *in vitro* is low, kinase activity is biologically relevant, since a kinase-dead (K33R) version of CDKB1 fails to rescue the *cdkb1-1* mutant (Table 4.1).

CDKA1-associated kinase activity is largely dependent on CYCA1 and independent of CYCB1

CDKs are critically dependent on cyclin binding for enzymatic activity (Jeffrey et al. 1995). We assessed whether CDKA1 activity is affected in mutants in which cyclin A or cyclin B is inactivated (*cyca1Δ* or *cycb1-1* [p.Leu288>Pro]). Activation of CDKA1 kinase is largely eliminated in the *cyca1Δ* background (Fig. 4.2D, E). This is despite the fact that the *cyca1Δ* mutant successfully replicates DNA and executes mitotic divisions (Figs. 2.3, 4.2D), and so cannot be explained by a simple failure to proceed through the cell cycle. The phenotype of the

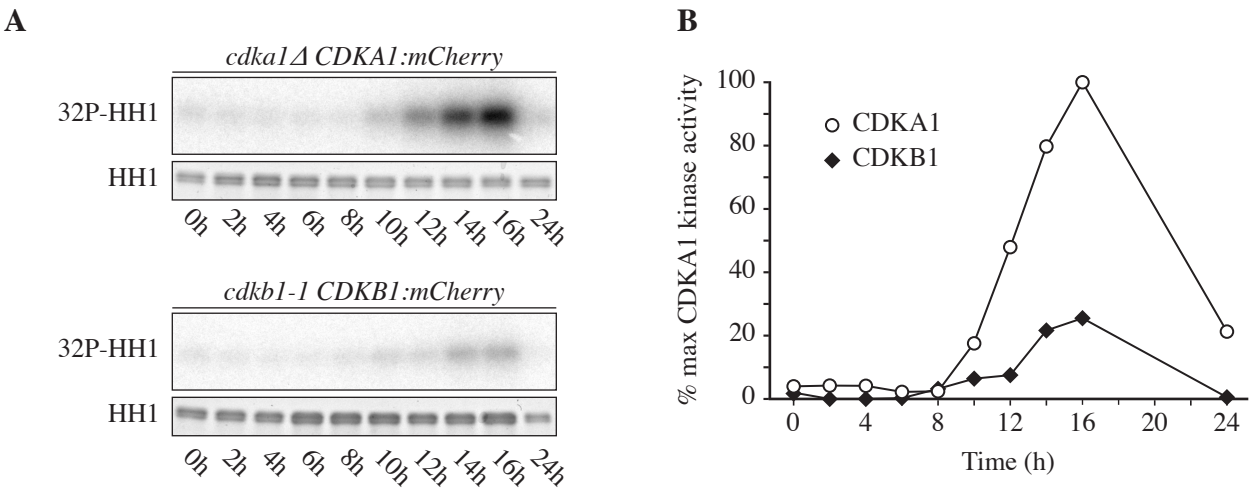

Figure 4.7 Activity of CDKA1 against histone H1 is greater than that of CDKB1.

(A) Kinase activity of immunoprecipitated CDKA1- and CDKB1-mCherry against histone H1 throughout the cell cycle. **(B)** Quantification of signal in (A) as % of maximum activity of CDKA1-mCherry during the time-course.

Table 4.1 Kinase dead (K33R) CDKB1-mCherry fails to rescue temperature-sensitive lethality of the *cdkb1-1* mutant.

Transforming DNA[a]	Number Resistant to Paromomycin[b]	Number Alive at 33ºC[c]
no DNA	0	0
no DNA	0	0
no DNA	0	0
pKA1 (wt)	100	122
pKA1 (wt)	156	100
pKA1 (wt)	2	6
pKA16 (K33R)	293	0
pKA16 (K33R)	66	0
pKA16 (K33R)	134	0

[a]200fmol cut with ScaI. pKA1 encodes wild type CDKB1-mCherry. pKA16 has K33R mutation (kinase dead CDKB1-mCherry)

[b]One quarter of the transformation was plated on TAP + paromomycin and grown at 21ºC.

[c]One quarter of the transformation was plated on TAP and grown at 33ºC.

cyca1Δ mutant is considerably less severe than that of the *cdka1Δ* mutant (Fig. 2.3C, D), indicating that CDKA1 must have CYCA1-independent biological activity. This activity may be due to activation of CDKA1 by other cyclins, but if this is the case, these complexes must have low biochemical activity, at least in the absence of CYCA1.

In contrast, CDKA1 kinase activity rises on schedule in the *cycb1-1* mutant, with no diminution in amount, despite the strong inhibition of progression to mitosis in this mutant (Fig. 4.2D, E). We therefore conclude that the normal activation of CDKA1 is largely dependent on CYCA1 and independent of CYCB1. A simple model to explain this is that CYCA1 is the primary biochemical activator of CDKA1.

We confirmed CYCA1-dependent activation of CDKA1 kinase in *cycb1*-deficient backgrounds with the *cycb1-3* (p.Glu325>Lys) allele (Fig. 4.8A), which has a more uniform cell cycle arrest than *cycb1-1* (data not shown).

The decline in CDKA1-associated kinase activity at the end of the cell cycle depends on CDKB1, CYCB1, and the APC

In fungi and animals, the anaphase promoting complex targets mitotic cyclins for destruction, eliminating CDK kinase activity at the end of the cell cycle. This is essential to allow mitotic exit and relicensing of DNA replication origins. We asked whether the APC is required for inactivation of CDKA1 in *Chlamydomonas* by assessing CDKA1-associated kinase activity in the *cdc27-6* APC mutant. The initial rise in CDKA1 kinase activity is similar to wild type in the *cdc27-6* mutant. In wild type, CDKA1 kinase activity falls as cell division cycles are completed. In the *cdc27-6* mutant, however, a high level of activity is maintained (Fig. 4.2F, G). Therefore, the APC is required for inactivation of CDKA1 as cells exit the multiple division cycles.

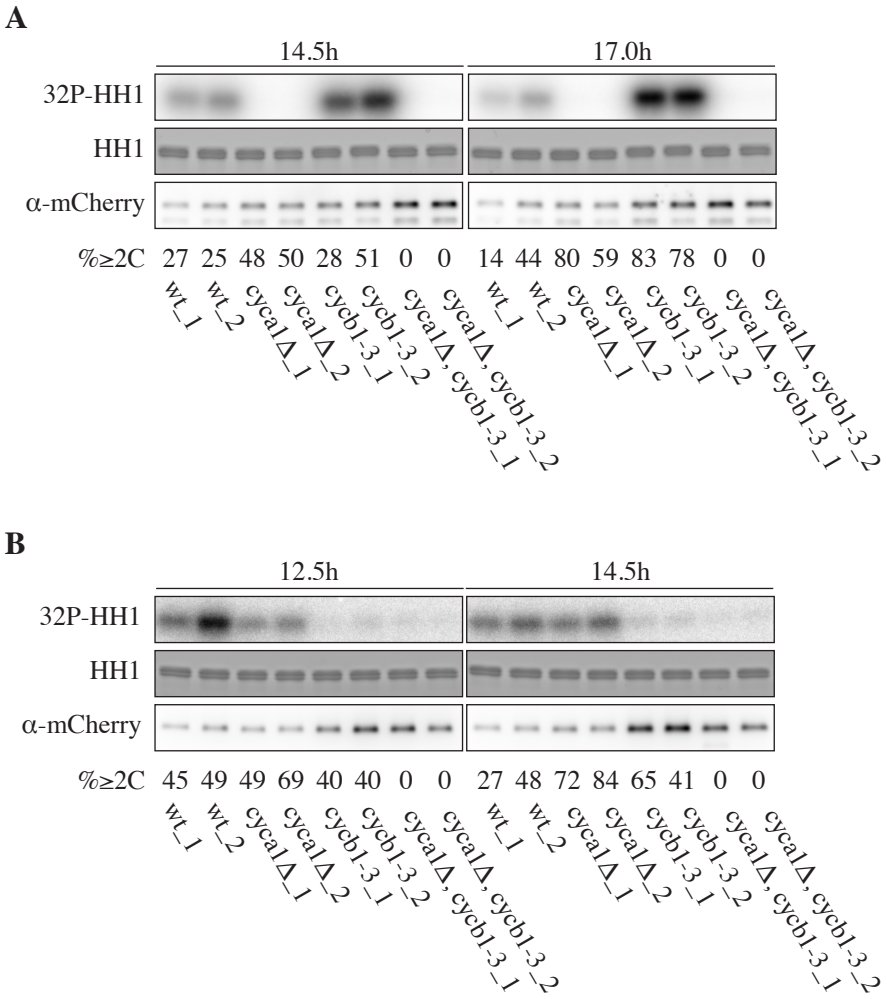

Figure 4.8 Cyclin-dependence of CDKA1 and CDKB1 protein kinase activity.

Kinase activity of immunoprecipitated CDKA1 and CDKB1 against histone H1 in wild type, *cyca1Δ*, *cycb1-3*, and c*yca1Δ cycb1-3* mutants. Two independent segregants of each genotype were examined at two time-points. **(A)** CDKA1. **(B)** CDKB1. CDKA1-associated kinase activity is dependent on CYCA1 in the presence or absence of CYCB1; CDKB1-associated kinase activity is dependent on CYCB1 in the presence or absence of CYCA1.

As mentioned previously, of the *Chlamydomonas* cyclins, only CYCA1 and CYCB1 contain canonical destruction boxes, making them good candidates for APC targeted destruction (Fig. 3.2). Since CDKA1 activity is independent of cyclin B (Fig 4.2D, E), the APC may inactivate CDKA1 at the end of the cell cycle by targeting CYCA1 for destruction.

In addition to the APC, CDKB1 is required for inactivation of CDKA1-associated kinase (Fig. 4.2F, G). This finding is consistent with the previous report that bulk CKS1-associated kinase activity remains at a high level in arrested *cdkb1-1* mutants (Tulin and Cross 2014). One possible interpretation of this result is that in the absence of functional CDKB1, competition between CDKA1 and CDKB1 for cyclins is reduced. To test this, we examined the effect of inactivating CYCB1 on CDKA1-associated kinase. The results were almost identical to the results of inactivating CDKB1 (Fig. 4.2D, E), arguing against cyclin competition as the mechanism for CDKA1 activation (since in this experiment CDKB1 is wild type, and available cyclins are reduced by inactivation of *CYCB1*). Overall, these results suggest that CYCB1 and CDKB1 may inactivate the CYCA1-CDKA1 complex.

CDKB1-associated kinase activity is dependent on CYCB1 and independent of CYCA1; it is strongly repressed by the APC

Similarly, we examined cyclin dependence of CDKB1-associated kinase activity. Consistent with the delayed onset of division in the *cyca1Δ* mutant (Fig. 2.3C, D), the onset of peak CDKB1 protein and kinase activity is also delayed, but rises to normal levels (Fig. 4.4C, D). In contrast, in the *cycb1-1* mutant, CDKB1 kinase activity is greatly diminished, even though CDKB1 protein accumulates to very high levels (Fig. 4.4C, D). We conclude that CDKB1 kinase activity is largely dependent on cyclin B and, aside from timing, independent of cyclin A.

Notably, this is the opposite pattern of cyclin dependence to that of CDKA1, which is dependent on CYCA1 but independent of CYCB1.

CDKB1 kinase activity is strikingly elevated in the *cdc27-6* mutant (Fig. 4.4E, F), indicating that the APC is critical for restricting CDKB1 activity. Since CDKB1 is largely dependent on CYCB1 but not CYCA1 for activity, and CYCB1 (but not CDKB1) contains a canonical destruction box (Fig. 3.2), the APC most likely inhibits CDKB1 by targeting CYCB1 for destruction. CYCB1 may be the major biochemical activator of CDKB1 kinase.

While APC prevents loss of CDKA1 kinase activity, APC inactivation has a much greater effect on CDKB1 activity (compare Figs. 4.2F, G and 4.4E, F). We lack a mechanistic explanation for this difference at present.

Summary

Characterization of mCherry-tagged CDKA1 and CDKB1 transgenes shows some common aspects in their behavior and regulation during the cell cycle in *Chlamydomonas* and also unveils some key differences that may reflect their divergent functions. Both proteins are found in the nucleus. CDKA1 in particular is also found near the base of the flagella, potentially reflecting a role in coordinating the ciliary and mitotic cycles. Others have identified both CDKA1 and CYCA1 (which we speculate is the primary activator of CDKA1) in the ciliary transition zone (Diener et al. 2015), corroborating our findings here.

Expression levels and kinase activities of both kinases are induced during cell division, although CDKA1 protein is present throughout the extended growth period whereas CDKB1 protein is undetectable until just before the multiple cell divisions begin. This order of appearance is probably at least partly ensured by CDKA1-dependent induction of CDKB1

expression and also rapid degradation (by an unknown mechanism) of CDKB1 at the end of the multiple division cycles.

The kinase activities of both CDKA1 and CDKB1 fall rapidly at the end of the multiple division cycles as flagellated newborn cells hatch from the mother cell wall. At least part of this inhibition can be attributed to the activity of the APC. A likely explanation is that the APC inhibits CDKA1 and CDKB1 by targeting their activating cyclin subunits for destruction. Indeed, we find that CYCA1 and CYCB1, the only two of the *Chlamydomonas* cyclins with APC-targeted destruction box motifs, are required for the activity of these kinases in a seemingly modular fashion. CYCA1, but not CYCB1, activates CDKA1. CYCB1, but not CYCA1, activates CDKB1. CYCA1 seems to be required specifically for the timing of CDKB1 expression and kinase activity, which is consistent with its role in activating CDKA1 (since CDKA1 is known to influence expression of CDKB1). CYCB1 along with CDKB1, on the other hand, are *inhibitors* of CDKA1 kinase activity. This set of interactions sets up the possibility for a negative feedback loop between these CDKs and may ensure the proper ordering of their activation and thus the cell cycle events that they direct.

Due to poor cell cycle synchrony, we are unable to determine whether the kinase activity of CDKA1 or CDKB1 oscillates during each individual cell division during the rapid cycles that follow the extended growth phase. When the APC is inactivated in *Chlamydomonas*, cells arrest with once-replicated DNA (Fig. 3.1) and high kinase activity of both CDKA1 and CDKB1 (Figs. 4.2F, G and 4.4E, F). This implies that the APC is required for re-replication of the genome and inhibition of CDK activity. APC degradation of DNA re-replication inhibitors at the end of the cell cycle is well understood in both animals (McGarry and Kirschner 1998) and fungi (Nguyen et al. 2001). In *Chlamydomonas* APC is not required for the first round of DNA replication, but

is required for the subsequent round. It seems a conservative assumption that APC is also required in each ensuing division in order to allow DNA replication to begin again. This would presumably also result in the oscillation of CDK activity due to their periodic downregulation by the APC every cycle.

Some sort of biological sensor of CDK activity that could be tracked in live cycling cells would be useful to determine whether CDK activity oscillates during these rapid, asynchronous divisions in *Chlamydomonas*. Without such a tool, it may be productive to consider first whether CYCA1 and CYCB1, likely the activating subunits of CDKA1 and CDKB1, oscillate in abundance during these divisions. Time-lapse microscopy of individual cells expressing CYCA1 and CYCB1 with fluorescent tags could be used to this end. Inducible expression of a non-degradable CYCA1 or CYCB1 in a population of dividing cells may also be informative. Assuming the degradation of a given cyclin is required for re-replication but inessential for nuclear division in each individual cycle, then the population in which a non-degradable version is induced should arrest with a mixture of cell clusters with 2C, 4C, 8C, and 16C DNA content (depending on how many divisions had occurred previous to induction of non-degradable cyclin), each nucleus arresting with 1C DNA content.

Chapter 5 CDKA1 is connected to ribosome biogenesis and inositol metabolism and may function in a parallel pathway with TOR1

Synthetic lethal screens can enable the identification of functionally interacting components of essential biological pathways and can also uncover the individual molecular players of compensating parallel pathways. Here we isolate synthetic lethal interactors with the mutant *cdka1-1* and identify multiple mutations in genes with predicted roles in ribosome biogenesis and inositol lipid metabolism. Evidence from other systems suggests that both of these pathways are intimately connected with the nutrient-sensing TOR pathway. Null *cdka1* mutants are hypersensitive to the TOR inhibitor rapamycin, suggesting TOR acts in a parallel pathway to CDKA1. We speculate that synthetic lethal interactors with *cdka1-1* may comprise upstream and downstream components of the TOR pathway in *Chlamydomonas*.

A synthetic lethal screen with *cdka1-1* should uncover parallel pathways that contribute to cell cycle progression

The temperature-sensitive (ts) *cdka1-1* allele was originally discovered as a double mutant named *ts301* (Tulin and Cross 2014). Upon backcrossing and sequencing, it was found that lethality at restrictive temperature depended on the presence of two mutations, one in *CDKA1* and another in a predicted subunit of the mediator complex, *MED6*. One possible explanation for their interaction is that CDKA1 and MED6 act coordinately to control the transcription of some essential gene or subset of genes; CDKA1 itself is known to promote the transcription of a large set of genes coincident with the onset of cell division (Tulin and Cross 2015).

In general, synthetic lethal interactions, like that between *cdka1-1* and *med6-1*, can be explained mechanistically as occurring either between two compensating pathways or within a single pathway whose activity is essential for viability. In the between pathways scenario (Fig. 5.1A), two pathways independently drive an essential biological process, such that even complete abrogation of any component of one pathway is compatible with viability, since the output of the alternative pathway is sufficient to maintain the essential process. In the within pathway scenario (Fig. 5.1B), on the other hand, the output of a single pathway is essential. Individual hypomorphic mutations in components of this pathway are tolerated, but mutations in multiple components can reduce the output of the pathway below a survivable threshold.

Genetic interactions tend to occur between genes that have some common function. Because of this, a set of interacting genes can give clues as to the function of any given query gene (Boone et al. 2007). We therefore endeavored to identify new mutations that exhibit synthetic lethality with the *cdka1-1* allele to gain further insight into CDKA1 function. Given that *CDKA1* is an inessential gene in *Chlamydomonas* (see Chapter 2), as it is in *Arabidopsis* and likely all Viridiplantae, genes identified in a synthetic lethal screen probably play a role in some compensating pathway that contributes to cell cycle progression in the absence of *CDKA1*.

Design of the *cdka1-1* synthetic lethal screen and isolation of mutants

To identify synthetic lethal interactors, we set up a pipeline for isolating and identifying conditional mutations that result in synthetic lethality with *cdka1-1* at restrictive temperature (Fig. 5.2). The *cdka1-1* mutant is mutagenized with ultraviolet light, mutant cells are allowed to grow at permissive temperature (21ºC), and mutant colonies are robotically picked to an array as described (Tulin and Cross 2014). These arrayed mutant colonies are then replica plated and

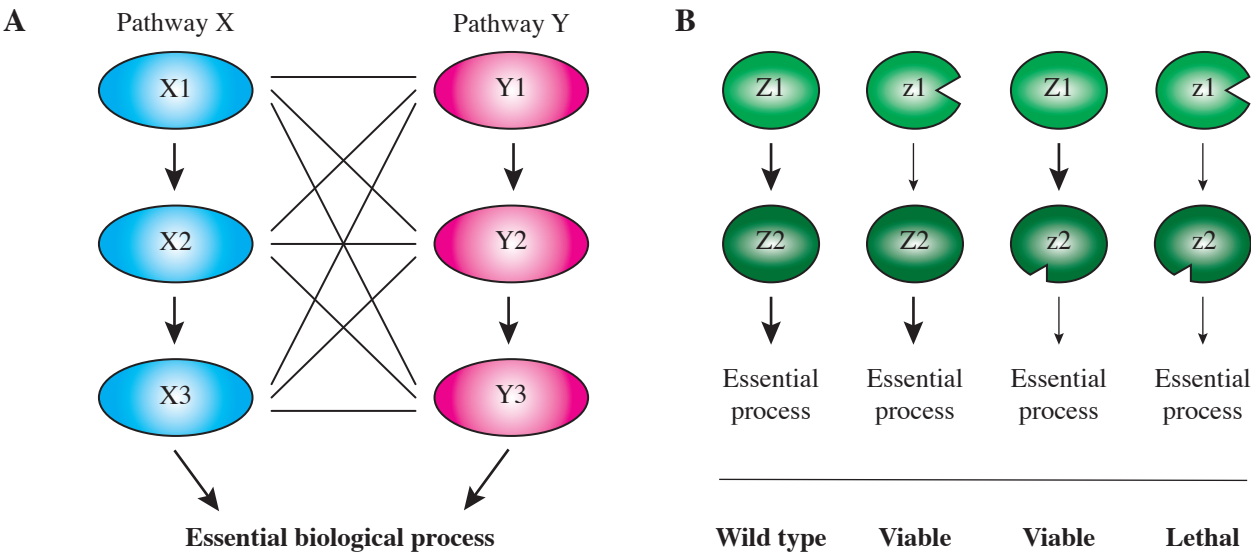

Figure 5.1 Two models for mechanisms underlying synthetic lethal interactions.

Adapted from (Boone et al. 2007).

(A) Some synthetic lethal interactions are explained by interaction 'between' two pathways each independently contributing to some essential biological process. Elimination of one pathway can be compensated by the activity of the other, maintaining viability in a sort of 'buffering' mechanism. Thin lines indicate potential interactions between pathways. **(B)** Other synthetic lethal interactions are explained by interaction 'within' a single essential pathway. Here, hypomorphic mutations in individual components (represented by modified ovals with lower-case 'z1' or 'z2') are compatible with viability, but multiple mutations reduce the output of the pathway below a viable threshold and result in lethality (rightmost pathway) .

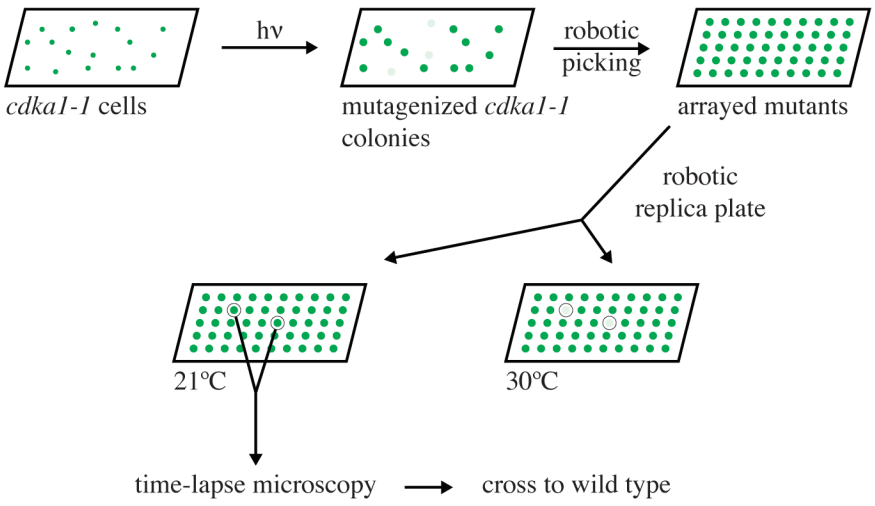

Figure 5.2 Schematic of *cdka1-1* synthetic lethal screen.

The *cdka1-1* mutant is exposed to ultraviolet radiation (hν) to induce mutations. Mutagenized cells are allowed to form colonies at permissive temperature, and these colonies are robotically picked to a new plate in a regularly spaced array. Arrayed plates are then replica plated to permissive (21ºC) and restrictive (30ºC) temperature and visually inspected for defective biomass accumulation at restrictive temperature. Temperature-sensitive mutants are assessed by time-lapse microscopy at restrictive temperature. Mutants from a phenotypic subset are then crossed to wild type to determine whether lethality is synthetic with *cdka1-1*.

visually screened for reduced biomass accumulation at restrictive temperature. For this screen, we use a restrictive temperature of 30ºC instead of 33ºC as in (Tulin and Cross 2014), since *cdka1* mutants show some reduction in biomass accumulation at 33ºC, but not at 30ºC (Fig. 2.2).

Approximately 35,000 individual mutants were screened, and of these, 162 had defective biomass accumulation at 30ºC. A subset of these ts mutants were analyzed by time-lapse microscopy and crossed to wild type to determine genetic interaction with the *cdka1-1* mutation. In total, fifteen *cdka1-1* synthetic lethal (*csl*) mutants were isolated and analyzed further.

Time-lapse microscopy of ts lethal mutants in the *cdka1-1* background

Ninety-four mutants were imaged by time-lapse microscopy at restrictive temperature (30ºC) as described (Tulin and Cross 2014). Of these, ~1/3 underwent multiple divisions during the time-lapse. We assume these are not *bona fide* ts lethal mutants or else only result in lethality after the first set of divisions. In either case, we excluded these mutants from further analysis.

In an effort to enrich for synthetic lethal interactors with *cdka1-1*, we focused on mutants with a phenotype that resembles the original *cdka1-1 med6-1* mutant. At restrictive temperature, *cdka1-1 med6-1* exhibits normal growth but fails to undergo cell division; cells arrest with a round, intact morphology (Tulin and Cross 2014). We thus excluded any mutants that have obvious growth defects (class 3) or that undergo cell lysis (class 2) at restrictive temperature in favor of mutants with robust growth that remain intact (class 1, Fig. 5.3).

Whether this phenotypic subset is enriched for synthetic interactors with *cdka1-1* is not known, but theoretically, this is the expected phenotype from *cdka1 csl* mutants. *CDKA1* plays a role in promoting the transition from the growth phase to the division phase in the *Chlamydomonas* cell cycle (see Chapter 2). While *CDKA1* promotes the timely occurrence of

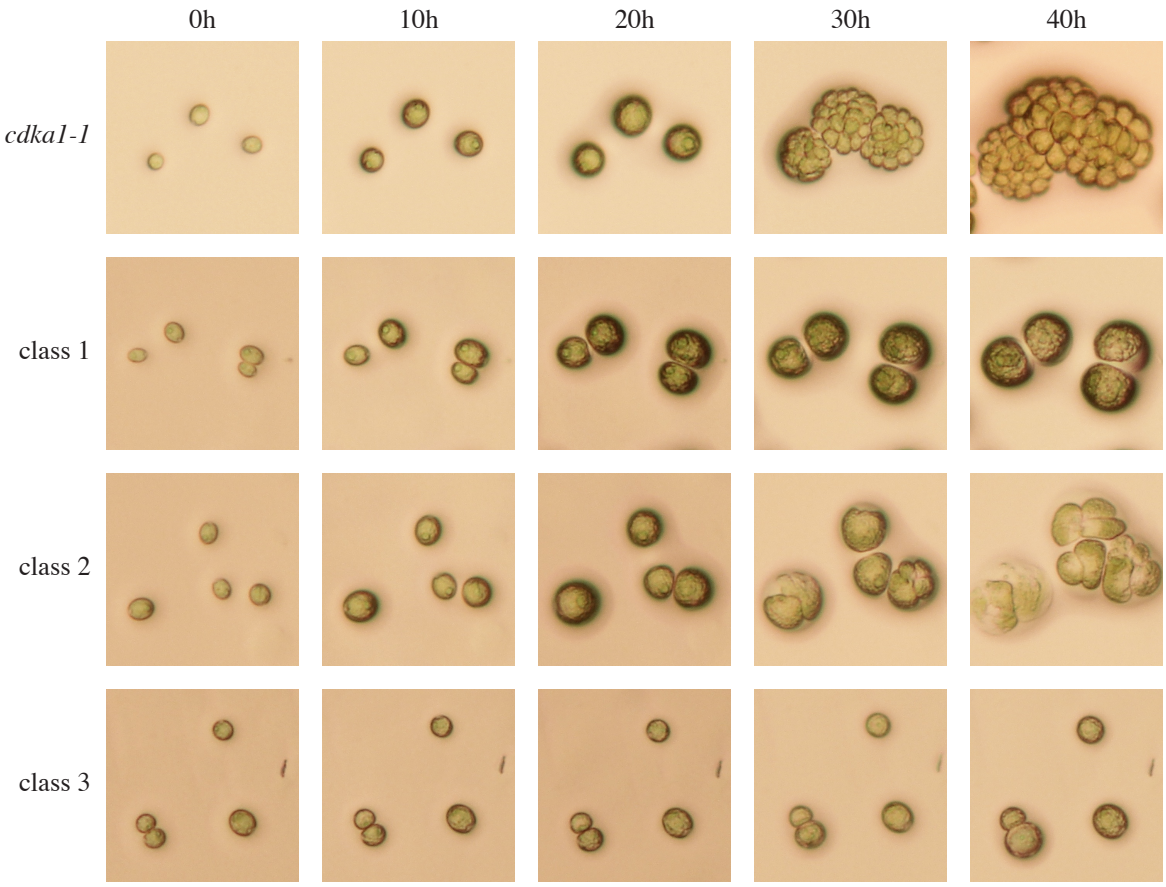

Figure 5.3 Phenotypic classes of ts lethal mutants in the *cdka1-1* background.

The parent *cdka1-1* mutant and representatives of temperature-sensitive lethal mutants created in the *cdka1-1* background imaged at 0, 10, 20, 30, and 40h at restrictive temperature (30ºC). The *cdka1-1* parent spends the first 20-30h in the growth phase, followed by a rapid series of divisions between 20 and 30h. Class 1 mutants, comprising ~1/2 of ts lethal mutants analyzed, exhibit normal growth and arrest as large, round, intact cells. Classes 2 and 3 together make up the other half of mutants, in roughly equal proportion. Class 2 mutants have normal growth, but undergo cell lysis after an apparent attempt at division. Class 3 mutants have severely retarded growth. The class 1 mutant depicted here is *cdka1-1 csl13-1*.

this transition, it is not absolutely required for it, implying the existence of late-acting back-up mechanisms. Impairment of these back-up mechanisms in a *cdka1-1* mutant background should result in synthetic lethality. Presumably, such a double mutant will fail to traverse the growth-to-division transition, causing cells to arrest with a pre-division morphology.

Determination of synthetic lethality and time-lapse microscopy of *csl* mutants

In order to identify synthetic lethal interactors with *cdka1-1*, mutants from phenotypic class 1 (Fig. 5.3) were crossed to a wild type strain. By segregating the *cdka1-1* and candidate *csl* mutations, we can determine whether the candidate *csl* mutation independently causes ts lethality or whether lethality only occurs in a mutant *cdka1* background. Several mutants, when crossed to wild type, showed a 2-to-2 segregation pattern for viability-lethality at restrictive temperature, indicating the presence of a single mutation that causes ts lethality on its own. These mutants were not analyzed further. For true *cdka1-1* synthetic lethal mutants, however, only one quarter of progeny in a cross to wild type will be lethal at high temperature, and all such progeny will have the *cdka1-1* mutation. We identified fifteen such mutants.

Time-lapse microscopy of segregants from crosses of *cdka1-1 csl* mutants to wild type serves to illustrate the synthetic nature of ts lethality (Fig. 5.4B, D) and also reveals phenotypic variability among the *csl* mutants. Some *csl* mutants are essentially indistinguishable from wild type at 30ºC—they grow at a normal rate and produce microcolonies that are comparable in size and cell number to those produced by wild type cells (Figure 5.4A). Other *csl* mutants, however, exhibit delayed division compared to wild type and exhibit slower growth, forming smaller microcolonies (Figure 5.4C).

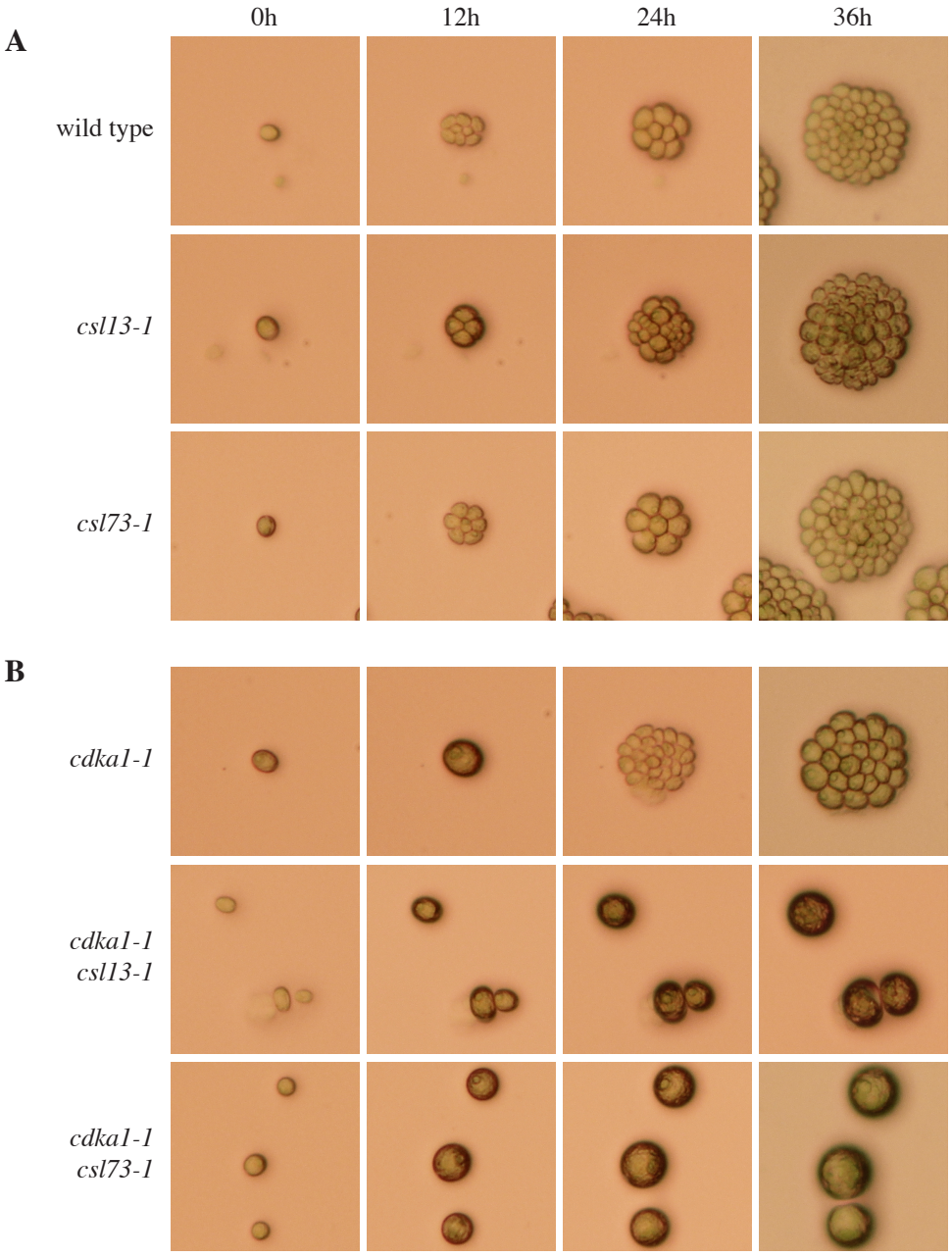

Figure 5.4 Time-lapse microscopy of representative *csl* and *cdka1-1 csl* mutants.
(A) Some *csl* mutants are comparable to wild type in growth and division timing. They grow and divide at a normal rate and form microcolonies of comparable size to wild type. **(B)** In a *cdka1-1* background, these mutations result in lethality at restrictive temperature.

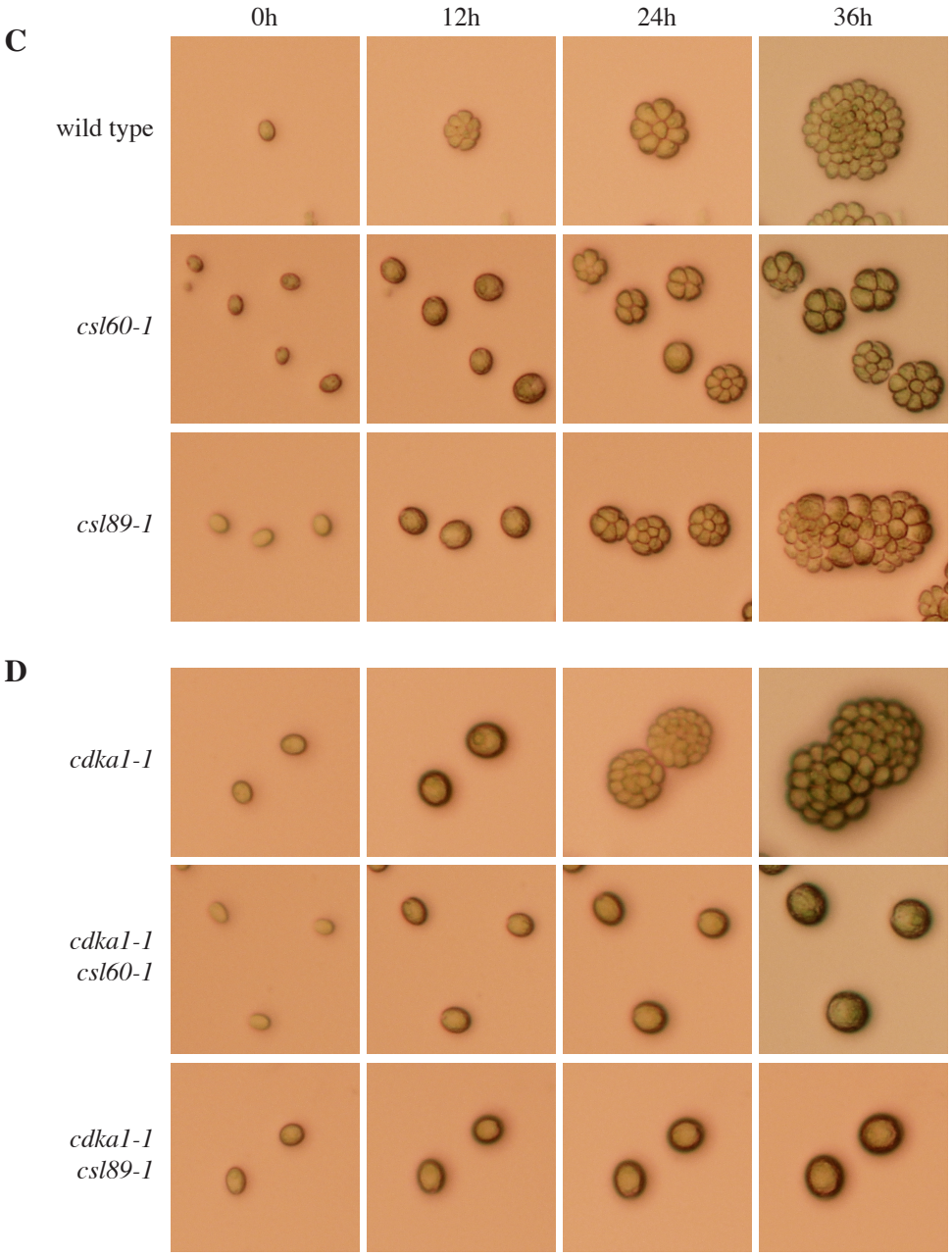

Figure 5.4 Time-lapse microscopy of representative *csl* and *cdka1-1 csl* mutants. **(C)** Some *csl* mutants exhibit slow growth compared to wild type and, probably as a result of their slow growth, delayed division. These mutants form microcolonies that are smaller than those formed by individual wild type cells. **(D)** In a *cdka1-1* background, these mutations also result in lethality at restrictive temperature.

Identification of causative mutations

In order to identify causative mutations in the *csl* mutants, we sequenced genomic DNA from a pool of ts lethal segregants from crosses of the *cdka1-1 csl* mutants to wild type—a technique called bulked segregant analysis (Michelmore and Kesseli 1991). In this approach, 10-12 ts lethal segregants are isolated from a cross of *cdka1-1 csl* to wild type, and these segregants are cultured independently. The cultures are mixed in equal proportion and DNA from the mixture is purified and processed for paired-end 100bp Illumina sequencing. The principle underlying this approach is that causative mutations will be represented in 100% of the reads from the pooled DNA, whereas non-causative ('passenger') mutations will segregate randomly and, on average, will be represented in 50% of the reads. The frequency of any given mutation in the pool depends on its genetic distance from the causative mutation, such that closely linked mutations will also be represented in 100% of the reads. The computational process for identification of single nucleotide polymorphisms (SNPs) is described in (Tulin and Cross 2014).

For most of the *csl* mutants, there is at least one genomic region where mutant SNPs are covered by 100% of reads in the pool (Figure 5.5). These regions range in size from single isolated uniform SNPs to genomic regions spanning 1.5Mbp within which all mutant reads are uniform. For the *csl* mutants, tetrad analysis reveals that a single locus is responsible for synthetic lethality in the *cdka1-1* background, so we assume only one mutation is causative.

By identifying genomic regions with uniform mutant SNPs, bulked segregant analysis aids in the identification of a subset of mutations as likely candidates for causality. However, other methods are required to determine which, if any, of the sometimes many candidate mutations underlie synthetic lethality with *cdka1-1*.

Figure 5.5 Mutant read frequency in DNA from bulked segregant pools of *cdka1-1 csl* mutants.

Genomic regions where mutant SNPs are detected in 100% of reads from a pool of mutant segregants likely contain the causative mutation. Mutant read frequency is plotted against position along the chromosome. For *csl8,* both a chromosome with a uniform region (16) and one without any uniform SNPs (14) are depicted. For the remaining mutants (mutant name depicted above x-axis), only one chromosome is depicted for illustration. Red triangles represent mutations that change protein coding sequence; open blue circles represent all other mutations. Note: some primary *cdka1-1 csl* mutants were backcrossed to wild type several times before the generation of bulked segregant pools. Extended SNP-deficient regions on some chromosomes are likely accounted for by crossovers with wild type chromosomes that occurred during these crosses. For *csl95* no uniform SNPs were detected, but many SNPs approach uniformity on chromosome 13.

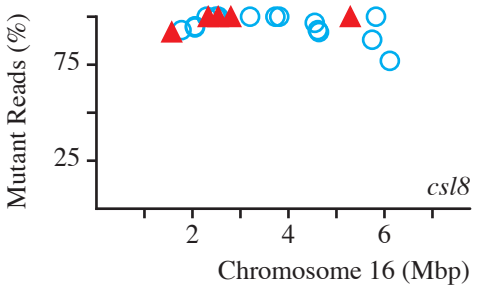
Mutant Reads (%)
75
25
csl8
2
4
6
Chromosome 16 (Mbp)

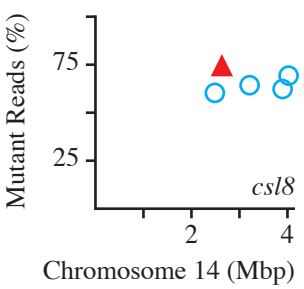
Mutant Reads (%)
75
25
csl8
2
4
Chromosome 14 (Mbp)

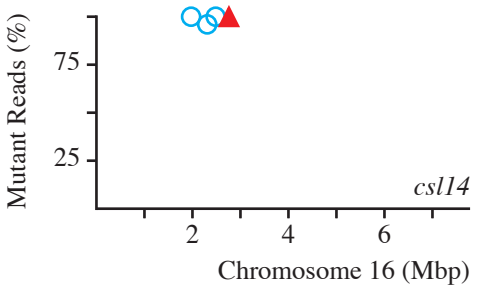
Mutant Reads (%)
75
25
csl14
2
4
6
Chromosome 16 (Mbp)

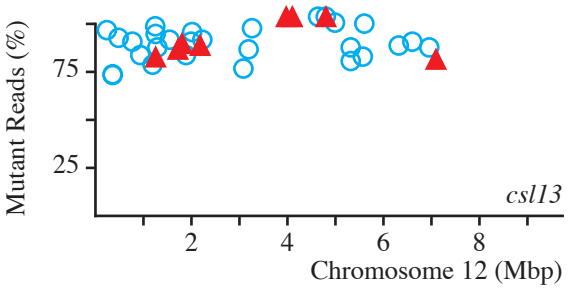
Mutant Reads (%)
75
25
csl13
2
4
6
8
Chromosome 12 (Mbp)

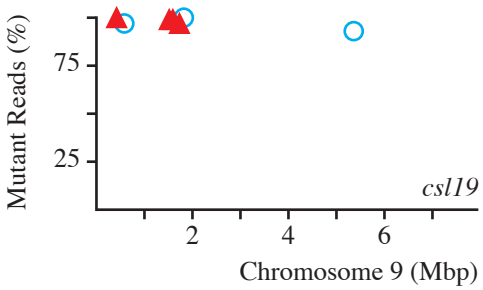
Mutant Reads (%)
75
25
csl19
2
4
6
Chromosome 9 (Mbp)

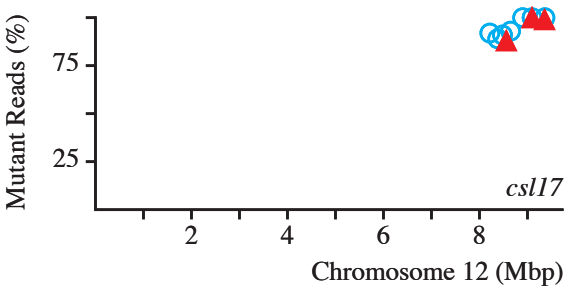
Mutant Reads (%)
75
25
csl17
2
4
6
8
Chromosome 12 (Mbp)

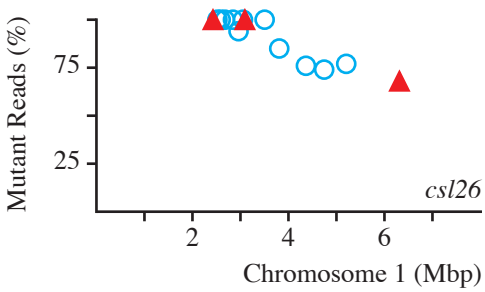
Mutant Reads (%)
75
25
csl26
2
4
6
Chromosome 1 (Mbp)

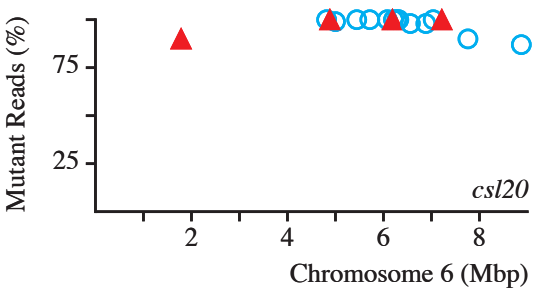
Mutant Reads (%)
75
25
csl20
2
4
6
8
Chromosome 6 (Mbp)

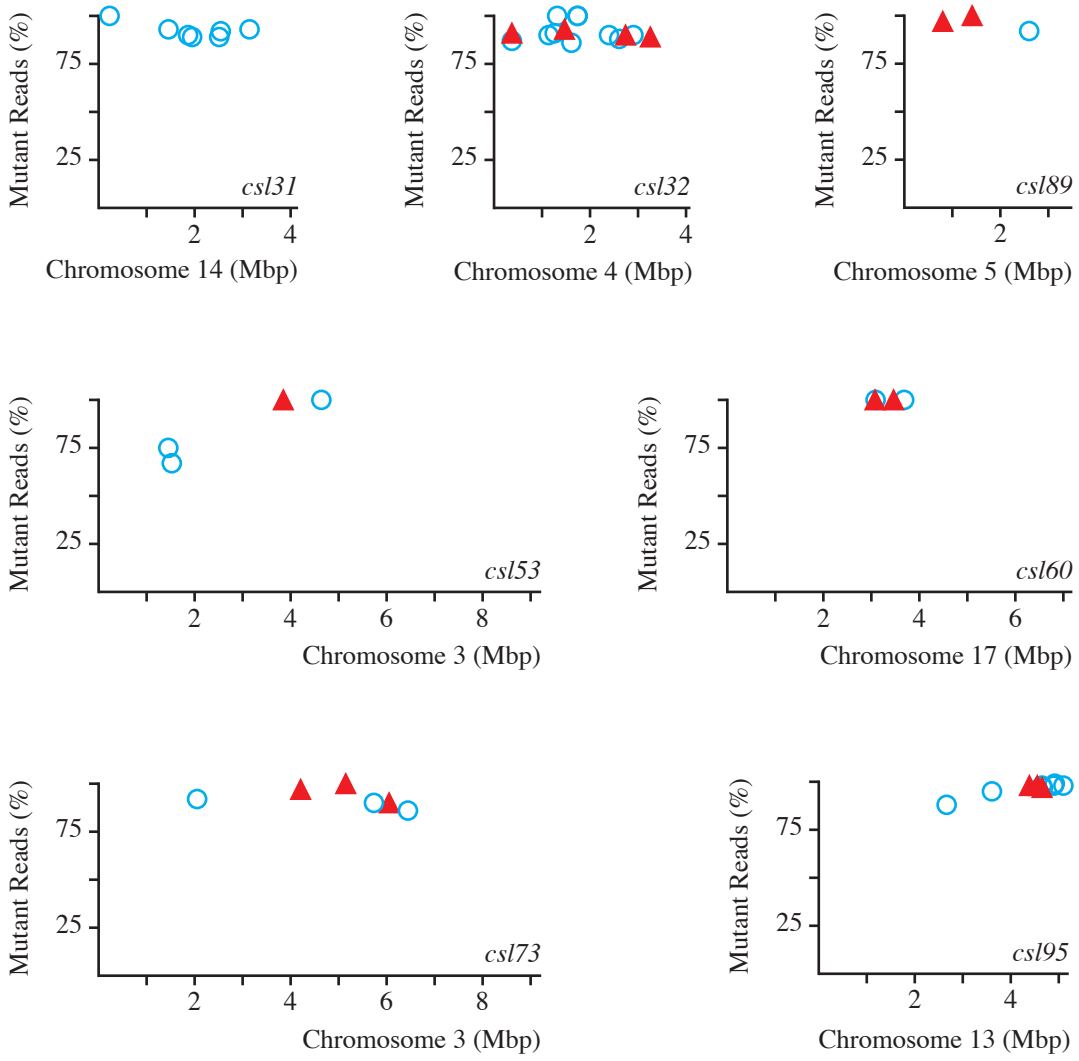
Mutant Reads (%)
75
25
csl31
2
4
Chromosome 14 (Mbp)
Mutant Reads (%)
75
25
csl32
2
4
Chromosome 4 (Mbp)
Mutant Reads (%)
75
25
csl89
2
Chromosome 5 (Mbp)
Mutant Reads (%)
75
25
csl53
2
4
6
8
Chromosome 3 (Mbp)
Mutant Reads (%)
75
25
csl60
2
4
6
Chromosome 17 (Mbp)
Mutant Reads (%)
75
25
csl73
2
4
6
8
Chromosome 3 (Mbp)
Mutant Reads (%)
75
25
csl95
2
4
Chromosome 13 (Mbp)

Of the uniform SNPs, we only considered those that result in a change to protein coding sequence (referred to herein as 'functional SNPs'). For six of the fifteen *csl* mutants (*csl14*, *17*, *19*, *53*, *73*, and *89*), there is only one uniform functional SNP, and this SNP is assigned the highest likelihood of causality (Table 5.1). For four of the *csl* mutants (*csl31*, *32*, *76*, and *95*), either no uniform SNPs are detected or none of the uniform SNPs are functional. For the remaining five *csl* mutants (*csl8*, *13*, *20*, *26*, and *60*), there are multiple (2-4) uniform functional SNPs. For each of these mutants, only one of the uniform functional SNPs occurs in a conserved region in an *Arabidopsis thaliana* homolog. These mutations are assigned as the best candidate for causality (Table 5.1). Sequences that natural selection has maintained since the divergence of green algae from land plants are likely critical for fitness, and thus mutations that disrupt these conserved motifs are more likely to cause deleterious phenotypes. More to the point, conservation is an empirically useful feature for predicting causality of mutations in ts lethal mutants in *Chlamydomonas* (Tulin and Cross 2014; Cross et al. 2017).

We undertook two additional approaches to increase our confidence in the assignment of causative mutations. In one approach, we extended the bulked segregant analysis, which is essentially a genetic mapping exercise, by genotyping the candidate causative mutation in question in ts lethal segregants from crosses of the *csl* mutants to the *cdka1Δ*^{paro} mutant (this allele is easily followed in crosses by simply determining paromomycin resistance). Genotyping was performed with toe-hold primers (Byrom et al. 2014) or by Sanger sequencing of a small PCR-amplified segment of DNA containing the candidate causative mutation. In all the *csl* mutants examined in this way, all ts lethal segregants tested harbored the candidate causative mutation (Table 5.1). Additionally, in mutants where it was examined, the candidate causative mutation was maintained through three backcrosses to wild type (Figure 5.1).

Table 5.1. Best candidate *csl* mutations and evidence for causality.

Mutant	Best Candidate Gene[a]	Gene Name[b]	Mutation[c]	Mapping[d]	Reversion[e]
csl8	Cre16.g663050	*GBP4*[*]	p.Ser572>Met	6 segs + 3bx	N/A
csl13	Cre12.g523050	*CCT11*	p.Glu2295>Lys	2 segs + 3bx	2 pseudo
csl14	Cre16.g662800	*PRP4*	p.Gly11>Lys	N/A	N/A
csl17	Cre12.g542800	*RPC2*	p.Phe454>Leu	3bx	N/A
csl19	Cre09.g404650	*VPS51*[*]	mis-splice	N/A	2 psuedo
csl20	Cre06.g290500	*VPS15*[†]	p.Asp285>Asn	18 segs	N/A
csl26	Cre01.g019200	*RRP1*[#]	p.Lys16>Ter	N/A	1 true + 8 pseudo
csl31	no candidate	N/A	N/A	N/A	N/A
csl32	no candidate	N/A	N/A	N/A	N/A
csl53	Cre03.g170750	*RNP3*	p.Val134>Glu	N/A	2 pseudo
csl60	Cre17.g724850	*RRB1*[#]	p.Glu468>Lys	N/A	1 true + 2 pseudo
csl73	Cre03.g182100	*IPK*	mis-splice	10 segs + 3bx	1 true
csl76	no candidate	N/A	N/A	N/A	N/A
csl89	Cre05.g244236	*GCD14*[#]	mis-splice	12 segs + 3bx	1 true + 1 pseudo
csl95	no candidate	N/A	N/A	N/A	N/A

[a]Gene model in which the best candidate mutation occurs (Phytozome v5.5).

[b]If the *Chlamydomonas* gene lacks a name, a BLAST search is conducted against the proteomes of *Arabidopsis thaliana*, *Saccharomyces cerevisiae*, and *Homo sapiens* and the best BLAST hit from one of these is used.

[c]Mutation nomenclature is as recommended by the Human Genome Variation Society.

[d]Number of segregants (segs) that retain the putative causal mutation and the number of backcrosses (bx) in which the putative causal mutation has been maintained.

[e]Number of identified true reversions (mutations that revert exactly to wild type) and pseudo-reversions (intragenic mutations predicted to restore function) of candidate causal mutation.

[*]Best *Homo sapiens* BLAST hit.

[†]Best *Arabidopsis thaliana* BLAST hit.

[#]Best *Saccharomyces cerevisiae* BLAST hit.

Despite the fact that bulked segregant analysis and careful genetic mapping can increase our confidence that the assigned candidate causative mutation is correct, the possibility that the true causative mutation is closely linked cannot be excluded. Furthermore, there is a distinct possibility that the true causative mutation was not detected in the original analysis of whole genome sequence data. This could occur if the mutation falls either within a gap in the reference assembly or within a repetitive region that fails to align to the reference, for instance. Indeed, there are many such blocks of unknown sequence in the *Chlamydomonas* reference genome, and on closer analysis, some of them do contain exons (Tulin and Cross 2016).

A second approach—the isolation and sequencing of revertants—circumvents both of these problems. A large fraction of mutations induced by ultraviolet radiation are transitions, and cytosine to thymine transitions at dipyrimidine sites are particularly common (Brash 2015). We find that coding sequence changes due to UV-induced mutations can oftentimes be corrected by single nucleotide transitions, many occurring at dipyrimidine sites. Since the *cdka1-1 csl* mutants are lethal at restrictive temperature, revertants can be isolated by exposing mutant cells to ultraviolet light and incubating the mutagenized population at high temperature. Theoretically, viability should be restored if either the *cdka1-1* or *csl* mutation is reverted. Reversion of *cdka1-1* was avoided in some cases by crossing *csl* mutants to the *cdka1Δ*^{paro} allele and isolating revertants in this background. Successful reversion of the candidate causative mutation was detected by Sanger sequencing for seven of the *csl* mutants (Table 5.1). We never sequenced more than ten revertants per mutant, so the chance of detecting a spurious reversion in a passenger mutation is exceedingly unlikely. We therefore consider the causality of these mutations definitive.

Two pathways emerge: ribosome biogenesis and phosphoinositide metabolism

Very little is known regarding the function of most of the *CSL* genes in *Chlamydomonas*. Mutations in two *CSL* genes have been identified previously. *csl20* and *csl26* are new alleles of *gex63* and *gex26*, respectively—alleles previously isolated in a screen for ts lethal cell cycle mutants (Tulin and Cross 2014). Indeed, *csl26* exhibits lethality at 33ºC, despite its viability at a more permissive 30ºC. The *csl20* allele, however, is viable even at 33ºC. The mutations in *csl20* and *gex63* are in the same region of the protein (Cre06.g290500; *csl20*: p.Asp285>Asn, *gex63*: p.Ser288>Phe) in residues exactly conserved between *Chlamydomonas* and *Arabidopsis*. The mutation in *csl20*, however, is much less severe than that in *gex63* [according to Blosum63 scoring (Henikoff and Henikoff 1993)], which could explain the viability of this allele at higher temperatures.

In other organisms, homologs of the *CSL* genes are involved in diverse molecular functions, including pre-mRNA splicing, translation initiation, and vacuolar protein sorting (Lustig et al. 1986; Anderson et al. 1998; Pahari et al. 2014). Two pathways, however, are hit multiply in the *CSL* set. Multiple *CSL* genes are predicted to play a role in ribosome biogenesis. Yeast homologs of both *CSL26* and *CSL53* are involved in critical steps in the processing of ribosomal RNA (rRNA) (Andrew et al. 1976; Lee and Baserga 1999), and the yeast homolog of *CSL60* promotes the transcription of ribosomal proteins and the assembly of the 60S ribosomal subunit (Iouk et al. 2001). Inositol lipid metabolism is also encountered as the predicted function in multiple *CSL* genes. The yeast homologs of *CSL20* and *CSL13* (*VPS15* and *FAB1*, respectively) act consecutively in a pathway generating various phophoisoforms of the membrane lipid phosphatidylinositol (PI). VPS15, together with VPS34, forms a complex that phosphorylates PI to generate phosphatidylinositol 3-phosphate (PI(3)P) (Stack et al. 1993).

FAB1 functions downstream of the VPS34/VPS15 complex, converting PI(3)P to phosphatidylinositol 3,5-bisphosphate ($PI(3,5)P_2$) (Cooke et al. 1998). The isolation of a mutation in *CSL73* also suggests a connection to phosphoinositide metabolism. Homologs of *CSL73* are inositol kinases targeting various phosphorylated forms of the water-soluble free inositol ring (Yang and Shears 2000), precursors of which are generated by cleavage of the inositol ring from membrane phosphoinositides by phospholipase C (York et al. 1999).

We became interested in the possibility that both ribosome biogenesis and phosphoinositide metabolism might have a common connection to the TOR pathway. In Opisthokonts, the phospholipid kinases VPS34/15 and FAB1, like TOR, respond to the availability of nutrients (such as glucose and amino acids) and their activity is required for the phosphorylation of canonical TOR targets (Byfield et al. 2005; Nobukuni et al. 2005; Bridges et al. 2012). Furthermore, the enzymatic product of FAB1, $PI(3,5)P_2$, is required for the activation and localization of TOR to the vacuolar membrane and recruits known binding partners and substrates of TOR (Bridges et al. 2012; Jin et al. 2014). TOR is also a key regulator of ribosome biogenesis, promoting transcription of genes encoding ribosomal proteins and driving the production and maturation of rRNA (Powers and Walter 1999). We hypothesize that many *CSL* genes may act either upstream or downstream of TOR in a parallel pathway to CDKA1.

Rapamycin sensitivity in the absence of CDKA1 suggests that TOR1 and CDKA1 act in parallel pathways

Given that *CSL* homologs in other systems either activate or are activated by TOR, we speculated that TOR inhibition might create a *csl*-like phenotype—synthetic lethality with *cdka1*. *TOR1* mutants in *Chlamydomonas* are not available, but TOR1 can be targeted with the

macrolide rapamycin. As in Opisthokonts (Aylett et al. 2016), rapamycin restricts the growth of *Chlamydomonas* by inhibiting TOR1 as part of a complex with the protein FKBP12 (Crespo et al. 2005). We observe that *Chlamydomonas* exhibits slow growth when exposed to rapamycin at concentrations as low as 100nM, but is nonetheless viable at concentrations up to 1μM. *cdka1* mutants, however, exhibit hypersensitivity to the drug, with a dose-dependent progressive reduction in viability (Figure 5.6). This synthetic interaction, observed in both missense and null alleles of *CDKA1*, suggests that *CDKA1* and *TOR*1 act in parallel pathways such that their combined impairment results in lethality.

Summary

Here we have conducted a small scale genetic screen to identify conditional mutations that result in synthetic lethality in the *cdka1-1* mutant. The inessentiality of *CDKA1* in plants implies that synthetic lethal interactors are part of a parallel pathway that acts alongside *CDKA1* to promote some essential biological function, likely the initiation of the cell cycle. Homologs of the *CSL* genes have a wide range of molecular functions, but multiple *CSL* genes implicate ribosome biogenesis and inositol lipid metabolism as important parallel pathways to *CDKA1*. A speculative connection to TOR is supported by an experiment demonstrating the hypersensitivity of *cdka1* mutants to the TOR inhibitor rapamycin.

We propose a mostly speculative model as a framework to guide future experiments (Figure 5.7). In this model, the TOR1 kinase acts alongside CDKA1 as a critical driver of cell cycle initiation. Specific phosphoisoforms of PI, generated by the enzymatic activity of lipid kinases, act upstream of TOR1 as activators, and ribosome biogenesis is subsequently induced by an activated TOR1. Whether the phospholipid kinases activate TOR1 in *Chlamydomonas* is

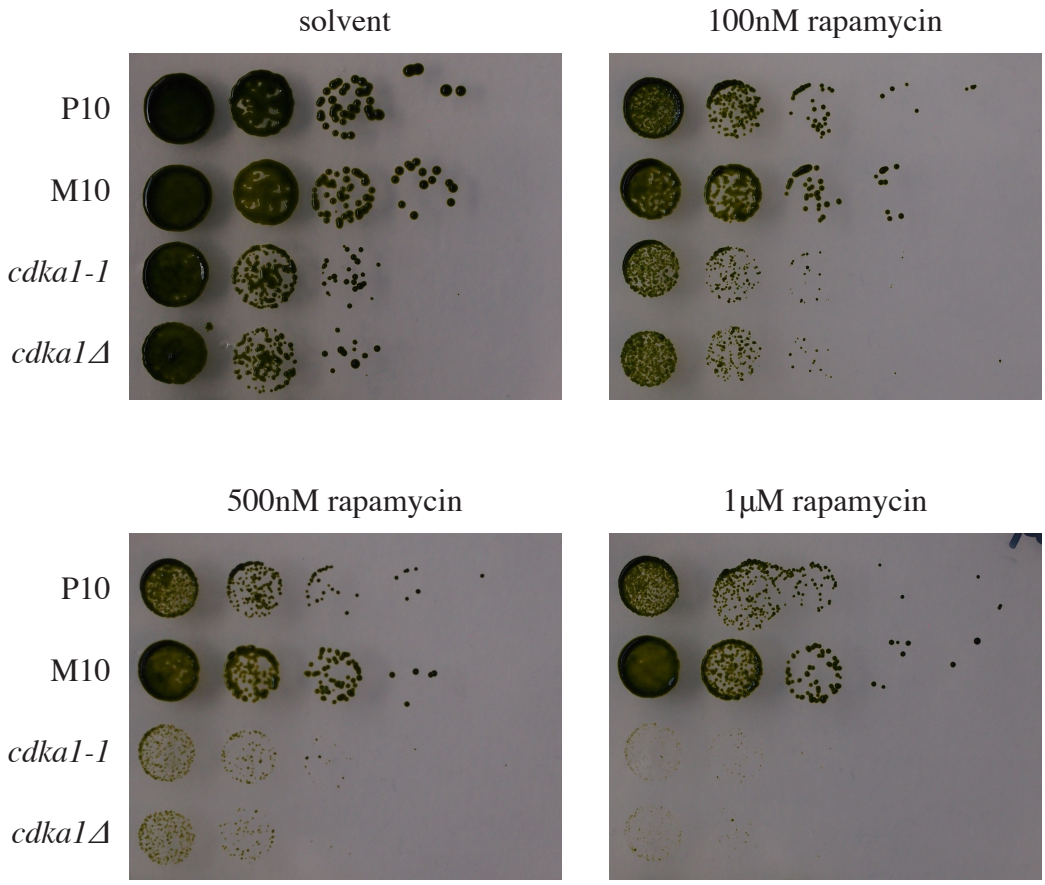

Figure 5.6 *cdka1* mutants are hypersensitive to rapamycin.

Both the missense mutant *cdka1-1* and the disruption mutant *cdka1Δ* are more sensitive to rapamycin than wild type. Wild type strains [P10 and M10 (Tulin and Cross 2014)] exhibit some growth reduction on rapamycin-containing plates, as evidenced by the formation of smaller colonies compared to plates containing only the ethanol solvent. Both *cdka1* mutants, on the other hand, exhibit a dose-dependent loss of viability when grown on rapamycin. All plates were incubated at 30ºC under continuous illumination. Dilutions are ten-fold.

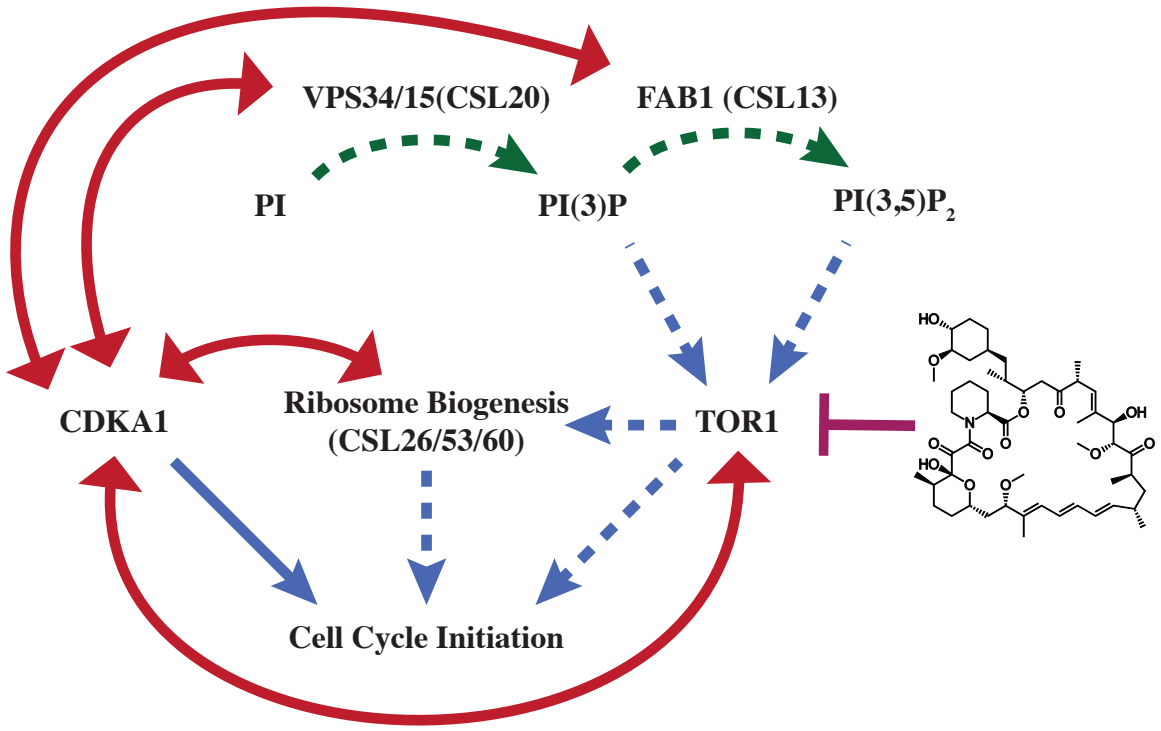

Figure 5.7 A speculative model incorporating CSL and TOR1 in a parallel pathway to CDKA1 in promoting initiation of the cell cycle.

In this model, the *CSL* gene products are presumed to carry out the same function as their homologs in Opisthokonts. The generation of PI(3)P and PI(3,5)P_2 by the lipid kinases VPS34/15 and FAB1, respectively, both contribute to the activation of TOR1. TOR1 then, either on its own or via its activation of ribosome biogenesis, promotes the initiation of the cell cycle alongside CDKA1, providing a back-up mechanism driving this process in the absence of CDKA1 activity. The solid blue arrow indicates the known role of CDKA1 in promoting cell cycle initiation. Dashed blue arrows indicate putative positive regulation based on findings from Opishtokonts. Dashed green arrows indicate putative enzymatic reactions. Synthetic lethal interactions are indicated by solid red double arrows. The purple bar represents the known inhibition of TOR1 by rapamycin (whose chemical structure is depicted to the right of the bar).

an open question. Experiments quantifying phosphorylation of the canonical TOR1 substrate S6K1 (which exists in single copy in the *Chlamydomonas* genome) in the *csl20* and *csl13* mutants would be useful in this regard. Localization of TOR1 may also be affected in these mutants and could be assessed with immunofluorescence microscopy using antibodies against TOR1. TOR1 in Chlamydomonas is normally localized at the apical end of the cell body near the base of the flagella (Díaz-Troya et al. 2008). Perhaps reflecting similar roles, this is also where CDKA1 is found (see Chapter 4).

Also unknown is the role of TOR1 in ribosome biogenesis in *Chlamydomonas* or whether the presumed impairment of ribosome biogenesis upon rapamycin treatment mediates synthetic lethality with *cdka1-1*. A whole genome transcription profile of rapamycin treated cells, quantifying the effect of the drug on levels of transcripts encoding rRNA and ribosomal proteins could demonstrate whether TOR1 regulates ribosome biogenesis in *Chlamydomonas*, at least at the level of transcription. The mechanism whereby combined TOR1 inhibition and mutation of *CDKA1* leads to lethality, and whether this is mediated by a resultant inhibition of ribosome biogenesis, is difficult to probe directly. Evidence from budding yeast suggests Whi5 mediates a delay in Start in response to inhibition of ribosome biogenesis (Bernstein et al. 2007). Assuming there are similarly acting regulatory molecules in *Chlamydomonas*, perhaps downstream effectors negatively regulated by either *CDKA1* or *TOR1*, they may be identified by a suppressor screen for mutations that rescue the *cdka1* mutant on rapamycin. Identification of such genes could begin to unravel the interaction between these two kinases.

Most of the connections in this model are currently speculative, but what is clear is that CDKA1 and TOR1 function in parallel pathways contributing to an essential biological process since their combined impairment results in lethality. Genes identified in this small scale synthetic

lethal screen might provide a glimpse into upstream and downstream components of the TOR1 pathway in *Chlamydomonas*. The functional association of TOR1 with CDKA1 may suggest a close coordination between nutrient sensing, cell growth, and cell division.

Chapter 6 Discussion

Specialization of CDKs in the plant kingdom: CDKB1 replaces CDK1

In Opisthokonts, CDK1 is an essential inducer of mitosis. In *Arabidopsis*, the plant CDK1 homolog, CDKA1, is dispensable, although plants lacking CDKA1 are severely compromised in both cell proliferation and development (Nowack et al. 2012). In *Chlamydomonas*, the mutant *cdka1-1* is delayed for cell cycle entry at restrictive temperature (Tulin and Cross 2014). Here, by the isolation of null alleles, we demonstrate that the CDK1 homolog in *Chlamydomonas* is inessential for viability. CDKA1 is nevertheless required for timely cell cycle initiation, both for the first division after the extended growth period and also for the multiple subsequent divisions that follow before cells hatch and start the cycle anew. Despite timing defects, mutants lacking CDKA1 eventually carry out all the events of the cell cycle successfully.

Thus, in *Chlamydomonas*, CDKA1 is not essential for DNA replication or mitosis, but instead has a primary role in regulating the transition from growth to division. Similar results in *Arabidopsis* (Nowack et al. 2012) suggest a divergence of function after the split of Viridiplantae from Opisthokonts. Assuming CDKB1 was acquired in the plant lineage after the split from Opisthokonts, its acquisition may have allowed for subfunctionalization (Lynch and Force 2000; Lynch et al. 2001). Once CDKB gained the ability to regulate mitosis, CDKA1, no longer an essential gene, lost the ability to promote mitosis and became specialized in the promotion of cell cycle initiation. Alternatively, it could be that the ancestor of plants and Opisthokonts had both CDK1 and CDKB1 and that, in some manner, CDKB1 was lost in the Opisthokonts and CDK1 was co-opted as the mitotic inducer. Other explanations are possible.

CYCA1-CDKA1 activity is likely the primary trigger for cell cycle initiation

In animals, A-type cyclins, in association with CDK2 or CDK1, play an important role in the promotion of DNA replication (Pagano et al. 1992) and the early events of mitotic entry (Pagano et al. 1992; Gong and Ferrell 2010). (CDK2 is a close relative of CDK1 that arose within the animal lineage.) Whereas animal genomes typically encode one or two A-type cyclins, in plants, the A-type cyclin family is greatly expanded. *Arabidopsis* has ten A-type cyclins that fall into three separate families (Vandepoele et al. 2002). The various cyclins are expressed in distinct but overlapping patterns in different tissues and developmental stages. Some A-type cyclins respond specifically to certain plant hormones or developmental signals (Vanneste et al. 2011; Polko et al. 2015). Some regulate the transition from mitotic cycles to endocycles (Imai et al. 2006).

Chlamydomonas has only one A-type cyclin, CYCA1, providing a simplified model for understanding cyclin A function in plants. We find that CYCA1 is inessential, but regulates the transition from growth to division in a similar manner to CDKA1. CYCA1 is also specifically required for full biochemical activation of CDKA1. This activation probably explains the ability of CYCA1 to promote the growth to division transition. Preliminary mass spectrometry results (see below) suggest that CYCA1 is bound to CDKA1 *in vivo*. Together, these results suggest that CYCA1 is likely the primary biochemical activator of CDKA1 in *Chlamydomonas* and the activity of the CYCA1-CDKA1 complex may be the primary trigger for cell cycle initiation.

Cell cycle delay is considerably longer in the *cdka1Δ* mutant than in the *cyca1Δ* mutant. This implies that CDKA1 may have additional cyclin activators besides CYCA1 or perhaps that CDKA1 has cyclin-independent activities. *Arabidopsis* CDKA1 can bind to multiple cyclins, and it is critically dependent on cyclin binding for biochemical activity (Harashima and Schnittger 2012). It seems likely then that CDKA1 is simply activated by multiple cyclins.

CYCB1-CDKB1 is probably the primary inducer of mitosis

In fungi, B-type cyclins regulate both DNA replication and mitosis (Bloom and Cross 2007). In the animal kingdom, B-type cyclins, in association with CDK1, promote entry to mitosis, and their degradation by the APC is essential for completion of the cell cycle (Morgan 2007; Murray and Kirschner 1989; Murray et al. 1989). Degradation of cyclin B is also critical in plants, since non-degradable (destruction box mutant) cyclin B inhibits late mitotic events (Weingartner et al. 2004). In *Arabidopsis*, the CYCB1 family (comprising 4 of the 12 *Arabidopsis* B-type cyclins) is involved in DNA repair, possibly in conjunction with members of the CDKB1 family (Weimer et al. 2016). It may also have a role in regulating mitosis (Schnittger et al. 2002).

As with A-type cyclins, *Chlamydomonas* presents a much simpler system than land plants for analyzing the role of B-type cyclins in the plant kingdom. Its genome encodes only one B-type cyclin, *CYCB1*. We find that *CYCB1* is an essential gene and is required for the formation of mitotic spindles; it is not essential for DNA replication, although replication is delayed upon its inactivation. These and other phenotypes are very similar to those of *cdkb1-1* (Tulin and Cross 2014). This may be explained by direct activation of CDKB1 by CYCB1. Consistently, we find that CYCB1, but not CYCA1, is required for robust activation of CDKB1 kinase activity. Taken together, these results strongly suggest that CYCB1 is the main activator of CDKB1, and that the CYCB1-CDKB1 complex is the predominant mitotic inducer.

Immunoprecipitation of CYCA1 and CYCB1 would allow a direct test of the idea that these cyclins are the biochemical activators of CDKA1 and CDKB1, respectively. Preliminary mass spectrometry experiments (S. Obado, K. Atkins, F. Cross, M. Rout, unpublished) show that CYCA1 but not CYCB1 co-immunoprecipitates with CDKA1, and CYCB1 but not CYCA1 co-immunoprecipitates with CDKB1, supporting this simple biochemical model.

CYCB1 and CYCA1 are likely targets of the APC

The sequences of both CYCA1 and CYCB1 contain canonical destruction boxes near their amino termini. This suggests they may be targeted for destruction by the APC in *Chlamydomonas*. Consistently, both CDKA1 and CDKB1 (whose activity depends on the cyclins CYCA1 and CYCB1, respectively) have elevated kinase activity upon APC inactivation. Epistasis experiments are consistent with APC-targeted destruction of CYCB1: the phenotype of *cycb1* single mutants and *cycb1 cdc27* double mutants are indistinguishable and are distinct from the phenotype of *cdc27* single mutants. A simple explanation for this interaction is that mutational inactivation of CYCB1 mimics the normal downregulation of CYCB1 by the APC. While almost all eukaryotic genomes encode homologs of APC subunits, the excavate *Giardia intestinalis* has none, and therefore degradation of cyclin B may occur by entirely different mechanisms (Gourguechon et al. 2013). This led to the suggestion that the last eukaryotic common ancestor (LECA) may have lacked the APC. However, if Viridiplantae is an outgroup to the other eukaryotic lineages (Rogozin et al. 2010), then the presence and functional conservation of APC in plants supports the ancient role of this complex in mitotic regulation. Sequence analysis and genetic experiments in *Chlamydomonas* support this notion.

Many further experiments can be devised to test whether cyclins are targeted by the APC for destruction in *Chlamydomonas*. Time-lapse microscopy of cells expressing CYCA1 or CYCB1 with fluorescent tags would establish whether these cyclins are degraded in each cell division. Assessing the abundance of CYCA1 and CYCB1 in the *cdc27* mutant would be an informative first step in determining whether their degradation is regulated by the APC. *In vitro* experiments with immunoprecipitated (or recombinant) *Chlamydomonas* APC and recombinant CYCA1 and CYCB1 would be useful to establish whether these cyclins are directly

ubiquitinated by this complex and could also be used to determine whether targeting depends on the presence of their destruction boxes.

A model for *Chlamydomonas* cell cycle control

We propose a working model for *Chlamydomonas* cell cycle control (Fig. 6.1). This model incorporates the role of cyclin-CDKs and the APC in promoting different cell cycle events and the circuitry of their regulatory interactions among themselves. Several putative feedback loops are indicated which may ensure switch-like behavior and temporal ordering of the activation of these regulatory molecules.

The activity of CDKA1 is proposed as the initiator of cell division. This is accomplished at least partly by induction of the mitotic transcriptome. Over 2000 genes are induced coincident with cell division, and many of these depend on CDKA1 for maximal expression (Tulin and Cross 2015). Interestingly *CYCA1* is among the genes whose transcription is CDKA1-dependent. Transcription of *CDKA1* itself, however, is independent of CDKA1 activity. Since CDKA1 promotes the transcription of CYCA1 and CYCA1 is likely a direct biochemical activator of CDKA1, this creates the potential for a positive feedback loop which may generate switch-like activation of CDKA1. The initial activity that 'flips' this putative switch could involve activation of CKDA1 by other cyclins whose transcription is independent of CDKA1 activity.

CDKA1 also drives the transcription of *CYCB1* and *CDKB1* (Tulin and Cross 2015), and we observe that CDKA1 is required for the timely accumulation of CDKB1 protein (Fig. 4.6). Since both CYCB1 and CDKB1 promote DNA replication and mitosis, it could be that CDKA1 drives cell cycle initiation simply by inducing their expression. We have begun to test this idea with a transgene driving *CDKB1* transcription from the *CDKA1* promoter, theoretically

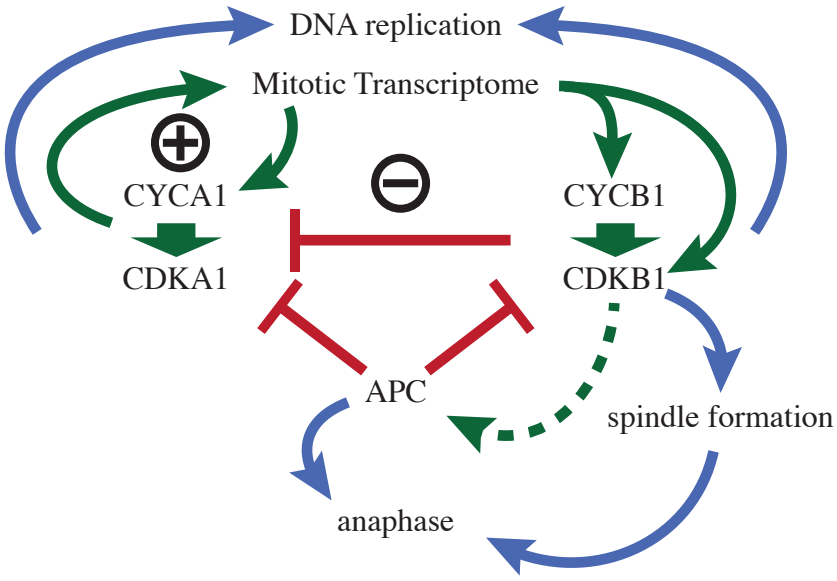

Fig. 6.1 Model for *Chlamydomonas* cell cycle control by CYCA1-CDKA1 and CYCB1-CDKB1.

We propose CYCA1 and CYCB1 as the predominant *in vivo* activators of CDKA1 and CDKB1, respectively (heavy green arrows). The anaphase-promoting complex negatively regulates CYCA1-CDKA1 and CYCB1-CDKB1. CYCB1-CDKB1 also negatively regulates CYCA1-CDKA1. CDKA1 activation of CYCA1 transcription represents a possible positive feedback loop (circled +). CDKA1 activation of CYCB1-CDKB1 with ensuing repression of CDKA1 by CYCB1-CDKB1 represents a possible negative feedback loop (circled -). Blue arrows indicate promotion of cell division cycle events. Green arrows and red bars indicate activating and inhibiting control circuitry respectively. Dashed green line indicates possible activation of the APC by CYCB1-CDKB1.

uncoupling *CDKB1* transcription from the activity of CDKA1. This transgene rescues *cdkb1-1* ts lethality, but shows little, if any, rescue of the delayed cell cycle initiation phenotype of *cdka1* disruption (data not shown). This implies that CDKA1 has unique functions beyond transcriptional induction of *CDKB1*. Since they are predicted to act as a complex, uncoupling both *CDKB1* and *CYCB1* transcription from CDKA1 activity may be sufficient to drive early divisions in the absence of CDKA1. Alternatively, CDKA1 may have roles, either inside or outside of transcriptional induction, that the CYCB1-CDKB1 complex simply cannot provide. It may also be that CDKA1-driven expression of CYCB1-CDKB1 is required for the proper order of cell cycle events. Premature mitosis induced by early expression of CYCB1-CDKB1 may increase the risk of aneuploidy and chromosome breakage if chromosome segregation occurs before chromosomes have completed replication, for instance.

CDKA1 activation of *CYCB1* and *CDKB1* transcription and the subsequent repression of CDKA1 kinase activity by CYCB1-CDKB1 may create a negative feedback loop. This circuit structure, of a negative feedback loop reinforced by positive feedback (CDKA1-> CYCA1-> CDKA1), operates in both animal (Pomerening et al. 2003) and fungal systems (Cross 2003). Recurrence of this regulatory architecture suggests conservation of the overall topology from an early ancestor, with individual molecules and mechanisms of interaction substituted along various lineages. Alternatively, diverse rudimentary control systems may converge to this arrangement over evolutionary time due to its optimality or due to various evolutionary constraints that prevent the evolution of alternative systems (historical constraints, pleiotropy, energetic requirements, etc.).

In Opisthokonts, the activity of the APC and the cyclin-CDKs oscillate out of phase with one another with a once-per-cell-cycle period. Various regulatory mechanisms ensure this

alternation of activity, including a negative feedback loop between the mitotic cyclin-CDKs and the APC (Morgan 2007). In animals cells, the phosphorylation of the APC by mitotic cyclin-CDKs allows binding, and thus activation, by the APC coactivator CDC20 (Qiao et al. 2016). Given the functional displacement of CDK1 by CDKB as the primary mitotic inducer in plants, it could be that CYCB1-CDKB1, in a similar fashion, enables activation of the APC by direct phosphorylation. If such an interaction exists in *Chlamydomonas* (dashed green arrow, Fig. 6.1), inhibition of CDKA1 by CYCB1-CDKB1 may be mediated by activation of the APC and thus degradation of the CDKA1-activator CYCA1. Consistent with this hypothesis, CDKA1 kinase activity is elevated in the absence of APC function.

We propose that initiation of DNA replication is redundantly controlled by the activity of CDKA1 and CDKB1 in complex with CYCA1 and CYCB1. Single mutations in *cdka1*, *cdkb1*, and *cycb1* result in a delay but not a complete block of DNA replication (Tulin and Cross 2014; see above), whereas the double mutants *cdka1 cdkb1* (Tulin and Cross 2014) and *cyca1 cycb1* (Atkins and Cross, forthcoming) completely fail to replicate the genome. One explanation is that the ancestor of CDKA1 and CDKB1 promoted all the events of the cell cycle, somewhat like CDK1 in fungi (see Introduction). Despite the specialization of CDKA1 and CDKB1 for different cell cycle events and the subsequent loss of some redundant functions, they may have preserved some degree of functional overlap, including initiation of DNA replication.

CYCB1 and CDKB1 are both required for spindle formation (Fig. 3; Tulin and Cross 2014) and likely function as a complex, suggesting CYCB1-CDKB1 phosphorylation of spindle-regulatory components. In contrast, the ability of *cyca1* and *cdka1* mutants to complete divisions implies that neither is required for spindle formation (or any other essential cell cycle event).

This represents clear evidence that that the mitotic function of CDK1 is not universal among the eukaryotes and in plants is likely the responsibility of B-type cyclins and B-type CDKs.

The connection of CDKA1 to inositol metabolism, ribosome biogenesis, and TOR

The inessentiality of CDKA1 in plants implies that back-up mechanisms exist to provide essential function in the absence of CDKA1 activity. In wild type cells, such parallel pathways probably work alongside CDKA1 to promote cell cycle initiation. We carried out an enhancer screen in the *cdka1-1* mutant in order to identify such pathways and gain a fuller picture of the control of cell cycle initiation in *Chlamydomonas*. The fraction of possible target genes that were identified in this screen is likely small since no double hits were identified (11/11 identified mutations are single hits); nevertheless, the screen unveiled multiple mutations in genes with predicted functions in two pathways—inositol metabolism and ribosome biogenesis.

We have not yet determined whether the genes identified in this screen carry out the same role as their sequence orthologs in Opisthokonts, but this is a conservative preliminary assumption. In Opisthokonts, both inositol lipid metabolism and ribosome biogenesis are connected to the TOR pathway. In both animals and fungi, inositol lipid kinases act upstream of TOR; they respond to the same external signals as TOR and their activity is required for the phosphorylation of canonical TOR substrates. Ribosome biogenesis is downstream of TOR. One of the primary functions of TOR is to induce the biogenesis of ribosomes as a response to anabolic hormones or the availability of nutrients.

We tested whether the combined depletion of TOR and CDKA1 activity would result in lethality. If TOR acts in a parallel pathway to CDKA1 to promote cell cycle progression, the

simultaneous impairment of TOR and CDKA1 should result in a failure to initiate the cell cycle and thus death. Indeed, *cdka1* mutants are hypersensitive to the TOR-inhibitor rapamycin.

TOR is recognized as a central regulator of both cell growth and cell cycle progression in Opisthokonts. Because of its multiple roles, the mechanisms of cell cycle regulation by TOR are sometimes unclear. TOR may act directly by modulating the cell cycle control machinery. Alternatively, it could be that cell cycle progression is influenced indirectly by the global effects of TOR activity on translation and cell growth. In budding yeast, the cell cycle is delayed by TOR inhibition, but this delay can be rescued by uncoupling the translation of the G1 cyclin Cln3 from TOR activity (Barbet et al. 1996). In a parallel result to our observation of rapamycin hypersensitivity of *cdka1* mutants, budding yeast mutants lacking the S-phase cyclin Clb5 are also hypersensitive to rapamycin. Additionally, the delay in DNA replication due to Clb5 deletion is significantly extended on rapamycin treatment, suggesting TOR and Clb5 may coordinately control this process (Tran et al. 2010). In plants, TOR can directly activate the cell cycle. In response to glucose, TOR directly phosphorylates and thus activates the transcription factor E2Fa, leading to the induction of S-phase genes and cell proliferation in the root meristem. TOR activation in this context may bypass the typical requirement for cyclin-CDK activation of E2F for the induction of cell divisions (Xiong et al. 2013).

The connection between TOR1 and cell cycle initiation in *Chlamydomonas* is unclear. We propose that mutations identified in the synthetic lethal screen with *cdka1-1* may identify components of the TOR1 pathway in *Chlamydomonas*. A robust assay for measuring TOR1 activity, perhaps measurement of the phosphorylation of a canonical substrate, would be useful for testing this idea. More detailed experiments are suggested in Chapter 5. Additionally, it may be useful to perform a synthetic lethal screen on a larger scale with more sophisticated

techniques. A 'dropout' viability screen using a deletion library may reveal additional pathways acting parallel to CDKA1 that were missed in the screen conducted here.

Future directions

Two aspects of the model we present are particularly intriguing, and their investigation could yield insight into the central mechanisms governing plant cell cycle regulation. The first is the possible positive feedback loop between CDKA1 and CYCA1. As suggested, this may generate switch-like activation of CDKA1, ensuring a swift and irreversible decision to initiate the cell division program. Uncoupling CYCA1 transcription from CDKA1 activity, by expressing CYCA1 from the CDKA1 promoter for instance, would abolish this positive feedback loop and may result in diminished CDKA1 activity and a consequent delay in cell cycle initiation. Expression of CYCA1 from an inducible promoter would enable a more careful evaluation of the positive feedback model. CDKA1 activity may be ultrasensitive to CYCA1 levels: brief induction of CYCA1 expression may be insufficient to activate the 'CDKA1 on' state, but some threshold level may promote sustained high CDKA1 activity and CYCA1 expression. If high CDKA1 activity is sufficient to initiate the cell cycle, it may be possible to induce early divisions by inducing CYCA1 expression during the extended growth period in *Chlamydomonas*.

Genetic experiments suggest that CDKA1 is probably activated by cyclins other than CYCA1. Activation of CDKA1 by cyclins whose transcription is independent of CDKA1 activity could 'flip' the putative CYCA1-CDKA1 switch described above. Both *CYCD1* and *CYCAB1* are transcribed around the time of cell division in a CDKA1-independent manner (Tulin and Cross 2015) and are good candidates for such an activity, should it exist. Targeted mutation of these loci may be worth pursuing, especially given recent advancement in

technologies for gene targeting in *Chlamydomonas* using engineered nucleases (Greiner et al. 2017). The ablation of various cyclins, in some combination, may lead to a delay or a failure of CDKA1 activation and CYCA1 expression and a subsequent delay in cell cycle initiation. Conversely, early misexpression of such cyclins may induce early divisions.

Alternatively, it may be possible to isolate non-CYCA1 activators of CDKA1 using forward genetics. Mutational inactivation of such activators in a *cyca1Δ* mutant background may very well mimic the behavior of the *cdka1Δ* mutant. Therefore, a repetition of the 'death delay' screen (Ch. 2) in the *cyca1Δ* mutant background may yield such mutations. This approach benefits from a lack of bias in searching for CDKA1-activators and the potential for isolation of conditional mutations, but is limited by the requirement for at least some degree of non-redundancy among activators.

Another interesting regulatory feature, supported by our biochemical experiments in various mutants, is the inhibition of CDKA1 kinase activity by CYCB1-CDKB1. We do not yet understand the mechanism of CDKA1 inhibition by CYCB1-CDKB1. One idea, suggested above, is that this inhibition may be mediated via CYCB1-CDKB1 activation of the APC and the subsequent APC-targeted destruction of the CDKA1-activator CYCA1 (Fig 6.1). This explanation is consistent with the known role of mitotic cyclin-CDKs and the APC in other systems, but involves many interactions whose existence in *Chlamydomonas* is not yet fully understood. Since CYCA1 is a major regulator of CDKA1 and is required for the elevated kinase activity of CDKA1 in the *cycb1-3* mutant (Fig. 4.8A), a simple first step would be to determine whether CYCA1 abundance is elevated in the *cdkb1-1* or *cycb1-5* mutants. If CYCA1 is elevated in this context, next steps would include determining whether CYCA1 is targeted by the APC (experiments are suggested in prior sections) and whether the APC is activated by CYCB1-

CDKB1. *In vitro* ubiquitination assays could be used to determine whether the APC is hypoactive in *cycb1* or *cdkb1* mutants, for instance. Alternatively, it may be that CYCA1 abundance is unperturbed by mutation of *CDKB1* or *CYCB1*. In this case, comparison by mass spectrometry of CDKA1 complexes immunoprecipitated from wild type and *cycb1*/*cdkb1* mutants may reveal differences in post-translational modifications or binding partners whose importance to CDKA1 activity could then be tested by *in vitro* kinase assays with recombinant proteins.

Conclusions

Many features of this model we present are familiar. Mitotic induction by B-type cyclins, downregulation of cyclin-CDKs by the APC, and the overall topology of interactions among regulators is similar to that of the Opisthokonts. Some features are novel, including the replacement of the mitotic inducer CDK1 by CDKB—the plant CDK1 homolog, CDKA1, rendered inessential and functioning primarily to induce the growth to division transition, likely in a complex with CYCA1. Biochemical experiments suggest the presence of a negative feedback loop operating between CYCA1-CDKA1 and CYCB1-CDKB1, with the possibility of positive feedback stabilizing the state of CYCA1-CDKA1 activation. Positive feedback may allow a switch-like decision to initiate cell division, and negative feedback may ensure orderly progression of the activity of the specific cyclin-CDKs (and thus the events they control). The TOR kinase may act somewhat redundantly alongside CDKA1 to promote initiation of the cell cycle, although more experiments are necessary to establish whether this is the case.

We have begun to elucidate the function of cyclins in *Chlamydomonas*. CYCA1 and CYCB1, the only A-type and B-type cyclins in the *Chlamydomonas* genome, are required for

activation of CDKA1 and CDKB1, respectively. Preliminary results suggest specific binding between CYCA1-CDKA1 and CYCB1-CDKB1, supporting a model whereby these cyclins directly activate their respective CDKs. The A-A and B-B pairings are further supported by the similarity of phenotypes upon inactivation of CYCA1/CDKA1 and CYCB1/CDKB1. Despite the relative promiscuity in binding between various CDKs and cyclins when overexpressed (Boruc et al. 2010), our results suggest cyclin-CDK pairing in *Chlamydomonas* is rather modular. Nevertheless, we expect CDKA1 has cyclin activators besides CYCA1 and that CYCA1 likely has CDKA1-indpendent biological activities, perhaps in complex with other CDKs. The relative simplicity of the *Chlamydomonas* system should continue to provide a deeper understanding of cyclin function in the plant kingdom as the function and regulation of these and other cyclins are further explored.

The plant and Opisthokont lineages have undergone separate evolutionary change for hundreds of millions of years, with exceedingly rare horizontal transfer of genetic material between them (Richards et al. 2009). It is rather striking then that certain features of cell cycle control are so well conserved. This must imply something profound about either the optimality of the control system or the constraints of evolution to build alternative systems. On the other hand, some features are significantly diverged, suggesting a degree of flexibility which may have played a role in the capacity of various lineages to develop their unique and diverse lifestyles. Alternatively, these variations may simply reflect the settlement of different lineages in local 'minima' in the fitness landscape (Wright 1932). Given the dependence of much of life on earth, including humanity, on various members of the plant kingdom, understanding the conservation and divergence of biological mechanisms in this kingdom, compared to the well-characterized animal and fungal lineages, may be of great utility.

Appendix A1 Methods

Alleles and strain construction

The *div19-2* (p.Pro569>Phe), *cdka1-1* (p.Phe147>Cys), *cdkb1-1* (p.Pro180>His, previously called *div48*), and *cdc27-6* (p.Met884>Ile, Gly885>Ser, previously called *div23-6*) mutants were described previously (Tulin and Cross 2014). The *cycb1-5* mutant (p.Glu325>Lys) was isolated by F. Tulin (unpublished). *cycb1-1* (p.Leu288>Pro) and *cycb1-3* (p.Glu325>Lys; same change as *cycb1-5*) were provided by M. Breker (unpublished). The disruption of CYCA1, designated *cyca1Δ*, was obtained from the Chlamydomonas Library Project (http://www.chlamylibrary.org). The disruption allele of *CDKA1*, designated *cdka1Δ*, has a 7-base pair deletion that disrupts codons 89-91, followed by an insertion of the Aph7" cassette (described below) just downstream of codon 93. The *cdka1Δ*^{paro} mutant has an insertion of the AphVIII cassette (also described below) that in codon 79. Genetic crosses were carried out as described (Dutcher 1995).

Transformation

Transformation was carried out by electroporation. Approximately 50x10^{6} cells were washed and suspended in CHES buffer (40mM sucrose, 10mM sorbitol, 10mM n-cyclohexyl-2-aminoethanesulfonic acid, pH=9.25) to 250μL. DNA was added to the cell suspension and the mixture was incubated on ice for 5min. Electroporation was then carried out using a Bio-Rad Gene Pulser on exponential protocol with pulse parameters of 500V, 50μF, 800Ω in a 2mm gap cuvette. After 15min, cells were suspended in 10mL of TAP + 40mM sucrose buffer to recover for 12-16h. After recovery, cells were collected by centrifugation and spread on selective media (TAP + 10μg/mL paromomycin or 10μg/mL hygromycin).

Death delay screen

For generation of insertional *tdd* mutants, the *div19-2* strain (backcrossed six times) was transformed in ten separate transformations with 0.5µg of the *AphVIII* cassette (conferring resistance to paromomycin) amplified from pSI103 using primers KA019 and KA020. Five separate transformations with 0.5µg of the *Aph7"* cassette (conferring resistance to hygromycin) were performed by amplifying from the pHyg3 plasmid using the same primers. Transformants were spread on selective media and allowed to form colonies for 48h at 21ºC under 14h light/10h dark cycles to induce partial synchrony.

To select for 'death delay' mutants, plates were transferred to 33ºC for 20h, followed by transfer to 21ºC for 48h to allow surviving mutants to proliferate. Plates were transferred again to 33ºC for 20h for another round of selection. Following two rounds of selection at 33ºC, plates were incubated at 21ºC until visible colonies had formed (8 days). All selection and recovery periods were under continuous illumination. Surviving colonies were picked manually, avoiding very small colonies. To characterize growth of these mutants, cells were grown on TAP agar plates for 20h at 33ºC and imaged on a Zeiss Axioskop 40 tetrad dissection microscope with a Canon EOS 50D digital camera. Cell area was measured using ImageJ.

For generation of UV-induced *tdd* mutants, a *div19-2* culture was grown in liquid TAP to an optical density at 750nm (OD_{750}) of 0.17. Cells were collected by centrifugation and spread on ten 100mm TAP agar plates at a density of ~2 million cells per plate. Plates were mutagenized by exposure to UV light for 0-2 minutes and incubated in the dark at 21ºC for two days. Selection was as described above except exposure to 33ºC was for 16h instead of 20h. Surviving colonies were picked manually, avoiding very small colonies.

Mutant identification

The genomic location of insertions was determined using either the RATE technique (Karlyshev et al. 2000) or the Hairpin PCR technique (Plecenikova et al. 2014). For RATE, primers KA021 and KA022 were used in separate single primer reactions to amplify flanking genomic DNA from the 5' and 3' end of the *AphVIII* insert, respectively (or the 3' and 5' ends of the *Aph7"* insert, respectively). illustra PuReTaq Ready-To-Go PCR Beads (GE Healthcare) were used with described cycling conditions (Karlyshev et al. 2000). Sanger sequencing was performed using primers KA023 or KA024 for fragments amplified with KA021 or KA022, respectively.

For hairpin PCR, gDNA was purified using the DNeasy® Plant Mini Kit (Qiagen). gDNA was cut with *NaeI*, *PmlI*, *PvuII*, and *StuI*. Cut gDNA (300ng) was ligated to a blunt-ended hairpin (1.6µM, KA025). PCR was performed with either primer KA021 or KA022 in combination with KA026 using Q5® High Fidelity DNA Polymerase (New England Biolabs). Nested PCR was performed using primers KA023 or KA024 (for those reactions with KA021 or KA022, respectively) in combination with KA026. Sanger sequencing was performed with either KA023 or KA024.

Mutations in UV-induced mutants were determined by amplifying two fragments covering the coding sequence of CDKA1 and sequencing these fragments from both ends by Sanger sequencing. The first fragment was amplified using the primers KA027 and KA028, the second fragment using primers KA029 and KA030. PCR was performed using Q5® High Fidelity DNA Polymerase (New England Biolabs) and standard cycling conditions.

Plasmid construction

Plasmids pKA11 and pKA1 were constructed using one-step isothermal assembly with the NEBuilder® HiFi DNA Assembly Master Mix (New England Biolabs). Primers used to construct plasmids are listed in Appendix A2. Genomic DNA (gDNA) for PCR was prepared as described (Lin et al. 2013). Both plasmids were constructed with pSI103 (obtained from the Chlamydomonas Resource Center) as a backbone, cut with the restriction enzyme *PsiI*. All PCR reactions were carried out with the Q5® High Fidelity DNA Polymerase (New England Biolabs) with standard cycling conditions.

To construct pKA11, the promoter and 5' UTR of CDKA1 were amplified from genomic DNA using the primers KA001 and KA002. Genomic DNA including coding sequence and introns of CDKA1 was amplified using primers KA003 and KA004. The stop codon, 3' UTR, and terminator of CDKA1 were amplified with primers KA007 and KA008. *Chlamydomonas* codon-optimized mCherry was amplified from the plasmid pBR29-mCherry (Rasala et al. 2013) with the primers KA005 and KA006. Sequence for a small linker $(3X\ GGGGS)_3$ was included in primers KA004 and KA005 between the coding sequences of CDKA1 and mCherry.

pKA1 was constructed in a similar manner. The promoter, 5' UTR, coding sequence and introns of CDKB1 were amplified from gDNA using primers KA009 and KA010. The stop codon, 3' UTR, and terminator of CDKB1 were amplified from gDNA using the primers KA013 and KA014. Again, sequence was included in the primers KA010 and KA001 to introduce a 3X GGGGS linker between the coding sequences of CDKB1 and mCherry.

pKA16 was constructed by overlap-extension PCR to introduce the K33R mutation. One fragment was amplified from pKA1 with the primers KA015 and KA016, another was amplified with primers KA017 and KA018. These fragments were fused by overlap extension PCR using

primers KA015 and KA018. The unified fragment was then cloned into pKA1 after removing a fragment flanked by *SfiI* and *XhoI*.

Timelapse microscopy

Cells are grown to saturation on TAP plates [prepared as described (Harris 2009)] at 21ºC under continuous illumination. Saturated cells are resuspended in liquid TAP, transferred to TAP agar plates, and placed at 33ºC with illumination. At various intervals, the plate is transferred to a heated, illuminated chamber on a Zeiss Axioskop 40 tetrad dissection microscope stage with calibrated positions, and bright-field images are captured. Custom MATLAB software segments individual cells and presents an interface for manual scoring of cell divisions across time-points. The scoring scheme yields reproducible results between experiments and between independent strains of the same genotype.

Appearance of a division plane at one time-point and not the prior implies that the division occurred sometime between those time-points. To be conservative, we assign time of division to the midpoint between these times. (A minor exception: the second time-point occurs 10h after plating, and we know that divisions almost never occur before 9h in this protocol. Therefore, divisions scored at 10h are assigned a time of division at 9.5h. These cells are rare).

For a cell to be scored, it must be in reasonable focus in all time-points, and contacted little or not at all by other cells so that a full view can be obtained. We require no cell lysis across the time-course. Most lysis occurs by the second time-point and presumably reflects initially inviable cells (possibly damaged in handling or plating). We also restrict attention to cells (the large majority) that exhibit significant growth (at least a two-fold increase in cell area).

Time-lapse microscopy for Chapter 5 was conducted in a similar manner except with a different microscope set-up and divisions were not quantitatively scored. Strains were incubated in 96-well plates in liquid TAP for two days at 21ºC. Cells were transferred to a TAP agar plate with a 96-pin replica tool (V&P Scientific). The plate was transferred to 30ºC under continuous illumination and cells were imaged at regular intervals with a Leica DMIRE2 microscope with a 10x/0.25NA bright-field objective, in a heated chamber. A motorized stage was used to revisit specific positions. Images were collected with a Canon EOS Rebel T2i.

Synchronization

Cells are grown to saturation on TAP agar plates at 21ºC under continuous illumination. Saturated cells are resuspended in TAP lacking nitrogen. Around 20 million cells (equivalent to 5mL of cells at OD_{750} of 0.4) of this suspension is spread on a 100mm TAP + 1.5% agar plate with ammonium chloride at 10% the typical amount (10% N-TAP). Cells are incubated at 21ºC with continuous illumination for 24h. During this time, most cells carry out two divisions, then arrest due to nitrogen deprivation. Nitrogen starved cells are resuspended, spread on 100% N-TAP agar plates, and incubated at 33ºC with continuous illumination. In this protocol, wild type cells exhibit little to no DNA replication or cell division for around 10 after transfer to 33ºC. Wild type cells then undergo 3-4 rapid sequential divisions. Entry into divisions is somewhat asynchronous but almost all wild type cells have completed divisions and hatched by 16h.

Flow cytometry

Flow cytometry was performed as described (Tulin and Cross 2014).

Immunostaining and fluorescence microscopy

Indirect anti-α-tubulin immunofluorescence and DNA detection (by SYTOX green) were performed on methanol-fixed cells as described (Tulin and Cross 2014). Images were collected using DeltaVision deconvolution microscopy. DIC images are from one in-focus z-slice. DNA images are blurred by Gaussian smoothing (σ=6) and presented as maximum intensity z-projections. Gaussian smoothing reduced the patchy appearance from maximum intensity projections due to occasional very bright pixels in some sections. α-tubulin images are maximum intensity z-projections without smoothing. All images are individually contrast-adjusted for clarity, so intensities should not be compared across images.

Transformation with tagged *CDKA1* and *CDKB1* transgenes

For generation of strains expressing mCherry-tagged CDKs, 1μg of uncut pKA11 or pKA1 was transformed into *cdka1-1 csl89* or *cdkb1-1*, respectively. For each transformation, expression of the integrated mCherry-tagged transgenes was assessed by Western blot in ten transformants after incubation at 33ºC for 16h following synchronization by nitrogen starvation. Untransformed parent strains were used as negative controls. Complementation of temperature-sensitivity was assessed by serial dilution of transformants. Transformants were grown on TAP agar plates and suspended in liquid TAP to an OD_{750} of 0.1. From this culture, five five-fold serial dilutions were made and 10μL of each dilution were dropped onto TAP agar plates. Untransformed parent strains and appropriate *csl89* or wild type strains were used as negative and positive controls, respectively.

Western blot

Protein samples for Western blot were prepared by lysing cells as described below (Immunoprecipitation and Protein Kinase Assay). For each sample, 20µg of lysate was used for Western blot. Western blot was performed according to standard methods. Anti-mCherry antibody (Thermo Fisher, M11217) was used at a dilution of 1:1000. Anti-AtpB antibody (Agrisera, AS05 085) and HRP-conjugated secondary antibodies (Thermo-Fisher, A18865; GE Healthcare, NA934) were all used at a 1:2000 dilution. Blots were imaged with an ImageQuant LAS 4000 imager (GE Healthcare). Quantification and contrast adjustment were performed using ImageJ.

Conjugation of LaM-2 nanobody to beads

LaM-2 nanobody (Fridy et al. 2014) was kindly provided by Peter Fridy. LaM-2 was conjugated to Dynabeads® M-270 Epoxy (Invitrogen, 14302D) essentially according to protocol; 1mg of LaM-2 was conjugated to 100mg of Dynabeads and resuspended in 700µL of PBS, pH = 7.4 with 50% (v/v) glycerol and stored at -20ºC.

Immunoprecipitation and protein kinase assay

Cells were collected by centrifugation, resuspended in 1mL of ice-cold LSHN buffer (10mM N-2-hydroxyethylpiperazine-N'-2-ethanesulfonic acid [HEPES; pH = 7.5], 50mM NaCl, 10% [v/v] glycerol), pelleted again by centrifugation and stored at -80ºC. For later time-points (10h-16h), approximately 20 million cells (5mL at an OD_{750} of 0.4) are sufficient; for earlier time-points, 20-100 million cells are required. 200µL of acid-washed glass beads (Sigma, G8772) were added to the cell pellet followed by addition of 250µL of RIPA buffer (50mM Tris [pH = 7.4], 150mM

NaCl, 1mM EDTA, 1% [v/v] Nonidet P-40 [NP-40], 0.5% [v/v] sodium deoxycholate, 0.1% [w/v] sodium dodecyl sulfate [SDS]) containing phosphatase inhibitors (10mM sodium pyrophosphate) and protease inhibitors (10% aprotinin [Sigma, A6279], 0.5mM phenylmethylsulfonyl fluoride, 10μg/mL of leupeptin, 10μg/mL of pepstatin). Cells were broken at 4ºC using a FastPrep FP120 Cell Disruptor (Thermo Electron Corporation) with two cycles of lysis for 20s each on setting 5. Lysate was microcentrifuged for 5min and transferred to a new tube. Protein concentration of lysates was determined using the Pierce BCA Protein Assay Kit (Thermo Scientific). 200μg of protein was diluted in RIPA buffer plus inhibitors to 200μL and added to 10μL nanobody-conjugated Dynabeads. Lysate was incubated with beads with rotation for 1h at 4ºC. Following binding, the beads were washed 4x with 1mL of RIPA buffer, 2x with 1mL HNN buffer (10mM HEPES [pH = 7.5], 250mM NaCl, 10% [v/v] glycerol, 0.1% [v/v] NP-40), and once with 1mL kinase buffer (10mM HEPES [pH = 7.5], 50mM KCl, 10mM $MgCl_2$, 1mM dithiothreitol). Beads were suspended to a final volume of 60μL in kinase buffer, and 15μL of the suspension was added to 5μL of master mix (1μL of 2mg/mL histone H1 [EMD Millipore, 382150], 2μL of 50μM ATP, 1μL of [γ-^{33}P]ATP [PerkinElmer, NEG502A001MC], and 1μL of water). This kinase reaction mixture was incubated at 30ºC for 15min, with mixing every 3min. Reactions were stopped by addition of 20μL of 2x SDS sample buffer with β-mercaptoethanol. 45μL of 2x SDS sample buffer was added to the remainder of the immunoprecipitate, and 12μL was loaded onto a polyacrylamide gel for Western blot after heating for 10min at 95ºC. For the kinase reaction, a polyacrylamide gel was run with 10μL of the kinase reaction. The free (γ-^{32}P)ATP was cut from the gel front, and gels were stained with GelCode Blue Stain Reagent (Thermo Scientific) to image histone H1. Quantification of radioactivity was by exposure to a

storage phosphor screen (Molecular Dynamics), and imaging with a Typhoon 9400 Variable Imager (Amersham Biosciences).

Live-cell confocal fluorescence microscopy

Synchronized cycling populations of cells were placed on thin TAP + 1.5% low melt agarose slabs for imaging. Confocal laser microscopy was performed using an inverted TCS SP8 confocal microscope (Leica) equipped with three HyD detectors and one PMT detector. Objective lens used was HC PL APO CS2 63x/1.40 oil with an optical zoom of 0.75x. Scan speed was 600Hz. Images were obtained with a resolution of 1024x1024 pixels. Time gating of 0.3-12.0 ns was used to eliminate chloroplast autofluorescence (Kodama 2016). mCherry images were acquired with excitation from the 587nm laser light and xyz scanning with the hybrid detector at 597-660nm with 4x line accumulation. Nuclear *ble-GFP* was imaged with excitation from the 489nm laser light and xyz scanning with the hybrid detector at 497-561nm with line averaging of 2x. Bright-field images were obtained with the PMT trans detector. ImageJ was used for average Z-projections and contrast adjustment as described in figures.

Nuclear concentration of CDKB1 (Figure 4.5G) was measured using confocal micrographs of a live, cycling population of *cdkb1-1 CDKB1-mCherry ble-GFP*. Individual nuclei were partitioned from ble-GFP images using ImageJ. Within the nuclear boundaries, pixel intensities were summed through the z-stack in the CDKB1-mCherry images. Nuclear concentration of CDKB1-mCherry is then calculated by dividing the sum of the pixel intensities by the number of pixels within the nuclear boundaries. Background fluorescence is subtracted from the signal using a correction factor determined from images of the *ble-GFP* (no CDKB1-mCherry) strain. Nuclear concentration is plotted against number of nuclei in a cell cluster. Red

circle and bars represent mean and standard deviation, respectively. The signal in one-cell and 16-cell nuclei is essentially background. The result indicates that CDKB1 does not have a protracted period of low abundance at any time during the S/M cycles, since this would produce a bimodal distribution of intensities in the 2, 4 and 8 nucleus cells (since these are still proliferating and about to undergo another division).

Synthetic lethal screen with *cdka1-1*

Cultures of the *cdka1-1* mutant (backcrossed six times) were grown in liquid TAP at 21ºC. Cultures were diluted to an OD_{750} of 0.1 and 25mL of the culture were transferred to a shallow plastic dish. Cells were exposed to UV light for 3.5min while shaking and incubated in the dark at 21ºC overnight. Several dilutions of the mutagenized culture were prepared, spread on TAP agar plates, and incubated at 21ºC under continuous illumination to allow mutant colonies to form. Individual mutant colonies were then robotically picked using the RapidPick™ colony picker (Hudson Robotics) and transferred either into a 384-well plate filled with liquid TAP or in an ordered array onto a solid TAP + 1.5% agar plate. Arrayed mutants were replica plated at both 21ºC and 30ºC and visually screened for defective biomass accumulation at 30ºC. We used a restrictive temperature of 30ºC instead of 33ºC as in (Tulin and Cross 2014) since *cdka1* mutants show some reduction in biomass accumulation at 33ºC, but not at 30ºC (Fig. 2.2). A phenotypic subset of ts lethal mutants were crossed to a wild type strain; tetrads were dissected and replica plated at both 21ºC and 30ºC to determine whether lethality was synthetic with the *cdka1-1* mutation. In some cases, *csl* mutants were crossed to the $cdka1\Delta^{paro}$ mutant and synthetic lethality at 30ºC was observed with this allele as well.

Preparation of genomic DNA and sequence analysis

Ten to twelve ts lethal segregants were isolated in crosses of *cdka1-1 csl* mutants (either the primary mutants or a backcrossed strain) to wild type and were cultured independently. Segregants were combined in equal proportion and their pooled genomic DNA was prepared and sequenced as described in (Tulin and Cross 2014). Sequence analysis and SNP identification are as described in (Tulin and Cross 2014).

Toe-hold primer genotyping

We used 'toe-hold' primers (Byrom et al. 2014) for genotyping in PCR-based mapping of the putative causative *csl* mutations. Essentially, two end-point PCRs are carried out: one reaction with a primer pair that only allows efficient amplification from a wild type template and another reaction with a primer pair that only allows efficient amplification from a mutant template. We used a 4-nucleotide toe-hold when designing primers. Genomic DNA (gDNA) is prepared from segregants by suspending cells in 1x VENT buffer [100mM KCl, 100mM $(NH_4)_2SO_4$, 20mM $MgSO_4$, 1% Triton-X-100, 200mM Tris-HCl, pH = 8.8] with 20µg of proteinase K and incubating for 1h at 58ºC followed by 0.5h at 95ºC. The two reaction mixtures (one for wild type, one for mutant) are prepared by combining 10pmol of both forward and reverse primer, 0.5µL of the crude gDNA prep, and ddH_2O to 25µL and adding this mixture to illustra PuReTaq Ready-To-Go PCR Beads (GE Healthcare). We found empirically that 40-45 cycles of 95ºC/30s, 60ºC/30s, 72ºC/30s is sufficient to detect PCR product when 10µL of the final reaction product is loaded on a 1% SB agarose gel and visualized under UV light after staining with ethidium bromide. All primer pairs were verified as discriminating appropriately between wild type and mutant alleles with strains verified by Sanger sequencing as harboring the expected allele.

Revertant isolation and sequencing

A given *cdka1 csl* mutant (with either the *cdka1-1* or *cdka1Δ*^{paro} allele) is cultured in liquid TAP at 21ºC under continuous illumination. Approximately 50 million cells (50mL of culture at OD_{750} of 0.1) are spread on individual 100mm TAP + 1.5% agar plates and exposed to UV light for 0-3min. Plates are wrapped in aluminum foil immediately after mutagenesis and kept in the dark overnight. Following dark incubation, the foil is removed and plates are incubated at 30ºC under continuous illumination to select for rescue of ts lethality. Viable colonies are used to prepare gDNA as described above ('Toe-hold primer genotyping') and the candidate SNP is amplified by PCR using appropriate primers and touch-down PCR (Korbie and Mattick 2008). PCR products were sequenced by Sanger sequencing.

Appendix A2 Primers

Primer Name	Sequence 5'-3'
KA001	TATCTCGGTCTATTCTTTTGATTTACATGATGCAGGTGTGGAGG
KA002	CATGATTAGGCCCCCAGCGC
KA003	AGGTGGCGCTGGGGGCCTAATC
KA004	CACCACCGCCGCTACCGCCGCCGCCGGAGCCGCCACCACCGCGCATCACGCCCATTCCGC
KA005	GGCTCCGGCGGCGGCGGTAGCGGCGGTGGTGGCTCGATGGTGTCCAAGGGCGAGGAG
KA006	CCGGCACCGGTGCTGCTGCTCATCACTTGTACAGCTCGTCCATGC
KA007	TGATGAGCAGCAGCACCGG
KA008	AGGCCGAAATCGGCAAAATCCCTTAGTGCGACTTTTGATTCGCCA
KA009	TATCTCGGTCTATTCTTTTGATTTGCTCCAGAAGGTGGCAGAAG
KA010	CCGCTACCGCCGCCGCCGGAGCCGCCACCACCGCAGACAACGTTGGCGGCG
KA011	CCGGCGGCGGCGGTAGCGGCGGTGGTGGCTCGATGGTGTCCAAGGGCGAG
KA012	ACCGTGCCCACGCCCTCTCACTTGTACAGCTCGTCCATGC
KA013	TGAGAGGGCGTGGGCACGG
KA014	AGGCCGAAATCGGCAAAATCCCTTACGTGCAGAAACGTTGCCTTTG
KA015	ACGCAGCTGTGCGTGCGTGC
KA016	GCGGCACTTGCGCAGCGCGACCAGCTTCCC
KA017	TCGCGCTGCGCAAGTGCCGCCTTGAAATGG
KA018	CCGTAGTTCAAGAAAGCATC
KA019	CGTTGTAAAACGACGGCCAG
KA020	TTCCGGCTCGTATGTTGTGT
KA021	ACGCACCAATCATGTCAAGC
KA022	CGGGTACCCAGCTTTTGTTC
KA023	ACGCACCAATCATGTCAAGC
KA024	GGGTTAATTTCGAGCTTGGC
KA025	GGATCCGTAGTCCAAGTCTCACAGTCTATTTTTAGACTGTGAGACTTGGAGATGGGATCC
KA026	TAGACTGTGAGACTTGGAGATG
KA027	AGTAACCTGGAGAGCACCCT
KA028	CCTGTATTGTCCTGCGGCTT
KA029	CAGCGACGCTTCGGTTTATG
KA030	TCAGCCAATATGGCACGGTT

References

Adams K, Wendel J. 2005. Polyploidy and genome evolution in plants. *Curr Opin Plant Biol* **8**: 135–141.

Anderson J, Phan L, Cuesta R, Carlson BA, Pak M, Asano K, Björk GR, Tamame M, Hinnebusch AG. 1998. The essential Gcd10p-Gcd14p nuclear complex is required for 1-methyladenosine modification and maturation of initiator methionyl-tRNA. *Genes Dev* **12**: 3650–62.

Andrew C, Hopper A, Hall B. 1976. A yeast mutant defective in the processing of 27S r-RNA precursor. *Mol Gen Genet* **144**: 29–37.

Archambault V, Buchler NE, Wilmes GM, Jacobson MD, Cross FR. 2005. Two-Faced Cyclins with Eyes on the Targets. *Cell Cycle* **4**: 125–130.

Atkins K, Cross F. (forthcoming). Inter-regulation of CDKA1/CDK1 and the plant-specific cyclin-dependent kinase CDKB in control of the Chlamydomonas cell cycle. *The Plant Cell*.

Aylett C, Sauer E, Imseng S, Boehringer D, Hall M, Ban N, Maier T. 2016. Architecture of human mTOR complex 1. *Science* **351**: 48–52.

Barbet N, Schneider U, Helliwell S, Stansfield I, Tuite M, Hall M. 1996. TOR controls translation initiation and early G1 progression in yeast. *Mol Biol Cell* **7**: 25–42.

Bernstein K, Bleichert F, Bean J, Cross F, Baserga S. 2007. Ribosome Biogenesis Is Sensed at the Start Cell Cycle Checkpoint. *Mol Biol Cell* **18**: 953–964.

Bisova K, Krylov D, Umen J. 2005. Genome-wide annotation and expression profiling of cell cycle regulatory genes in Chlamydomonas reinhardtii. *Plant Physiol* **137**: 475–91.

Bloom J, Cross F. 2007. Multiple levels of cyclin specificity in cell-cycle control. *Nat Rev Mol*

Cell Biol **8**: 149–160.

Boone C, Bussey H, Andrews B. 2007. Exploring genetic interactions and networks with yeast. *Nat Rev Genet* **8**: 437–449.

Boruc J, Van den Daele H, Hollunder J, Rombauts S, Mylle E, Hilson P, Inzé D, De Veylder L, Russinova E. 2010. Functional modules in the Arabidopsis core cell cycle binary protein-protein interaction network. *Plant Cell* **22**: 1264–1280.

Boudolf V, Inzé D, De Veylder L. 2006. What if higher plants lack a CDC25 phosphatase? *Trends Plant Sci* **11**: 474–9.

Brandeis M, Rosewell I, Carrington M, Crompton T, Jacobs M, Kirk J, Gannon J, Hunt T. 1998. Cyclin B2-null mice develop normally and are fertile whereas cyclin B1-null mice die in utero. *Proc Natl Acad Sci U S A* **95**: 4344–9.

Brash D. 2015. UV Signature Mutations. *Photochem Photobiol* **91**: 15–26.

Breker M, Lieberman K, Tulin F, Cross F. 2016. High-throughput robotically assisted isolation of temperature-sensitive lethal mutants in Chlamydomonas reinhardtii *J Vis Exp*. **118**: e54831.

Bridges D, Ma J-T, Park S, Inoki K, Weisman L, Saltiel A. 2012. Phosphatidylinositol 3,5-bisphosphate plays a role in the activation and subcellular localization of mechanistic target of rapamycin 1. *Mol Biol Cell* **23**: 2955–62.

Byfield M, Murray J, Backer J. 2005. hVps34 is a nutrient-regulated lipid kinase required for activation of p70 S6 kinase. *J Biol Chem* **280**: 33076–82.

Byrom M, Bhadra S, Jiang Y, Ellington A. 2014. Exquisite allele discrimination by toehold hairpin primers. *Nucleic Acids Res* **42**: e120–e120.

Chevalier C, Bourdon M, Pirrello J, Cheniclet C, Gévaudant F, Frangne N. 2014.

Endoreduplication and fruit growth in tomato: evidence in favour of the karyoplasmic ratio theory. *J Exp Bot* **65**: 2731–2746.

Churchman M, Brown M, Kato N, Kirik V, Hülskamp M, Inzé D, De Veylder L, Walker J, Zheng Z, Oppenheimer D, et al. 2006. SIAMESE, a plant-specific cell cycle regulator, controls endoreplication onset in Arabidopsis thaliana. *Plant Cell* **18**: 3145–3157.

Connell-Crowley L, Solomon MJ, Wei N, Harper JW. 1993. Phosphorylation independent activation of human cyclin-dependent kinase 2 by cyclin A in vitro. *Mol Biol Cell* **4**: 79–92.

Cooke FT, Dove SK, McEwen RK, Painter G, Holmes AB, Hall MN, Michell RH, Parker PJ. 1998. The stress-activated phosphatidylinositol 3-phosphate 5-kinase Fab1p is essential for vacuole function in S. cerevisiae. *Curr Biol* **8**: 1219–22.

Cools T, Iantcheva A, Weimer AK, Boens S, Takahashi N, Maes S, Van den Daele H, Van Isterdael G, Schnittger A, De Veylder L. 2011. The Arabidopsis thaliana checkpoint kinase WEE1 protects against premature vascular differentiation during replication stress. *Plant Cell* **23**: 1435–48.

Crespo JL, Díaz-Troya S, Florencio FJ. 2005. Inhibition of target of rapamycin signaling by rapamycin in the unicellular green alga Chlamydomonas reinhardtii. *Plant Physiol* **139**: 1736–49.

Cross FR. 2003. Two redundant oscillatory mechanisms in the yeast cell cycle. *Dev Cell* **4**: 741–52.

Cross FR, Breker M, Lieberman K. 2017. Validated bayesian differentiation of causative and passenger mutations. *G3 (Bethesda)* **7**: 2081–2094.

Cross FR, Buchler NE, Skotheim JM. 2011. Evolution of networks and sequences in eukaryotic cell cycle control. *Philos Trans R Soc B Biol Sci*. **366**: 3532-44.

Cross FR, Umen JG. 2015. The Chlamydomonas cell cycle. *Plant J* **82**: 370–92.

Cruz-Ramírez A, Díaz-Triviño S, Blilou I, Grieneisen VA, Sozzani R, Zamioudis C, Miskolczi P, Nieuwland J, Benjamins R, Dhonukshe P, et al. 2012. A bistable circuit involving SCARECROW-RETINOBLASTOMA integrates cues to inform asymmetric stem cell division. *Cell* **150**: 1002–1015.

Dewitte W, Scofield S, Alcasabas AA, Maughan SC, Menges M, Braun N, Collins C, Nieuwland J, Prinsen E, Sundaresan V, et al. 2007. Arabidopsis CYCD3 D-type cyclins link cell proliferation and endocycles and are rate-limiting for cytokinin responses. *Proc Natl Acad Sci* **104**: 14537–14542.

Díaz-Troya S, Florencio FJ, Crespo JL. 2008. Target of rapamycin and LST8 proteins associate with membranes from the endoplasmic reticulum in the unicellular green alga Chlamydomonas reinhardtii. **7**: 212–222.

Diener DR, Lupetti P, Rosenbaum JL. 2015. Proteomic analysis of isolated ciliary transition zones reveals the presence of ESCRT proteins. *Curr Biol* **25**: 379–384.

Dissmeyer N, Weimer AK, De Veylder L, Novak B, Schnittger A. 2010. The regulatory network of cell-cycle progression is fundamentally different in plants versus yeast or metazoans. *Plant Signal Behav* **5**: 1613–8.

Dissmeyer N, Weimer AK, Pusch S, De Schutter K, Kamei CLA, Nowack MK, Novak B, Duan G-L, Zhu Y-G, De Veylder L, et al. 2009. Control of cell proliferation, organ growth, and DNA damage response operate independently of dephosphorylation of the Arabidopsis Cdk1 homolog CDKA;1. *Plant Cell* **21**: 3641–3654.

Dutcher SK. 1995. Mating and tetrad analysis in Chlamydomonas reinhardtii. *Methods Cell Biol* **47**: 531–40.

Dutcher SK, O'Toole ET. 2016. The basal bodies of Chlamydomonas reinhardtii. *Cilia* **5**: 18.

Ehler LL, Dutcher SK. 1998. Pharmacological and genetic evidence for a role of rootlet and phycoplast microtubules in the positioning and assembly of cleavage furrows in Chlamydomonas reinhardtii. *Cell Motil Cytoskeleton* **40**: 193–207.

Ehler LL, Holmes JA, Dutcher SK. 1995. Loss of spatial control of the mitotic spindle apparatus in a Chlamydomonas reinhardtii mutant strain lacking basal bodies. *Genetics* **141**: 945–60.

Eloy NB, Gonzalez N, Van Leene J, Maleux K, Vanhaeren H, De Milde L, Dhondt S, Vercruysse L, Witters E, Mercier R, et al. 2012. SAMBA, a plant-specific anaphase-promoting complex/cyclosome regulator is involved in early development and A-type cyclin stabilization. *Proc Natl Acad Sci* **109**: 13853–13858.

Fang S-C, de los Reyes C, Umen JG. 2006. Cell size checkpoint control by the retinoblastoma tumor suppressor pathway. *PLoS Genet* **2**: e167.

Fang S-C, Umen JG. 2008. A suppressor screen in Chlamydomonas identifies novel components of the retinoblastoma tumor suppressor pathway. *Genetics* **178**: 1295–1310.

Fisher DL, Nurse P. 1996. A single fission yeast mitotic cyclin B p34cdc2 kinase promotes both S-phase and mitosis in the absence of G1 cyclins. *EMBO J* **15**: 850–60.

Forzani C, Aichinger E, Sornay E, Willemsen V, Laux T, Dewitte W, Murray JAH. 2014. WOX5 suppresses CYCLIN D activity to establish quiescence at the center of the root stem cell niche. *Curr Biol* **24**: 1939–1944.

Fridy PC, Li Y, Keegan S, Thompson MK, Nudelman I, Scheid JF, Oeffinger M, Nussenzweig MC, Fenyö D, Chait BT, et al. 2014. A robust pipeline for rapid production of versatile nanobody repertoires. *Nat Methods* **11**: 1253–1260.

Geng Y, Yu Q, Sicinska E, Das M, Schneider JE, Bhattacharya S, Rideout WM, Bronson RT,

Gardner H, Sicinski P. 2003. Cyclin E ablation in the mouse. *Cell* **114**: 431–43.

Glotzer M, Murray AW, Kirschner MW. 1991. Cyclin is degraded by the ubiquitin pathway. *Nature* **349**: 132–138.

Gong D, Ferrell JE. 2010. The roles of cyclin A2, B1, and B2 in early and late mitotic events. *Mol Biol Cell* **21**: 3149–61.

Goto K, Johnson CH. 1995. Is the cell division cycle gated by a circadian clock? The case of Chlamydomonas reinhardtii. *J Cell Biol* **129**: 1061–9.

Gourguechon S, Holt LJ, Cande WZ. 2013. The Giardia cell cycle progresses independently of the anaphase-promoting complex. *J Cell Sci* **126**: 2246–55.

Greiner A, Kelterborn S, Evers H, Kreimer G, Sizova I, Hegemann P. 2017. Targeting of photoreceptor genes in Chlamydomonas reinhardtii via zinc-finger nucleases and CRISPR/Cas9. *Plant Cell* Advance online publication. doi:10.1105/tpc.17.00659.

Guo J, Song J, Wang F, Zhang XS. 2007. Genome-wide identification and expression analysis of rice cell cycle genes. *Plant Mol Biol* **64**: 349–360.

Harashima H, Dissmeyer N, Schnittger A. 2013. Cell cycle control across the eukaryotic kingdom. *Trends Cell Biol* **23**: 345–356.

Harashima H, Schnittger A. 2012. Robust reconstitution of active cell-cycle control complexes from co-expressed proteins in bacteria. *Plant Methods* **8**: 23.

Harris EH. 2009. *The Chlamydomonas Sourcebook: Introduction to Chlamydomonas and Its Laboratory Use*. Academic Press.

He J, Chao WCH, Zhang Z, Yang J, Cronin N, Barford D. 2013. Insights into degron recognition by APC/C coactivators from the structure of an Acm1-Cdh1 complex. *Mol Cell* **50**: 649–660.

Henikoff S, Henikoff JG. 1993. Performance evaluation of amino acid substitution matrices. *Proteins Struct Funct Genet* **17**: 49–61.

Heyman J, Van den Daele H, De Wit K, Boudolf V, Berckmans B, Verkest A, Kamei CLA, De Jaeger G, Koncz C, De Veylder L. 2011. Arabidopsis ULTRAVIOLET-B-INSENSITIVE4 maintains cell division activity by temporal inhibition of the anaphase-promoting complex/cyclosome. *Plant Cell* **23**: 4394–4410.

Holm C, Stearns T, Botstein D. 1989. DNA topoisomerase II must act at mitosis to prevent nondisjunction and chromosome breakage. *Mol Cell Biol* **9**: 159–68.

Holmes JA, Dutcher SK. 1989. Cellular asymmetry in Chlamydomonas reinhardtii. *J Cell Sci* **94**: 273–85.

Imai KK, Ohashi Y, Tsuge T, Yoshizumi T, Matsui M, Oka A, Aoyama T. 2006. The A-Type cyclin CYCA2;3 is a key regulator of ploidy levels in Arabidopsis endoreduplication. *Plant Cell* **18**: 382–396.

Iouk TL, Aitchison JD, Maguire S, Wozniak RW. 2001. Rrb1p, a yeast nuclear WD-repeat protein involved in the regulation of ribosome biosynthesis. *Mol Cell Biol* **21**: 1260–1271.

Iwata E, Ikeda S, Matsunaga S, Kurata M, Yoshioka Y, Criqui M-C, Genschik P, Ito M. 2011. GIGAS CELL1, a novel negative regulator of the anaphase-promoting complex/cyclosome, is required for proper mitotic progression and cell fate determination in Arabidopsis. *Plant Cell* **23**: 4382–93.

Jeffrey PD, Russo AA, Polyak K, Gibbs E, Hurwitz J, Massagué J, Pavletich NP. 1995. Mechanism of CDK activation revealed by the structure of a cyclinA-CDK2 complex. *Nature* **376**: 313–320.

Jin N, Mao K, Jin Y, Tevzadze G, Kauffman EJ, Park S, Bridges D, Loewith R, Saltiel AR,

Klionsky DJ, et al. 2014. Roles for PI(3,5)P2 in nutrient sensing through TORC1. *Mol Biol Cell* **25**: 1171–85.

Jorgensen P, Tyers M. 2004. How cells coordinate growth and division. *Curr Biol* **14**: R1014–R1027.

Karlyshev A V, Pallen MJ, Wren BW. 2000. Single-primer PCR procedure for rapid identification of transposon insertion sites. *Biotechniques* **28**: 1078–82.

Karol KG, McCourt RM, Cimino MT, Delwiche CF. 2001. The closest living relatives of land plants. *Science* **294**: 2351–3.

King RW, Glotzer M, Kirschner MW. 1996. Mutagenic analysis of the destruction signal of mitotic cyclins and structural characterization of ubiquitinated intermediates. *Mol Biol Cell* **7**: 1343–57.

Kodama Y. 2016. Time gating of chloroplast autofluorescence allows clearer fluorescence imaging in planta. *PLoS One* **11**: e0152484.

Korbie DJ, Mattick JS. 2008. Touchdown PCR for increased specificity and sensitivity in PCR amplification. *Nat Protoc* **3**: 1452–1456.

Kozar K, Ciemerych MA, Rebel VI, Shigematsu H, Zagozdzon A, Sicinska E, Geng Y, Yu Q, Bhattacharya S, Bronson RT, et al. 2004. Mouse development and cell proliferation in the absence of D-cyclins. *Cell* **118**: 477–491.

Kwee H-S, Sundaresan V. 2003. The NOMEGA gene required for female gametophyte development encodes the putative APC6/CDC16 component of the Anaphase Promoting Complex in Arabidopsis. *Plant J* **36**: 853–66.

Lee SJ, Baserga SJ. 1999. Imp3p and Imp4p, two specific components of the U3 small nucleolar ribonucleoprotein that are essential for pre-18S rRNA processing. *Mol Cell Biol* **19**: 5441–

52.

Lemieux C, Otis C, Turmel M. 2000. Ancestral chloroplast genome in Mesostigma viride reveals an early branch of green plant evolution. *Nature* **403**: 649–652.

Li X, Zhang R, Patena W, Gang SS, Blum SR, Ivanova N, Yue R, Robertson JM, Lefebvre PA, Fitz-Gibbon ST, et al. 2016a. An indexed, mapped mutant library enables reverse genetics studies of biological processes in Chlamydomonas reinhardtii. *Plant Cell* **28**: 367–387.

Li Y, Liu D, Ló Pez-Paz C, Olson BJ, Umen JG. 2016b. A new class of cyclin dependent kinase in Chlamydomonas is required for coupling cell size to cell division. *Elife*: **5**: e10767.

Lin H, Miller ML, Granas DM, Dutcher SK. 2013. Whole genome sequencing identifies a deletion in protein phosphatase 2A that affects its stability and localization in Chlamydomonas reinhardtii. *PLoS Genet* **9**: e1003841.

Lorenz S, Tintelnot S, Reski R, Decker EL. 2003. Cyclin D-knockout uncouples developmental progression from sugar availability. *Plant Mol Biol* **53**: 227–236.

Lustig AJ, Lin RJ, Abelson J. 1986. The yeast RNA gene products are essential for mRNA splicing in vitro. *Cell* **47**: 953–63.

Lynch M, Force A. 2000. The probability of duplicate gene preservation by subfunctionalization. *Genetics* **154**: 459–73.

Lynch M, O'Hely M, Walsh B, Force A. 2001. The probability of preservation of a newly arisen gene duplicate. *Genetics* **159**: 1789–804.

McGarry TJ, Kirschner MW. 1998. Geminin, an inhibitor of DNA replication, is degraded during mitosis. *Cell* **93**: 1043–53.

Melaragno JE, Mehrotra B, Coleman AW. 1993. Relationship between endopolyploidy and cell size in epidermal tissue of Arabidopsis. *Plant Cell* **5**: 1661–1668.

Mendell JE, Clements KD, Choat JH, Angert ER. 2008. Extreme polyploidy in a large bacterium. *Proc Natl Acad Sci U S A* **105**: 6730–4.

Merchant SS, Prochnik SE, Vallon O, Harris EH, Karpowicz SJ, Witman GB, Terry A, Salamov A, Fritz-Laylin LK, Marechal-Drouard L, et al. 2007. The Chlamydomonas genome reveals the evolution of key animal and plant functions. *Science* **318**: 245–250.

Michelmore RW, Kesseli R V. 1991. Identification of markers linked to disease-resistance genes by bulked segregant analysis: a rapid method to detect markers in specific genomic regions by using segregating populations. *Genetics* **88**: 9828–9832.

Morgan DO. 2007. *The Cell Cycle:Principles of Control*. ed. E. Lawrence. New Science Press.

Münzner P, Voigt J. 1992. Blue light regulation of cell division in Chlamydomonas reinhardtii. *Plant Physiol* **99**: 1370–5.

Murphy M, Stinnakre M-G, Senamaud-Beaufort C, Winston NJ, Sweeney C, Kubelka M, Carrington M, Bréchot C, Sobczak-Thépot J. 1997. Delayed early embryonic lethality following disruption of the murine cyclin A2 gene. *Nat Genet* **15**: 83–86.

Murray AW, Kirschner MW. 1989. Cyclin synthesis drives the early embryonic cell cycle. *Nature* **339**: 275–280.

Murray AW, Solomon MJ, Kirschner MW. 1989. The role of cyclin synthesis and degradation in the control of maturation promoting factor activity. *Nature* **339**: 280–286.

Nguyen VQ, Co C, Li JJ. 2001. Cyclin-dependent kinases prevent DNA re-replication through multiple mechanisms. *Nature* **411**: 1068–1073.

Nobukuni T, Joaquin M, Roccio M, Dann SG, Kim SY, Gulati P, Byfield MP, Backer JM, Natt F, Bos JL, et al. 2005. Amino acids mediate mTOR/raptor signaling through activation of class 3 phosphatidylinositol 3OH-kinase. *Proc Natl Acad Sci U S A* **102**: 14238–43.

Nowack MK, Harashima H, Dissmeyer N, Zhao X, Bouyer D, Weimer AK, De Winter F, Yang F, Schnittger A. 2012. Genetic framework of cyclin-dependent kinase function in Arabidopsis. *Dev Cell* **22**: 1030–40.

Oldenhof H, Zachleder V, Ende H. 2004. Blue light delays commitment to cell division in Chlamydomonas reinhardtii. *Plant Biol* **6**: 689–695.

Olson BJSC, Oberholzer M, Li Y, Zones JM, Kohli HS, Bisova K, Fang S-C, Meisenhelder J, Hunter T, Umen JG. 2010. Regulation of the Chlamydomonas cell cycle by a stable, chromatin-associated retinoblastoma tumor suppressor complex. *Plant Cell* **22**: 3331–3347.

Pagano M, Pepperkok R, Verde F, Ansorge W, Draetta G. 1992. Cyclin A is required at two points in the human cell cycle. *EMBO J* **11**: 961–71.

Pahari S, Cormark RD, Blackshaw MT, Liu C, Erickson JL, Schultz EA. 2014. Arabidopsis UNHINGED encodes a VPS51 homolog and reveals a role for the GARP complex in leaf shape and vein patterning. *Development* **141**: 1894–1905.

Peres A, Churchman ML, Hariharan S, Himanen K, Verkest A, Vandepoele K, Magyar Z, Hatzfeld Y, Van Der Schueren E, Beemster GTS, et al. 2007. Novel plant-specific cyclin-dependent kinase inhibitors induced by biotic and abiotic stresses. *J Biol Chem* **282**: 25588–96.

Plecenikova A, Slaninova M, Riha K. 2014. Characterization of DNA repair deficient strains of Chlamydomonas reinhardtii generated by insertional mutagenesis. *PLoS One* **9**: e105482.

Polko JK, van Rooij JA, Vanneste S, Pierik R, Ammerlaan AMH, Vergeer-van Eijk MH, McLoughlin F, Gühl K, Van Isterdael G, Voesenek LACJ, et al. 2015. Ethylene-mediated regulation of A2-Type CYCLINs modulates hyponastic growth in Arabidopsis. *Plant Physiol* **169**: 194–208.

Pomerening JR, Sontag ED, Ferrell JE. 2003. Building a cell cycle oscillator: hysteresis and bistability in the activation of Cdc2. *Nat Cell Biol* **5**: 346–351.

Powers T, Walter P. 1999. Regulation of ribosome biogenesis by the rapamycin- sensitive TOR-signaling pathway in Saccharomyces cerevisiae. *Mol Biol Cell* **10**: 987–1000.

Qiao R, Weissmann F, Yamaguchi M, Brown NG, Vanderlinden R, Imre R, Jarvis MA, Brunner MR, Davidson IF, Litos G, et al. 2016. Mechanism of APC/C CDC20 activation by mitotic phosphorylation. *Proc Natl Acad Sci U S A* **113**: E2570-8.

Rasala BA, Barrera DJ, Ng J, Plucinak TM, Rosenberg JN, Weeks DP, Oyler GA, Peterson TC, Haerizadeh F, Mayfield SP. 2013. Expanding the spectral palette of fluorescent proteins for the green microalga Chlamydomonas reinhardtii. *Plant J* **74**: 545–56.

Remm M, Storm CE, Sonnhammer EL. 2001. Automatic clustering of orthologs and in-paralogs from pairwise species comparisons. *J Mol Biol* **314**: 1041–52.

Richards TA, Soanes DM, Foster PG, Leonard G, Thornton CR, Talbot NJ. 2009. Phylogenomic analysis demonstrates a pattern of rare and ancient horizontal gene transfer between plants and fungi. *Plant Cell* **21**: 1897–911.

Riou-Khamlichi C, Menges M, Healy JM, Murray JA. 2000. Sugar control of the plant cell cycle: differential regulation of Arabidopsis D-type cyclin gene expression. *Mol Cell Biol* **20**: 4513–21.

Robbens S, Khadaroo B, Camasses A, Derelle E, Ferraz C, Inzé D, Van de Peer Y, Moreau H. 2005. Genome-wide analysis of core cell cycle genes in the unicellular green alga Ostreococcus tauri. *Mol Biol Evol* **22**: 589–597.

Rogozin IB, Basu MK, Csuros M, Koonin E V. 2010. Analysis of rare genomic changes does not support the unikont-bikont phylogeny and suggests cyanobacterial symbiosis as the point of

primary radiation of eukaryotes. *Genome Biol Evol* **1**: 99–113.

Santamaría D, Barrière C, Cerqueira A, Hunt S, Tardy C, Newton K, Cáceres JF, Dubus P, Malumbres M, Barbacid M. 2007. Cdk1 is sufficient to drive the mammalian cell cycle. *Nature* **448**: 811–815.

Sanz L, Dewitte W, Forzani C, Patell F, Nieuwland J, Wen B, Quelhas P, De Jager S, Titmus C, Campilho A, et al. 2011. The Arabidopsis D-Type cyclin CYCD2;1 and the inhibitor ICK2/KRP2 modulate auxin-induced lateral root formation. *Plant Cell* **23**: 641–660.

Schnittger A, Schöbinger U, Stierhof YD, Hülskamp M. 2002. Ectopic B-type cyclin expression induces mitotic cycles in endoreduplicating Arabidopsis trichomes. *Curr Biol* **12**: 415–20.

Scofield S, Jones A, Murray J. 2014. The plant cell cycle in context. *J Exp Bot* **65**: 2557–2562.

Spudich JL, Sager R. 1980. Regulation of the Chlamydomonas cell cycle by light and dark. *J Cell Biol* **85**: 136–45.

Stack JH, Herman PK, Schu P V, Emr SD. 1993. A membrane-associated complex containing the Vps15 protein kinase and the Vps34 PI 3-kinase is essential for protein sorting to the yeast lysosome-like vacuole. *EMBO J* **12**: 2195–204.

Thornton BR, Toczyski DP. 2003. Securin and B-cyclin/CDK are the only essential targets of the APC. *Nat Cell Biol* **5**: 1090–1094.

Tran LT, Wang'Ondu RW, Weng JB, Wanjiku GW, Fong CM, Kile AC, Koepp DM, Hood-Degrenier JK. 2010. TORC1 kinase and the S-phase cyclin Clb5 collaborate to promote mitotic spindle assembly and DNA replication in S. cerevisiae. *Curr Genet* **56**: 479–493.

Tulin F, Cross FR. 2014. A microbial avenue to cell cycle control in the plant superkingdom. *Plant Cell* **26**: 4019–38.

Tulin F, Cross FR. 2015. Cyclin-dependent kinase regulation of diurnal transcription in

Chlamydomonas. *Plant Cell* **27**: 2727-42.

Tulin F, Cross FR. 2016. Patching Holes in the Chlamydomonas Genome. *G3 (Bethesda)* **6**: 1899–910.

Vandepoele K, Raes J, De Veylder L, Rouzé P, Rombauts S, Inzé D. 2002. Genome-wide analysis of core cell cycle genes in Arabidopsis. *Plant Cell* **14**: 903–16.

Vanneste S, Coppens F, Lee E, Donner TJ, Xie Z, Van Isterdael G, Dhondt S, De Winter F, De Rybel B, Vuylsteke M, et al. 2011. Developmental regulation of CYCA2s contributes to tissue-specific proliferation in Arabidopsis. *EMBO J* **30**: 3430–41.

Wang Y, Hou Y, Gu H, Kang D, Chen Z, Liu J, Qu L-J. 2012. The Arabidopsis APC4 subunit of the anaphase-promoting complex/cyclosome (APC/C) is critical for both female gametogenesis and embryogenesis. *Plant J* **69**: 227–240.

Weimer AK, Biedermann S, Harashima H, Roodbarkelari F, Takahashi N, Foreman J, Guan Y, Pochon G, Heese M, Van Damme D, et al. 2016. The plant-specific CDKB1-CYCB1 complex mediates homologous recombination repair in *Arabidopsis*. *EMBO J* **35**: 2068–2086.

Weingartner M, Criqui M-C, Mészáros T, Binarova P, Schmit A-C, Helfer A, Derevier A, Erhardt M, Bögre L, Genschik P. 2004. Expression of a nondegradable cyclin B1 affects plant development and leads to endomitosis by inhibiting the formation of a phragmoplast. *Plant Cell* **16**: 643–57.

Wright S. 1932. The roles of mutation, inbreeding, crossbreeding and selection in evolution. *Proc 6th Int Congr Genet* **1**: 356–366.

Xiong Y, McCormack M, Li L, Hall Q, Xiang C, Sheen J. 2013. Glucose–TOR signalling reprograms the transcriptome and activates meristems. *Nature* **496**: 181–186.

Yang X, Shears SB. 2000. Multitasking in signal transduction by a promiscuous human Ins(3,4,5,6)P4 1-kinase/Ins(1,3,4)P3 5/6-kinase. *Biochem J* **351 Pt 3**: 551–5.

York JD, Odom AR, Murphy R, Ives EB, Wente SR. 1999. A phospholipase C-dependent inositol polyphosphate kinase pathway required for efficient messenger RNA export. *Science* **285**: 96–100.

Zhao X, Harashima H, Dissmeyer N, Pusch S, Weimer AK, Bramsiepe J, Bouyer D, Rademacher S, Nowack MK, Novak B, et al. 2012. A general G1/S-phase cell-cycle control module in the flowering plant Arabidopsis thaliana *PLoS Genet* **8**: e1002847.

Zones JM, Blaby IK, Merchant SS, Umen JG. 2015. High-resolution profiling of a synchronized diurnal transcriptome from Chlamydomonas reinhardtii reveals continuous cell and metabolic differentiation. *Plant Cell* **27**: 2743–69.